NASA
Technical
Paper
2167

August 1983

Wind-Tunnel Investigation of Leading-Edge Thrust on Arrow Wings in Supersonic Flow

Robert J. Mack

NASA

25th Anniversary
1958-1983

NASA Technical Paper 2167

1983

Wind-Tunnel Investigation of Leading-Edge Thrust on Arrow Wings in Supersonic Flow

Robert J. Mack

Langley Research Center
Hampton, Virginia

National Aeronautics and Space Administration

Scientific and Technical Information Branch

SUMMARY

Six uncambered wing models were tested in the Langley Unitary Plan Wind Tunnel to identify and study leading-edge thrust at supersonic speeds. Three of the models had arrow wing planforms and the other three had their planform leading edges modified to produce constant, 100-percent thrust from the half-semispan station to the tip. Wing airfoils had a maximum thickness of 4 percent and had three bluntness ratios (Leading-edge radius)/(Chord), which varied from sharp to blunt. The tests were conducted at Mach numbers of 1.6, 1.8, 2.0, and 2.16 with a stagnation temperature of 125.0°F and Reynolds numbers per foot of 2.0×10^6 and 5.0×10^6.

The test results showed that significant benefits from leading-edge thrust and nonlinear thickness effects can be generated with very little airfoil bluntness, that these benefits were lost when the airfoil was severely blunted, and that such benefits seem to be produced on wings with linear-theory-defined supersonic as well as subsonic leading edges. Predicted axial-force increments agree reasonably well with measured values when the airfoils were moderately blunt but were in poor agreement when the airfoils were sharp or very blunt. Agreement between available-thrust theoretical and experimental lift-drag polars and lift-drag ratio curves was good for wings with moderately blunt airfoils and fair for wings with sharp airfoils, but poor for wings with very blunt airfoils.

INTRODUCTION

Leading-edge thrust has long been a vital part of subsonic wing theory, but only recently has it become accepted as potentially exploitable on wings in supersonic flow. During the early supersonic transport feasibility studies, wings were designed with thin, sharp, airfoil sections as well as other thin or slender components to minimize wave drag. These airfoils worked admirably in reducing wave drag but theoretically eliminated the generation of useful leading-edge thrust; therefore, with little or no thrust theoretically expected, none was looked for. The same situation persisted when calculation methods for optimum camber and twist were introduced and applied to supersonic-cruise wing planform design.

However, experimental data did not always support the expectations of zero leading-edge thrust. Often sizable differences between measured and predicted axial forces were found (ref. 1, typical); differences that could be explained most simply by leading-edge thrust theory. A methodology for estimating leading-edge thrust on wings in supersonic flow had been introduced in reference 2. With the use of measured pressure distributions, it provided local and total leading-edge thrust coefficients. This method was supplanted by linear-theory solutions which replaced experimental with theoretical pressure distributions (ref. 3) and utilized digital computer technology to quickly and easily calculate distributed and total thrust coefficients. An improvement (ref. 4) permitted the effects of wing thickness, leading-edge radius, and Reynolds number to be included in an estimate of attainable or realizable leading-edge thrust. These improvements were combined with linear-theory thickness effects and nonlinear thickness effects to obtain a prediction method for modified linear-theory wing analysis (ref. 5).

Since effective leading-edge thrust seemed to be generated on some though not all wings with sharp leading-edge airfoils, it appeared logical that exploitable levels of thrust could be obtained by slightly modifying existing wing features. With both theory and experiment necessary to validate this idea, a series of flat-camber wing models were designed and built. These models would be used to determine the amounts of leading-edge thrust that could be generated, assess the potential benefits of a leading-edge tailoring method suggested in reference 3, expand the data base of performance for blunt-leading-edge wings at supersonic speeds, and check the prediction capabilities of the methods which were reported in references 4 and 5.

In this paper, a wind-tunnel study of leading-edge thrust and its effect on wing performance is reported. The wing models used in the tests are described, and the features specifically incorporated to generate desired distributions of thrust are highlighted. Results of the tests and comparisons of theory and experiment are presented and discussed.

SYMBOLS

A	aspect ratio, b^2/S
b	wing span
C_A	total axial-force coefficient
ΔC_A	$= C_A - C_{A,max}$
C_D	drag coefficient
ΔC_D	$= C_D - C_{D,o}$
C_L	lift coefficient
$C_{L_{\alpha,0}}$	$\partial C_L/\partial\alpha$ at $\alpha = 0$
C_m	pitching-moment coefficient
C_N	total normal-force coefficient
C_p	pressure coefficient
c	wing chord
$\bar{c}$	mean aerodynamic chord
c_a	section axial-force coefficient
c_n	section normal-force coefficient
c_t	section leading-edge thrust coefficient
L/D	lift-drag ratio, C_L/C_D
k_1,k_2,k_3,k_4	airfoil equation constants in figure 1(c) and table I

M	free-stream Mach number
p	pressure, lb/ft^2
R	Reynolds number per foot
r	leading-edge radius along free-stream direction (see table I)
r_b	body radius (see table I)
S	reference area, 300.0 in^2
T	temperature, °F
t	maximum wing thickness
x	distance along longitudinal axis
x'	longitudinal distance aft of leading edge
x_b	longitudinal distance to aft end of body (figs. 1(a) and (b))
x_t	longitudinal distance to leading edge of wing tip (figs. 1(a) and (b))
y	distance along spanwise axis
z	distance normal to X-Y symmetry plane in right-hand coordinate sense
α	angle of attack, deg
$\Delta\alpha$	$= \alpha - \alpha_{sym}$
β	$= (M^2 - 1)^{1/2}$
$\beta \cot \Lambda_{le}$	$= \dfrac{\tan (90^\circ - \Lambda_{le})}{\tan \mu}$
Δ	increment
Λ_{le}	leading-edge sweep angle, deg
μ	Mach angle, deg
ξ	$= x'/c$

Subscripts:

LT	linear theory
le	leading edge
max	maximum

min	minimum
NLT	nonlinear theory
NL,THK	nonlinear corrections due to wing thickness only
o	conditions at zero lift
r	root chord
s	stagnation conditions
sym	symmetry point on axial-force curves

MODELS

Design

Two wing planforms were chosen for the leading-edge thrust study: a reference planform and a thrust-limited planform. The reference planform was an arrow wing chosen because the analytic solutions for lift, drag, and 100-percent leading-edge thrust were readily available. A thrust limit (desired spanwise variation), for a design Mach number of 1.6, was imposed on the second planform after an analysis of data from references 1 and 6 showed that on uncambered, subsonic leading-edge wings, inboard-generated upwash tends to separate the outboard-wing air flow at modest angles of attack. This limit, explained in the section "Description," resulted in a gradual unsweeping of the leading edge which, as hypothesized in reference 3, would permit flow to remain attached at angles of attack beyond the range of small to modest.

Description

Figure 1 shows the reference arrow wing, the thrust-limited modified arrow wing, and the airfoils used on these wings. Table I has the dimensions associated with these wings. Both wing planforms had the same span, wing area, inboard sweep angle, and balance body. They differed mainly in the outer wing section where the modified arrow leading edge was unswept to achieve a constant value of 100-percent leading-edge thrust from half-semispan to tip. The airfoils had a maximum thickness of 4 percent at 45 percent of chord. Leading-edge bluntness, designated by $(r/c)_{le}$, was set at three values: "sharp," $(r/c)_{le}$ of about 0.0005 but, ideally, of 0.0; medium blunt, $(r/c)_{le} \approx 0.00235$; and blunt, $(r/c)_{le} \approx 0.00470$. Note expanded scale in figure 1(c) which was used to show the relative bluntness of the airfoils. Figure 2 shows the spanwise thrust variation (thrust limit) and its effect on leading-edge parameters at the design Mach number of 1.6. The method described in reference 3 was used to compute the modified leading edge, but the method of reference 5 was used to analyze the wing performance because this modified method became available about the time that the wind-tunnel tests were performed.

TEST CONDITIONS

The tests were conducted in the 4- by 4-foot low supersonic speed test section of the Langley Unitary Plan Wind Tunnel. Aerodynamic force measurements were made with the models in Mach 1.6, 1.8, 2.0, and 2.16 flow. To insure turbulent flow over the wing surfaces, a No. 50 size grit was applied along a 0.0625-in.-wide band 0.125 in. behind and normal to the leading edges. Reynolds numbers per foot of 2.0×10^6 and 5.0×10^6 were used in the tests. The lower Reynolds number was used on all models at all test Mach numbers whereas the higher Reynolds number was used only on the arrow wing models at Mach numbers of 2.0 and 2.16. Originally, the arrow wing models were scheduled to be tested at the higher Reynolds number at all test Mach numbers. However, the test-section angle-of-attack mechanism was unable to maintain model attitude, so data at Mach 1.6 and 1.8 were not obtained. Stagnation temperature and pressures are shown in the following table:

M	R	T_s, °F	p_s, lb/ft^2
1.6	2.0×10^6	125.0	1078.6
1.8	↓	↓	1153.8
2.0			1253.2
2.16			1349.0
1.6	5.0×10^6		2697.0
1.8	↓		2885.0
2.0			3134.0
2.16			3373.0

In table II, the test combinations of Mach numbers and Reynolds numbers are given. Base pressure was recorded and used to correct the force and pitching-moment data to free-stream conditions. Strain-gage accuracy and test data repeatability established average data limitations as follows:

Coefficient	Accuracy at R of -	
	2.0×10^6	5.0×10^6
C_N	±0.0040	±0.0020
C_A	±.0003	±.0002
C_m	±.0010	±.0004

RESULTS

Wind-tunnel data from the six wing models at Mach numbers of 1.6, 1.8, 2.0, and 2.16 are recorded in tables III through VIII. They were corrected for normal-force and moment flow-angularity effects as well as balance-bore misalignment. No corrections were made for grit drag since it was assumed to be small and well within the accuracy limits of the instrumentation.

Although conventional correction techniques removed flow-angularity effects from the normal-force and moment data, they did not simultaneously remove these effects from the axial-force data. It is shown in subsequent sections why this occurred and how the axial-force data were treated to obtain meaningful information on leading-edge thrust.

A sampling of data was extracted and used to prepare figures 3 to 6 which are plots of $\left(C_{L_{\alpha,0}}\right)^{-1}$, $C_{m,o}$, $\Delta C_m/\Delta C_L$, and $C_{D,min}$ as a function of M and $(r/c)_{le}$. These parameters provide information on the merits of planform, camber and twist (if any), and thickness. Figure 3 shows measured $\left(C_{L_{\alpha,0}}\right)^{-1}$ for comparing the relative performance of the two planforms and three bluntness ratios at the test Mach numbers. For a flat camber wing which is not generating leading-edge thrust, $\left(C_{L_{\alpha,0}}\right)^{-1}$ and the drag-due-to-lift parameter $\left(\Delta C_D/C_L^2\right)_o$ are equal. When both leading-edge thrust and vortex effects are present, $\left(\Delta C_D/C_L^2\right)_o$ will usually be less than $\left(C_{L_{\alpha,0}}\right)^{-1}$. Since thrust effects are discussed later, values of $\left(C_{L_{\alpha,0}}\right)^{-1}$ were compared to determine whether nonlinear bluntness and/or thickness effects were present as an influence on planform performance.

The data in figure 3 suggest that leading-edge bluntness is a nonlinear factor in $\left(C_{L_{\alpha,0}}\right)^{-1}$, which changes very little with Mach number. These differences in $\left(C_{L_{\alpha,0}}\right)^{-1}$ could be caused by variations in distance between shock and wing leading edge. Leading-edge local Mach numbers would then vary with bluntness, and the effect would be felt across the entire wing surface. None of this would influence $C_{m,o}$ which is camber-surface sensitive. In figure 4, $C_{m,o}$ is seen to be about zero (within measurement tolerances); this indicates that the wing camber surfaces are effectively flat plate. The zero-lift stability parameter $\left(\Delta C_m/\Delta C_L\right)_o$ (fig. 5) shows both expected and unexpected variations with Mach number, planform, and bluntness. For both wing planforms, the sharp and medium-blunt airfoil data have similar levels and trends as the Mach number increases. Data for the blunt airfoil parallel and almost overlay the data for the sharp and medium-blunt airfoils on the modified arrow wing but are separated by a sizable gap for the arrow wing in figure 5(a). A closer examination of this bluntness effect is shown in figure 5(b). The modified arrow wing $\left(\Delta C_m/\Delta C_L\right)_o$ is seen to be virtually constant across the range of bluntness parameter - $(r/c)_{le}$ between 0.0005 and 0.00470. For the arrow wing, $\left(\Delta C_m/\Delta C_L\right)_o$ is almost constant between $(r/c)_{le} = 0.0005$ and 0.00235 but then increases markedly between $(r/c)_{le} = 0.00235$ and 0.00470. This sensitivity is probably caused by the inherently conical nature of attached flow over arrow wings. Effects of leading-edge bluntness which are introduced at the wing apex spread over the whole wing. In contrast, the decreasing leading-edge sweep on the modified arrow wing alters the conical nature established at the apex and spreads these modified effects over a proportionately larger outboard wing area.

Similar thickness effects are evident in the comparisons of $C_{D,min}$ in figure 6. Data for the blunt and medium-blunt arrow wings in figure 6(a) are coincident at Mach 1.6 and 1.8. Beyond Mach 1.8, the data for the medium-blunt wing change in trend from the data for the blunt wing and continue to decrease at Mach 2.0 and 2.16 in a manner paralleling the data for the sharp wing. Figure 6(b) shows nearly the same data for the sharp and the medium-blunt modified arrow wing, which are noticeably separated from and less than the data for the blunt wing at all test Mach numbers. The sensitivity of the arrow wing to leading-edge bluntness, which was noted in figure 5(b) for $(\Delta C_m/\Delta C_L)_o$ is also seen in figure 6(c). Compared with the data for the sharp and the blunt leading edges, the $C_{D,min}$ data for the medium-blunt leading edge are unusually close at Mach 1.6 and 1.8. This closeness is caused by the more rapid increase in $C_{D,min}$ for the arrow wing when $(r/c)_{le}$ increases from 0.0005 to 0.00235 as compared with an almost static response from the modified arrow wing over the same range of Mach number and bluntness conditions.

The results in figures 3 to 6 suggest that leading-edge bluntness has some effect on lift as well as drag characteristics. This effect is probably because of the range of $(r/c)_{le}$ used on the models - from sharp (approximately 0.0005) to 0.00470. These radius-chord values are measured in the free-stream direction. When measured normal to the wing leading edge, these values are about twice as large.

At the beginning of the section "Results," it was mentioned that the normal-force and the moment flow-angularity corrections did not simultaneously remove flow-angularity effects from the axial-force data. Theoretically, uncambered wings in uniform flow should generate axial-force data which are symmetrical about zero angle of attack. Figure 7 shows samples of experimental ΔC_A $(\Delta C_A = C_A - C_{A,max})$ plotted against α for the sharp and blunt arrow wings. For sharp leading edges (figs. 7(a) and (b)) ΔC_A distributions are much more symmetrical at small angles of attack than the ΔC_A distributions for blunt leading edges (figs. 7(c) and (d)) but still showed asymmetry at the angles of attack greater than ±5.0°. Mach number was also a factor. The offset in angle of attack for ΔC_A symmetry increased with test Mach number. Differences in all ΔC_A data at angles of attack of +15.0° and -15.0° ranged from 0.0014 to 0.0044, but most of the ΔC_A differences were closer to about 0.0025 than to either of the extreme values. Errors in C_D caused by these variations were no worse than about 2.5 percent.

An examination of the models revealed no significant surface departures from design symmetry, and the plots of $C_{m,o}$ (fig. 4), did not suggest the presence of camber or twist; therefore, the asymmetry of the axial-force data was hypothesized as due to throat asymmetry in the Unitary Plan Wind Tunnel design. This idea was verified by reference 7 and by an analysis which showed that the tunnel upwash fields could produce the data asymmetry. Since the amount of work required to obtain upwash field corrections for each model at each angle of attack, Mach number, and Reynolds number was found to be excessive, the origin for ΔC_A plotted against α was shifted to a "symmetry" point α_{sym}. Consequently, both model-upright and model-inverted axial-force coefficients were used to generate a band rather than a line of experimental data. In this modified format, ΔC_A plotted against $\Delta\alpha$ $(\Delta\alpha = \alpha - \alpha_{sym})$, data could be compared with theoretical predictions with the expectation that meaningful conclusions could be made.

Comparisons of theory and experiment presented in the section "Analysis and Discussion" are interpreted in the light of current supersonic wing theory. In these comparisons, the effects of wind-tunnel upwash are obvious. Nevertheless, the trend and magnitude of these upwash effects can be seen as small compared with the axial forces generated by the wings.

ANALYSIS AND DISCUSSION

Supersonic wing performance is conventionally analyzed by computing lift and drag-due-to-lift contributions on a zero-thickness wing, and adding zero-lift wave drag plus skin-friction drag components. By adding suitable modifications to linearized theory along the avenues of the analysis outlined in reference 5, the aerodynamic performance estimates of wings can include nonlinear thickness effects. Some insight can be obtained about the magnitude and behavior of these nonlinear forces from comparison of measured and predicted ΔC_A at $\Delta\alpha = 5.0°$ over the test Mach number range. Negative ΔC_A is shown to be caused by more than just leading-edge thrust. Comparisons of measured and predicted ΔC_A are examined to determine both the levels of axial force obtained and the capabilities of linear and nonlinear methods to estimate the magnitude and behavior of the various contributions. After the predicted and measured ΔC_A of each wing are compared, plots of ΔC_A at $\Delta\alpha = 5.0°$ as a function of leading-edge bluntness parameter $(r/c)_{le}$ and $\beta \cot \Lambda_{le}$ are presented so that possible optimum values of blunting can be sought. The hypothesis concerning the advantages of a thrust-limited leading edge over a straight leading-edge planform is examined in another set of plots of ΔC_A as a function of $\Delta\alpha$ at the design Mach number of 1.6. In the final set of figures, measured and predicted lift-drag ratios and lift-drag polars are compared.

Nonlinear Effects

Wind-tunnel and theoretical values of ΔC_A at $\Delta\alpha = 5.0°$ are compared in figure 8. The theory is only for leading-edge thrust which becomes zero at Mach 2.0 - the linear-theory sonic leading-edge condition. At Mach 1.6, there is trend agreement between available thrust and measured ΔC_A. However, agreement in magnitude varies from poor to reasonably good. At and beyond Mach 2.0, trend and magnitude agreement disappears, for although theoretical ΔC_A due to leading-edge thrust becomes zero, experimental ΔC_A is still finite. These nonlinear effects can be explained in a general way by an analysis based on figure 9.

On the left-hand side of figure 9, linear theory assumes a Mach cone at the wing apex. In the standard method for calculating lift and drag due to lift, the wing has a flat camber surface, and airfoil thickness contributes only wave drag. Hence, the flow is pictured as attached to the leading edge all along the span but with an upwash component that is mathematically singular. The plots of C_p against x and C_p against z show the influence of this singularity.

On the right-hand side of figure 9, a more realistic nonlinear theory places a shock surface at the wing apex so that at stations along the semispan leading edge, a Mach number less than free-stream value is felt. The flow stagnation point is now at a small distance behind and under the leading edge. Part of the flow continues along the chord while the other part goes around the leading edge to produce a locally negative ΔC_A due to leading-edge thrust as long as it stays attached to the wing surface. No leading-edge singularity is present; therefore, these local normal and axial forces will be less than linear theory values. Local pressures are also constrained by real-flow vacuum limitations. Therefore, the normal and axial forces predicted by a nonlinear theory will be less than those from linear theory.

Since the analysis method of reference 5 is a modified linear theory, a separate calculation of leading-edge thrust is required just as with regular linear theory. However, the corrections mentioned previously, the vacuum limit on negative C_p values and the estimates of nonlinear thickness effects, available leading-edge thrust, and vortex flow effects are included. The superposition of these nonlinear thickness effects on the available thrust (fig. 8) is seen in figure 10. Since the curve for 100-percent leading-edge thrust is only for reference, nonlinear effects are not added to it.

Agreement between measured and predicted ΔC_A values and trends is reasonably good for the medium-blunt wing across the test Mach number range, and good for the very blunt wing for Mach numbers greater than about 1.9. Although the magnitude is still underpredicted for the sharp-leading-edge wing, the trends are in good agreement. Thus, a significant contribution to negative ΔC_A can come from nonlinear thickness influences. Typical behavior with angle of attack is shown in figure 11 for the wing models at a Mach number of 1.6 with the nonlinear values of ΔC_A due to thickness predicted by the method of reference 5. It has been assumed that the flow remains attached at all angles of attack.

Linear theory would give $\Delta C_A = 0$ at all angles of attack when the wing has a flat camber surface and is producing no leading-edge thrust. Any ΔC_A which exceeds the nonlinear thickness values could be considered as leading-edge thrust until the angles of attack where flow separation effects become noticeable. In the next section, it is shown that this oversimplified and overoptimistic view is not always correct.

Leading-Edge Thrust

Comparison of theory and experiment are shown in figures 12 to 17 with ΔC_A and $\Delta\alpha$ as the variables at each of the test Mach numbers. Since the theory curves for flat wings are symmetrical about $\alpha = 0$, the previously mentioned $\Delta\alpha$ shift was used so that results at two Mach numbers could be put on each plot. The upper and lower bounds of the experimental data band are determined by model-upright and model-inverted data.

Arrow wings.- The first set of comparisons, figures 12 to 14, show theory and experiment for the reference arrow wings. Available leading-edge thrust theory predicts that little or no thrust is generated by sharp-leading-edge wings; a preplanned reference condition against which the blunt-wing data were to be compared. Figure 12 reveals that the ability of the sharp-leading-edge wing to generate negative ΔC_A is underestimated by the nonlinear thrust theory. The experimental ΔC_A is considerably larger than that predicted at subsonic leading-edge test Mach numbers (fig. 12(a)). Obviously, a true zero-radius leading edge cannot be put on a real wing; thus, $(r/c)_{le} \approx 0.0005$ which was used to obtain the theory curves was an approximate bluntness value. Additional departures from expectations were noted at Mach 2.0 and 2.16 (fig. 12(b)) where linear theory predicts a sonic and a supersonic leading edge, respectively, and no leading-edge thrust. Perhaps the nonlinear thickness effects are being underestimated, or real flow effects due to the apex-attached shock wave are permitting substantial leading-edge thrust generation at these test Mach numbers.

Although the available leading-edge thrust for the sharp-leading-edge wing was underpredicted, the trends in the experimental and theoretical curves are in close agreement. It may be that local Reynolds number effects are producing an artificial leading-edge-radius phenomenon at the nose of a sharp airfoil. Since the data base was built mainly on results from airfoils in the medium-blunt category, the experimental and theoretical ΔC_A curves from these arrow wings should be in close agreement.

This supposition is verified in figure 13(a) where the agreement is seen to be very good. However, the sonic and supersonic leading-edge theoretical decrements seen in the sharp-leading-edge wing comparison (fig. 12(b)) appear again in figure 13(b). The difference between experiment and theory in this moderately blunt-leading-edge data is smaller than in the sharp-airfoil data.

Comparisons of theory and experiment for the blunt-leading-edge wing (fig. 14) show that the theory is overpredicting leading-edge thrust and nonlinear thickness benefits at Mach 1.6 and 1.8 but is in closer agreement with experiment at Mach 2.0 and 2.16. Figure 14 seems to clearly demonstrate that from a viewpoint of leading-edge thrust, blunting can easily be overdone. However, it is also possible that both leading-edge thrust and nonlinear thickness effects are overpredicted.

With these comparisons (figs. 12 to 14), the relative merits of increasing leading-edge bluntness can be seen and understood. The sharp- and medium-blunt-leading-edge wings are providing exploitable amounts of leading-edge thrust while suffering relatively small nonlinear disturbance penalties. On the blunt wings, however, negative ΔC_A appears to be caused mostly by nonlinear thickness effects and the predicted thrust levels may not be experimentally realized.

Modified arrow wings.- The second set of comparisons (figs. 15 to 17) shows theory and experiment for the modified arrow wings. Very similar to the observations made from the arrow-wing plots, the leading-edge thrust is underpredicted on the sharp wing (fig. 15), fairly well predicted on the medium-blunt wing, (fig. 16), and overpredicted on the blunt wing (fig. 17). It is again seen that nonlinear thickness effects grow in importance with increases in airfoil bluntness, and that negative ΔC_A is apparently being generated at sonic and supersonic leading-edge conditions; these contributions (both thrust and nonlinear thickness effects) disappear with increasing bluntness.

However, another aspect of leading-edge thrust, probably nonlinear in origin, appeared in the comparisons of experimental and theoretical data for the modified arrow wing. At low angles of attack, the sharp and, to a lesser extent, the medium-blunt wings are generating more than 100-percent theoretical leading-edge thrust. Even with the nonlinear, thickness-induced correction added to the 100-percent reference curve, the wing appears to be outperforming theory by a small increment. This phenomenon is seen clearly at Mach 1.8 in figure 15(a), is almost lost at Mach 1.8 in figure 16(a), and is gone at Mach 1.8 in figure 17(a).

At Mach 1.8, linear theory predicts that the inboard panels have subsonic leading edges, the outboard section has a supersonic leading edge, and the section at about 0.72 semispan has a sonic leading edge where leading-edge thrust goes to zero and remains at zero out to the wing tip. If local nonlinear effects are changing the Mach number normal to the leading edge enough to permit effective subsonic conditions to extend beyond the sonic condition station, then thrust will continue to be generated at stations which have a slightly supersonic leading edge. Since the leading-edge sweep is decreasing so gradually on these modified arrow wings, this hypothesis seems to be correct and suggests an area for further study.

Airfoil bluntness.- Thus far, it has been seen that negative ΔC_A - available leading-edge thrust plus nonlinear thickness effects - has been generated on wings with linear-theory-defined subsonic and supersonic leading edges. At the heart of both of these contributions is leading-edge bluntness. A comparison of ΔC_A at $\Delta\alpha = 5.0°$ for the different values of $(r/c)_{le}$ and wing planforms is shown in figure 18. These ΔC_A values were the conservative data from figures 12 to 17, and $\Delta\alpha = 5.0°$ was selected because it was close to the $(L/D)_{max}$ point on most of the wing models. In figure 19, ΔC_A at $\Delta\alpha = 2.0°$ is also shown to examine conditions where available and full leading-edge thrust are, in theory, nearly equal. An average $(r/c)_{le}$ of 0.0005 was used for the sharp airfoil wings. Since this is an approximate value, a dashed line was sketched in figure 18 between the nonlinear ΔC_A value at $(r/c)_{le} = 0.0$ and the total ΔC_A value at $(r/c)_{le} = 0.00235$.

On the three plots (figs. 18(a) to (c)), a maximum negative ΔC_A was found in a range $0.0005 \leq (r/c)_{le} \leq 0.0010$. There are indications that this value is both Mach number and Reynolds number dependent. However, the high Reynolds number data are too sparse, the spread in wing $(r/c)_{le}$ too coarse, and the influence of test section upwash too apparent to permit definite conclusions to be made. There seems to be just enough data to suggest further studies in this area. In figure 19, ΔC_A from experiment and nonlinear theory for the arrow wings is compared over the bluntness range at Mach 1.6 and at $\Delta\alpha = 2.0°$ and $5.0°$. At $\Delta\alpha = 2.0°$, the theory curve increases much slower than at 5.0°, and fairly good agreement between predicted and measured ΔC_A is seen over a bluntness range of $0.0 < (r/c)_{le} < 0.0030$. However, at $\Delta\alpha = 5.0°$, good agreement is seen over a more restricted range of about $0.0010 < (r/c)_{le} < 0.0025$. At $(r/c)_{le} = 0.00470$, theory and experiment curves are diverging with the spread being more exaggerated at $\Delta\alpha = 5.0°$. These comparisons suggest that thrust is being lost less rapidly for sharp leading edges and the non-linear thickness effects are overestimated for subsonic leading edges and very blunt airfoils.

Another aspect of bluntness is its effect on ΔC_A at various values of $\beta \cot \Lambda_{le}$. Data for the arrow wing are plotted in figure 20 and show that the gap in ΔC_A narrows for the sharp and medium-blunt wings as $\beta \cot \Lambda_{le}$ decreases. At the same time, the magnitude of ΔC_A is increasing with decreasing $\beta \cot \Lambda_{le}$ for all the bluntness ratios tested but most rapidly for the medium-blunt airfoil. Since a decrease in $\beta \cot \Lambda_{le}$ provides a lower Mach number normal to the leading edge and a higher potential for thrust generation, the plot suggests, again, that airfoil bluntness can easily be overapplied.

Reynolds number.- It was mentioned earlier that the Reynolds number data were too sparse to permit any firm conclusions to be made. Figure 21 shows this clearly but also suggests that further gains in performance will be made for the less blunt rather than the more blunt airfoils.

Planform effects.- The purpose of the modified leading-edge wing models was to determine if leading-edge thrust benefits and attached flow could be maintained at the higher angles of attack. Comparisons of experimental ΔC_A plotted against $\Delta\alpha$ at Mach 1.6 for the two planforms are presented in figure 22. In each case, the sharp, medium-blunt, or blunt arrow wing is compared with its modified arrow wing counterpart. Mach 1.6 data only are shown because this was the design condition for the leading-edge modification. A $\Delta\alpha$ scale was used and peak ΔC_A points were overlaid on each plot so as to minimize wind-tunnel upwash effects as consistently and as effectively as possible. Since overall performance was the prime considera-tion, no attempt to isolate available leading-edge thrust or nonlinear thickness effects was made.

In all three comparisons, data at low $\Delta\alpha$ overlapped. This overlapping was unexpected for two reasons: (1) the arrow wing should produce 33 percent more theoretical leading-edge thrust than the modified arrow wing and (2) the nonlinear thickness effects were slightly less for the modified arrow wing than for the arrow wing. If production of available thrust were to explain this phenomenon, then it would follow that the arrow wing is losing thrust at a proportionally faster rate than the modified arrow wing. More likely, however, nonlinear thickness effects are increasing faster on the arrow wing than on the modified arrow wing (see fig. 11) and the net result is the approximately equal negative ΔC_A levels measured.

At the higher angles, the comparisons show that vortex generation and/or flow separation effects appear sooner on the arrow than on the modified arrow wings. The trends are noticeable although not always large and dramatic.

To the conclusions already noted, these also can be added at this point in the analysis. Very little airfoil blunting is needed to generate measurable amounts of negative ΔC_A (leading-edge thrust and nonlinear thickness effects). If bluntness is desirable for other design conditions than supersonic cruise and/or maneuver, leading-edge sweep should be locally increased, if possible, so as to keep a high percentage of full theoretical thrust. A gradual decrease in the outboard wing sweep, on the other hand, can help keep the flow attached and delay flow separation.

Lift-Drag Performance

Thus far, available leading-edge thrust and nonlinear thickness effects have been identified as the components of a negative ΔC_A increment. Since the net effect was found to be significant, these influences on the drag and the lift-drag ratio should readily be seen.

Figure 23 shows measured and predicted lift-drag polars and lift-drag ratios for the six wing models at the design Mach number of 1.6 and a Reynolds number per foot of 2.0×10^6. The theory curves were obtained from the method of reference 5. On each plot, drag increments were added to make all theory curves agree with experiment at zero lift.

In these comparisons, the experimental data were seen to be sandwiched between the linear-theory 0- and 100-percent curves except at $C_L > 0.5$ $(\alpha > 10.0°)$ where increasing flow separation seriously violates the analytical model. Between these theoretical boundaries, the nonlinear available thrust curves agree well with experiment for the medium-blunt wings (figs. 23(b) and (e)). This ageement was to be expected inasmuch as the available thrust data base was derived from similar bluntness wings and is a logical consequence of the good agreement between theory and experiment seen in figures 13(a) and 16(a).

In figures 23(a) and (d), the leading-edge thrust was conservatively underpredicted; thus the drag is overestimated and the lift-drag ratio is underestimated. Granted that the agreement between theory and experiment is not as good as for the medium-blunt wings, it must be realized that these sharp-wing theory predictions would contain no unpleasant surprises when the model was tested or the configuration was flown.

Figures 23(c) and (f) show the effects of overestimated leading-edge thrust and readily demonstrate the diminished returns from overdoing airfoil bluntness. However, a closer examination reveals that even the linear, 0-percent thrust curves agree fairly well with experiment up to about $C_L \approx 0.4$ $(\alpha \approx 8.0°)$.

The increment between experimental and zero-thrust, nonlinear theory $(L/D)_{max}$ shows the benefits accruing from small-to-moderate leading-edge blunting. These increments are as much as $\Delta(L/D)_{max} \approx 0.48$ on these models and are obtained with little or no drag penalties. Since some airfoil bluntness is desirable for various aspects of subsonic flight, it would seem logical to tailor this bluntness so as to be useful in the supersonic regime also.

CONCLUDING REMARKS

A wind-tunnel study has been performed to measure and identify the leading-edge thrust being generated on six wing models in supersonic flow and determine its effects on overall performance. Test data were measured at Mach numbers of 1.6, 1.8, 2.0, and 2.16 and at Reynolds numbers per foot of 2.0×10^6 and 5.0×10^6. Asymmetric upwash field effects were found in the axial-force data and, since they could not be readily removed at each angle of attack and Mach number condition, were compensated for by use of an angle-of-attack shift suggested by symmetry at low angle of attack.

Both leading-edge thrust and nonlinear thickness effects were hypothesized as present in the measured axial-force data. Comparisons of theory and experiment indicated that negative ΔC_A (total axial-force coefficient minus maximum axial-force coefficient) was being produced on all the wings at all the Mach numbers where subsonic and sonic leading-edge conditions exist.

Unexpectedly large amounts of negative ΔC_A were found in the sharp-wing data at both subsonic and supersonic leading-edge conditions. Analysis indicated that a leading-edge bluntness ratio from 0.0005 to 0.001 would suffice to produce benefits with minimum drag penalty.

The medium-blunt wing models produced axial-force data that were closely matched by predictions from nonlinear theory methods. However, the theory underpredicted the negative ΔC_A from sharp wings and overpredicted the negative ΔC_A from blunt wings. Lift-drag ratios predicted from both zero-thrust linear and nonlinear theory agreed fairly well with the measured blunt-wing values in the design Mach 1.6 comparisons.

Another interesting departure from theory was noted at Mach 1.8 for the sharp and medium-blunt airfoil, modified arrow wings. More negative ΔC_A was measured than full-thrust theory predicted which suggested that at this mixed subsonic-supersonic leading-edge situation, real flow effects were permitting additional negative ΔC_A to be produced.

Comparisons of experimental and theoretical values of maximum lift-drag ratio showed that available leading-edge thrust and nonlinear thickness effect benefits obtained from small to moderate leading-edge blunting could improve peak lift-drag ratio with little or no drag penalty.

Test data seemed to indicate that the arrow wing planform is more sensitive to leading-edge bluntness than the modified arrow planform. The sensitivity was especially evident in the data for the zero-lift stability parameter and the minimum drag coefficient.

Further areas of study were suggested by the results of this investigation. The first is a study of leading-edge thrust on wings with low bluntness airfoils. A second is a study of benefits accrued by varying the semispan location at which a decrease in wing sweep is initiated. A third could be an investigation of thrust generation on wings with slightly supersonic or subsonic leading edges. A fourth could be a study of leading-edge thrust at Mach numbers above 2.2. A fifth, and perhaps the most important, could be a study of Reynolds number effects both global over the wing and local at the leading edge.

Langley Research Center
National Aeronautics and Space Administration
Hampton, VA 23665
May 13, 1983

REFERENCES

1. Carlson, Harry W.: Aerodynamic Characteristics at Mach Number 2.05 of a Series of Highly Swept Arrow Wings Employing Various Degrees of Twist and Camber. NASA TM X-332, 1960.

2. Sotomayer, William A.; and Weeks, Thomas M.: A Semi-Empirical Estimate of Leading Edge Thrust For a Highly Swept Wing in Supersonic Flow. AFFDL-TM-76-63-FXM, U.S. Air Force, Sept. 1976.

3. Carlson, Harry W.; and Mack, Robert J.: Estimation of Leading-Edge Thrust for Supersonic Wings of Arbitrary Planform. NASA TP-1270, 1978.

4. Carlson, Harry W.; Mack, Robert J.; and Barger, Raymond L.: Estimation of Attainable Leading-Edge Thrust for Wings at Subsonic and Supersonic Speeds. NASA TP-1500, 1979.

5. Carlson, Harry W.; and Mack, Robert J.: Estimation of Wing Nonlinear Aerodynamic Characteristics at Supersonic Speeds. NASA TP-1718, 1980.

6. Carlson, Harry W.: Pressure Distributions at Mach Number 2.05 on a Series of Highly Swept Arrow Wings Employing Various Degrees of Twist and Camber. NASA TN D-1264, 1962.

7. Jackson, Charlie M., Jr.; Corlett, William A.; and Monta, William J.: Description and Calibration of the Langley Unitary Plan Wind Tunnel. NASA TP-1905, 1981.

TABLE I.- MODEL DIMENSIONS

(a) Wing planform parameters

	Arrow wing	Modified arrow wing
b, in.	32.648	32.648
S, in^2	300.0	300.0
x_{max}, in.	28.274	28.274
x_b, in.	21.377	21.377
x_t, in.	28.274	26.351
x_r, in.	18.378	17.638
t/c	0.04	0.04
A	3.55	3.55
Λ_{le}, deg	60	Variable (60 to 54)
$\bar{c}$, in.	12.252	11.528
r_b, in., for -		
$0 \leqslant x \leqslant 14.00$ in.	$\frac{x(28.0 - x)}{224.00}$	$\frac{x(28.0 - x)}{224.00}$
$14.00 \leqslant x \leqslant x_b$	0.875	0.875

(b) Airfoil parameters

$$\left[z/c = k_1\xi^{1/2} + k_2\xi + k_3\xi^{3/2} + k_4\xi^2\right]$$

$(r/c)_{le}$	k_1	k_2	k_3	k_4
0.0	0.0	0.12990	-0.12229	-0.00762
.00235	.06854	-.14299	.23438	-.15994
.00470	.09693	-.25603	.38212	-.22303

TABLE II.- WIND-TUNNEL TEST SCHEDULE

Model	M	$R = 2.00 \times 10^6$	$R = 5.00 \times 10^6$
Arrow wing:			
Sharp leading edge	1.6 and 1.8	X	
	2.0 and 2.16	X	X
Medium-blunt leading edge	1.6 and 1.8	X	
	2.0 and 2.16	X	X
Blunt leading edge	1.6 and 1.8	X	
	2.0 and 2.16	X	X
Modified arrow wing:			
Sharp leading edge	1.6, 1.8, 2.0, and 2.16	X	
Medium-blunt leading edge	1.6, 1.8, 2.0, and 2.16	X	
Blunt leading edge	1.6, 1.8, 2.0, and 2.16	X	

TABLE III.- FORCE COEFFICIENTS FOR ARROW WING WITH SHARP LEADING EDGE

(a) $R = 2.0 \times 10^6$; M = 1.6 and 1.8

M = 1.6

MODEL UPRIGHT

α,deg	C_N	C_A	C_L	C_D	C_m
-5.87	-.28818	.00893	-.2858	.0384	.0849
-3.84	-.19068	.01024	-.1896	.0230	.0583
-2.90	-.14607	.01115	-.1453	.0185	.0454
-1.88	-.09592	.01191	-.0955	.0151	.0303
-.82	-.04542	.01258	-.0452	.0132	.0150
.17	.00135	.01273	.0013	.0127	.0005
1.17	.05023	.01241	.0500	.0134	-.0140
2.18	.10204	.01140	.1015	.0153	-.0291
3.15	.14825	.01042	.1475	.0185	-.0436
4.14	.19789	.00928	.1967	.0235	-.0577
5.23	.25204	.00807	.2503	.0310	-.0726
6.16	.29553	.00713	.2931	.0388	-.0837
7.22	.34397	.00634	.3404	.0495	-.0948
8.18	.38526	.00579	.3805	.0606	-.1025
9.16	.42472	.00549	.4184	.0730	-.1088
10.19	.46544	.00522	.4572	.0875	-.1159
11.21	.50776	.00483	.4971	.1035	-.1246
12.18	.54692	.00448	.5337	.1198	-.1326
13.17	.58598	.00408	.5696	.1375	-.1407
14.23	.62941	.00359	.6092	.1582	-.1494
15.22	.66593	.00314	.6418	.1778	-.1568
.18	.00195	.01274	.0019	.0127	.0007

MODEL INVERTED

α,deg	C_N	C_A	C_L	C_D	C_m
6.02	.28450	.00699	.2822	.0368	-.0815
4.01	.18806	.00916	.1870	.0223	-.0556
3.06	.14327	.01029	.1425	.0179	-.0419
2.04	.09328	.01134	.0928	.0147	-.0271
1.02	.04277	.01221	.0425	.0130	-.0119
.03	-.00380	.01272	-.0038	.0127	.0020
-.99	-.05593	.01257	-.0557	.0135	.0180
-1.99	-.10346	.01184	-.1030	.0154	.0321
-2.98	-.15281	.01109	-.1520	.0190	.0468
-3.98	-.20311	.01030	-.2019	.0244	.0612
-5.00	-.25235	.00955	-.2506	.0315	.0746
-5.97	-.29634	.00890	-.2938	.0397	.0861
-6.97	-.34221	.00848	-.3387	.0499	.0967
-7.50	-.36515	.00827	-.3609	.0559	.1010
-7.93	-.38200	.00814	-.3772	.0608	.1040
-8.97	-.42352	.00817	-.4171	.0741	.1108
-9.98	-.46390	.00814	-.4555	.0884	.1174
-11.00	-.50557	.00806	-.4947	.1044	.1257
-11.98	-.54284	.00794	-.5294	.1204	.1330
-12.99	-.58413	.00779	-.5674	.1389	.1415
-13.97	-.62127	.00767	-.6010	.1574	.1493
-15.01	-.66201	.00751	-.6375	.1787	.1569

M = 1.8

MODEL UPRIGHT

α,deg	C_N	C_A	C_L	C_D	C_m
-5.78	-.25370	.00933	-.2515	.0348	.0716
-4.80	-.21254	.00982	-.2110	.0276	.0611
-3.82	-.17083	.01039	-.1698	.0217	.0500
-2.81	-.12676	.01103	-.1261	.0172	.0377
-1.81	-.08239	.01168	-.0820	.0143	.0250
-.78	-.03900	.01217	-.0388	.0127	.0123
.19	.00195	.01231	.0019	.0123	.0004
1.21	.04795	.01195	.0477	.0130	-.0128
2.20	.09030	.01126	.0898	.0147	-.0253
3.21	.13620	.01030	.1354	.0179	-.0381
4.17	.17893	.00947	.1778	.0225	-.0500
5.14	.22104	.00862	.2194	.0284	-.0615
6.18	.26437	.00782	.2620	.0362	-.0722
7.19	.30516	.00717	.3019	.0453	-.0822
8.17	.34439	.00652	.3400	.0554	-.0913
9.16	.38220	.00593	.3764	.0667	-.0999
10.21	.42132	.00534	.4137	.0799	-.1084
11.17	.45417	.00487	.4446	.0927	-.1152
12.19	.49190	.00454	.4799	.1083	-.1222
13.17	.52392	.00418	.5092	.1235	-.1272
14.15	.55426	.00425	.5364	.1396	-.1315
15.19	.58895	.00413	.5673	.1583	-.1369
16.20	.62325	.00390	.5974	.1776	-.1439
17.16	.65607	.00362	.6258	.1970	-.1504
13.20	.52566	.00421	.5108	.1241	-.1277
.17	.00193	.01227	.0019	.0123	.0003

MODEL INVERTED

α,deg	C_N	C_A	C_L	C_D	C_m
5.98	.25184	.00763	.2497	.0338	-.0694
5.00	.21211	.00841	.2106	.0269	-.0588
4.00	.16849	.00928	.1674	.0210	-.0472
3.00	.12377	.01014	.1231	.0166	-.0346
1.98	.08002	.01112	.0796	.0139	-.0220
.97	.03543	.01187	.0352	.0125	-.0094
-.02	-.00472	.01219	-.0047	.0122	.0023
-.99	-.04905	.01208	-.0488	.0129	.0152
-1.98	-.09219	.01156	-.0917	.0147	.0279
-3.01	-.13833	.01090	-.1376	.0181	.0405
-4.03	-.18368	.01030	-.1825	.0232	.0534
-5.01	-.22483	.00977	-.2231	.0294	.0641
-5.97	-.26520	.00932	-.2628	.0369	.0742
-7.01	-.30727	.00885	-.3039	.0463	.0845
-8.03	-.34657	.00850	-.3420	.0568	.0936
-8.99	-.38352	.00818	-.3775	.0680	.1018
-10.00	-.42025	.00788	-.4125	.0808	.1097
-10.99	-.45607	.00769	-.4462	.0945	.1172
-12.00	-.49057	.00752	-.4783	.1094	.1231
-12.98	-.52233	.00758	-.5073	.1247	.1278
-13.99	-.55446	.00771	-.5362	.1415	.1320
-15.01	-.58853	.00779	-.5664	.1599	.1384
-15.99	-.62047	.00772	-.5943	.1784	.1446
-17.00	-.65540	.00773	-.6245	.1990	.1518

TABLE III.- Continued

(b) $R = 2.0 \times 10^6$; $M = 2.0$ and 2.16

M = 2.0

MODEL UPRIGHT

α,deg	C_N	C_A	C_L	C_D	C_m
-5.95	-.23383	.00951	-.2316	.0337	.0642
-4.91	-.19438	.00991	-.1928	.0265	.0542
-3.94	-.15793	.01033	-.1568	.0212	.0447
-2.93	-.11780	.01090	-.1171	.0169	.0340
-1.93	-.07920	.01138	-.0788	.0140	.0230
-.95	-.04106	.01176	-.0409	.0124	.0124
.05	-.00324	.01187	-.0033	.0119	.0019
1.04	.03397	.01158	.0338	.0122	-.0084
2.06	.07658	.01108	.0761	.0138	-.0206
3.07	.11721	.01032	.1165	.0166	-.0315
4.04	.15633	.00966	.1553	.0207	-.0419
5.06	.19509	.00901	.1935	.0262	-.0519
6.04	.23272	.00841	.2305	.0328	-.0613
7.04	.26878	.00785	.2658	.0407	-.0699
8.07	.30591	.00732	.3018	.0502	-.0784
9.06	.34105	.00687	.3357	.0605	-.0862
10.04	.37489	.00642	.3680	.0717	-.0938
11.05	.40739	.00596	.3987	.0839	-.1006
12.05	.44081	.00560	.4299	.0975	-.1077
13.05	.47253	.00525	.4591	.1118	-.1141
14.05	.50278	.00496	.4865	.1269	-.1199
15.06	.53544	.00468	.5158	.1436	-.1259
16.06	.56462	.00442	.5414	.1604	-.1316
17.03	.59325	.00447	.5659	.1781	-.1354
18.01	.62032	.00436	.5886	.1959	-.1399
19.05	.65292	.00416	.6158	.2170	-.1466
20.06	.68346	.00388	.6407	.2381	-.1521

MODEL INVERTED

α,deg	C_N	C_A	C_L	C_D	C_m
6.14	.23244	.00795	.2303	.0328	-.0615
5.10	.19295	.00860	.1914	.0257	-.0518
4.14	.15579	.00926	.1547	.0205	-.0422
3.11	.11526	.01004	.1145	.0163	-.0315
2.15	.07798	.01080	.0775	.0137	-.0206
1.12	.03648	.01143	.0363	.0121	-.0093
.12	-.00037	.01175	-.0004	.0117	.0012
-.88	-.03835	.01172	-.0382	.0123	.0118
-1.88	-.07996	.01138	-.0795	.0140	.0233
-2.87	-.11996	.01091	-.1193	.0169	.0342
-3.85	-.15744	.01043	-.1564	.0210	.0443
-4.86	-.19768	.01008	-.1961	.0268	.0547
-5.87	-.23454	.00968	-.2323	.0336	.0639
-6.86	-.27142	.00937	-.2684	.0417	.0726
-7.90	-.30858	.00911	-.3044	.0514	.0808
-8.89	-.34335	.00884	-.3379	.0618	.0887
-9.88	-.37605	.00859	-.3690	.0730	.0958
-10.85	-.40806	.00843	-.3992	.0851	.1025
-11.83	-.43974	.00827	-.4287	.0983	.1091
-12.87	-.47309	.00813	-.4594	.1133	.1158
-13.89	-.50564	.00806	-.4889	.1292	.1222
-14.86	-.53441	.00797	-.5145	.1448	.1273
-15.89	-.56521	.00794	-.5414	.1624	.1329
-16.88	-.59354	.00810	-.5656	.1801	.1370
-17.85	-.62028	.00817	-.5879	.1979	.1414
-18.89	-.65318	.00820	-.6154	.2192	.1479
-19.86	-.68283	.00817	-.6394	.2397	.1535

M = 2.16

MODEL UPRIGHT

α,deg	C_N	C_A	C_L	C_D	C_m
-5.85	-.21430	.00983	-.2122	.0316	.0561
-4.86	-.17984	.01015	-.1783	.0253	.0477
-3.84	-.14294	.01054	-.1419	.0201	.0388
-2.86	-.10680	.01096	-.1061	.0163	.0295
-1.84	-.07003	.01145	-.0696	.0137	.0197
-.84	-.03366	.01173	-.0335	.0122	.0100
.16	.00079	.01175	.0008	.0118	.0009
1.16	.03610	.01150	.0359	.0122	-.0086
2.15	.07552	.01100	.0750	.0138	-.0192
3.17	.11329	.01042	.1125	.0167	-.0291
4.13	.14829	.00985	.1472	.0205	-.0384
5.15	.18501	.00931	.1834	.0259	-.0473
6.17	.22152	.00878	.2193	.0325	-.0561
7.13	.25362	.00827	.2506	.0397	-.0637
8.15	.28766	.00783	.2836	.0485	-.0714
9.15	.32112	.00744	.3159	.0584	-.0786
10.16	.35256	.00706	.3458	.0691	-.0857
11.13	.38270	.00667	.3742	.0804	-.0921
12.13	.41481	.00638	.4042	.0934	-.0990
13.17	.44623	.00604	.4331	.1075	-.1052
14.16	.47572	.00577	.4599	.1219	-.1111
15.16	.50572	.00551	.4867	.1376	-.1171
16.15	.53594	.00529	.5133	.1542	-.1229
17.17	.56532	.00504	.5386	.1717	-.1288
18.13	.59051	.00492	.5597	.1885	-.1325
19.16	.61988	.00486	.5840	.2080	-.1373
20.18	.65019	.00464	.6087	.2286	-.1433

MODEL INVERTED

α,deg	C_N	C_A	C_L	C_D	C_m
9.03	.31352	.00713	.3085	.0562	-.0768
8.05	.28152	.00753	.2777	.0469	-.0694
7.04	.24753	.00799	.2447	.0383	-.0619
6.05	.21400	.00851	.2119	.0310	-.0540
5.06	.17888	.00906	.1774	.0248	-.0457
4.05	.14232	.00964	.1413	.0197	-.0367
3.04	.10533	.01030	.1046	.0159	-.0272
2.03	.06776	.01097	.0673	.0134	-.0172
1.04	.03201	.01141	.0318	.0120	-.0077
.05	-.00331	.01165	-.0033	.0116	.0019
-.97	-.03803	.01165	-.0378	.0123	.0113
-1.97	-.07796	.01134	-.0775	.0140	.0218
-2.99	-.11559	.01095	-.1149	.0170	.0319
-3.96	-.15136	.01055	-.1503	.0210	.0409
-4.98	-.18761	.01024	-.1860	.0265	.0500
-5.95	-.22172	.00995	-.2195	.0329	.0581
-6.97	-.25752	.00968	-.2544	.0409	.0664
-7.99	-.29074	.00946	-.2866	.0498	.0740
-8.97	-.32287	.00926	-.3175	.0595	.0810
-9.97	-.35443	.00908	-.3475	.0703	.0879
-10.99	-.38666	.00892	-.3779	.0825	.0945
-11.96	-.41610	.00882	-.4052	.0949	.1008
-12.96	-.44644	.00875	-.4331	.1087	.1073
-13.96	-.47674	.00867	-.4606	.1234	.1132
-14.95	-.50605	.00860	-.4867	.1389	.1188
-15.97	-.53568	.00857	-.5126	.1556	.1246
-16.96	-.56404	.00859	-.5370	.1728	.1297

TABLE III.- Concluded

(c) $R = 5.0 \times 10^6$; $M = 2.0$ and 2.16

$M = 2.0$

MODEL UPRIGHT

α,deg	C_N	C_A	C_L	C_D	C_m
-5.83	-.22443	.00827	-.2224	.0310	.0595
-4.92	-.19245	.00876	-.1910	.0252	.0518
-3.84	-.15223	.00931	-.1513	.0195	.0418
-2.84	-.11574	.00992	-.1151	.0156	.0320
-1.80	-.07588	.01052	-.0755	.0129	.0212
-.71	-.03422	.01085	-.0341	.0113	.0101
-.05	-.00811	.01090	-.0081	.0109	.0029
1.21	.04402	.01060	.0438	.0115	-.0111
2.15	.08119	.00998	.0808	.0130	-.0212
3.15	.12027	.00918	.1196	.0158	-.0316
4.14	.15845	.00838	.1574	.0198	-.0415
5.23	.19925	.00753	.1977	.0256	-.0517
6.15	.23335	.00686	.2313	.0318	-.0598

MODEL INVERTED

α,deg	C_N	C_A	C_L	C_D	C_m
5.12	.19460	.00739	.1932	.0247	-.0510
4.17	.15986	.00818	.1588	.0198	-.0420
3.11	.11866	.00907	.1180	.0155	-.0316
2.12	.08034	.00992	.0799	.0129	-.0211
1.29	.04881	.01043	.0486	.0115	-.0125
.51	.01745	.01081	.0174	.0110	-.0040
-.52	-.02782	.01094	-.0277	.0112	.0082
-1.42	-.06591	.01078	-.0656	.0124	.0186
-1.94	-.08728	.01055	-.0869	.0135	.0243
-2.41	-.10483	.01030	-.1043	.0147	.0291
-2.91	-.12436	.01002	-.1237	.0163	.0342
-3.38	-.14283	.00974	-.1420	.0181	.0390
-3.91	-.16289	.00943	-.1619	.0205	.0442
-4.91	-.20004	.00890	-.1985	.0260	.0533
-5.93	-.23715	.00840	-.2350	.0328	.0622
-6.80	-.26764	.00799	-.2648	.0396	.0693

$M = 2.16$

MODEL UPRIGHT

α,deg	C_N	C_A	C_L	C_D	C_m
-5.79	-.21296	.00856	-.2110	.0300	.0544
-4.76	-.17865	.00899	-.1773	.0238	.0465
-3.79	-.14590	.00943	-.1450	.0191	.0384
-2.78	-.11002	.00994	-.1094	.0153	.0294
-1.85	-.07707	.01042	-.0767	.0129	.0209
-.70	-.03558	.01072	-.0354	.0112	.0101
.58	.01638	.01071	.0163	.0109	-.0035
.87	.02899	.01064	.0288	.0111	-.0069
1.18	.04148	.01052	.0413	.0114	-.0101
1.76	.06355	.01025	.0632	.0122	-.0156
2.10	.07591	.01004	.0755	.0128	-.0190
2.65	.09653	.00963	.0960	.0141	-.0244
3.28	.12025	.00914	.1195	.0160	-.0303
3.75	.13675	.00884	.1359	.0178	-.0346
4.22	.15345	.00852	.1524	.0198	-.0387
5.23	.18837	.00787	.1869	.0250	-.0472
6.18	.22096	.00730	.2189	.0310	-.0551
7.27	.25661	.00667	.2537	.0391	-.0631
8.22	.28733	.00614	.2835	.0471	-.0701

MODEL INVERTED

α,deg	C_N	C_A	C_L	C_D	C_m
6.02	.21007	.00723	.2082	.0292	-.0522
5.08	.17911	.00782	.1777	.0236	-.0448
3.99	.14165	.00856	.1407	.0184	-.0356
3.03	.10720	.00924	.1066	.0149	-.0271
1.96	.06865	.01001	.0683	.0124	-.0171
1.05	.03484	.01049	.0346	.0111	-.0083
.06	-.00313	.01079	-.0031	.0108	.0016
-1.06	-.05046	.01076	-.0502	.0117	.0139
-1.47	-.06491	.01066	-.0646	.0123	.0178
-1.98	-.08442	.01047	-.0840	.0134	.0228
-2.46	-.10169	.01024	-.1012	.0146	.0273
-3.03	-.12270	.00997	-.1220	.0164	.0325
-3.36	-.13404	.00981	-.1332	.0177	.0355
-4.05	-.15889	.00948	-.1578	.0207	.0415
-5.00	-.19123	.00908	-.1897	.0257	.0495
-6.04	-.22685	.00865	-.2247	.0325	.0580
-7.06	-.26001	.00825	-.2570	.0402	.0655
-8.07	-.29256	.00787	-.2886	.0489	.0727

TABLE IV.- FORCE COEFFICIENTS FOR ARROW WING WITH $(r/c)_{le} = 0.00235$

(a) $R = 2.0 \times 10^6$; $M = 1.6$ and 1.8

M = 1.6

MODEL UPRIGHT

α,deg	C_N	C_A	C_L	C_D	C_m
-5.02	-.23860	.00959	-.2368	.0304	.0689
-6.09	-.29034	.00871	-.2878	.0394	.0822
-4.06	-.19546	.01036	-.1942	.0242	.0565
-3.03	-.14459	.01113	-.1438	.0188	.0421
-2.03	-.09612	.01191	-.0956	.0153	.0281
-1.02	-.04648	.01266	-.0463	.0135	.0129
-.05	-.00001	.01305	-.0000	.0131	-.0009
.96	.05241	.01293	.0522	.0138	-.0167
1.91	.10182	.01239	.1013	.0158	-.0311
2.97	.15491	.01165	.1541	.0196	-.0463
3.96	.20499	.01096	.2037	.0251	-.0605
4.94	.25202	.01026	.2502	.0319	-.0732
5.93	.29817	.00969	.2956	.0404	-.0853
6.93	.34432	.00904	.3407	.0505	-.0965
7.96	.38941	.00844	.3845	.0623	-.1071
8.94	.42893	.00796	.4225	.0745	-.1143
9.95	.46798	.00754	.4596	.0883	-.1203
10.93	.50582	.00723	.4953	.1030	-.1269
11.93	.54465	.00710	.5314	.1195	-.1325
12.94	.58138	.00695	.5650	.1370	-.1390
13.90	.61738	.00668	.5977	.1548	-.1456
14.97	.65889	.00640	.6349	.1764	-.1540
15.96	.69658	.00609	.6681	.1974	-.1608

MODEL INVERTED

α,deg	C_N	C_A	C_L	C_D	C_m
5.82	.28796	.00948	.2855	.0386	-.0833
4.85	.24400	.01017	.2423	.0307	-.0710
3.81	.19509	.01084	.1939	.0238	-.0579
2.84	.14654	.01146	.1458	.0187	-.0441
1.84	.09741	.01212	.0970	.0152	-.0295
.79	.04481	.01272	.0446	.0133	-.0141
-.17	-.00128	.01294	-.0012	.0129	-.0008
-1.21	-.05748	.01254	-.0572	.0137	.0163
-2.18	-.10859	.01184	-.1081	.0160	.0312
-3.19	-.15897	.01103	-.1581	.0199	.0466
-4.20	-.20882	.01024	-.2075	.0255	.0604
-5.24	-.26042	.00941	-.2585	.0332	.0740
-6.20	-.30401	.00871	-.3013	.0415	.0859
-7.17	-.34709	.00803	-.3434	.0513	.0965
-8.17	-.39131	.00733	-.3863	.0629	.1067
-9.18	-.43281	.00673	-.4262	.0757	.1150
-10.19	-.47005	.00639	-.4615	.0895	.1198
-11.20	-.50818	.00604	-.4973	.1046	.1252
-12.18	-.54591	.00573	-.5324	.1207	.1315
-13.17	-.58146	.00537	-.5649	.1377	.1382
-14.21	-.62262	.00496	-.6024	.1576	.1457
-15.18	-.65884	.00452	-.6347	.1769	.1528
-16.19	-.69654	.00403	-.6678	.1981	.1599

M = 1.8

MODEL UPRIGHT

α,deg	C_N	C_A	C_L	C_D	C_m
-6.09	-.26265	.00944	-.2602	.0372	.0723
-5.04	-.22047	.00991	-.2187	.0293	.0616
-4.03	-.17669	.01051	-.1755	.0229	.0503
-3.08	-.13647	.01102	-.1357	.0183	.0393
-2.08	-.09169	.01154	-.0912	.0149	.0263
-1.05	-.04547	.01207	-.0452	.0129	.0125
-.10	-.00336	.01235	-.0033	.0124	.0007
.96	.04982	.01230	.0496	.0131	-.0146
1.93	.09503	.01199	.0946	.0152	-.0277
2.96	.14281	.01158	.1420	.0189	-.0412
3.93	.18517	.01120	.1840	.0239	-.0526
4.94	.22860	.01074	.2268	.0304	-.0642
5.94	.27063	.01028	.2681	.0382	-.0744
6.93	.30999	.00988	.3065	.0472	-.0841
7.95	.35001	.00947	.3453	.0578	-.0932
8.93	.38733	.00904	.3812	.0691	-.1019
9.93	.42413	.00868	.4163	.0817	-.1098
10.94	.46075	.00827	.4508	.0956	-.1172
11.91	.49388	.00790	.4816	.1097	-.1229
12.91	.52567	.00770	.5107	.1250	-.1265
13.99	.55943	.00761	.5410	.1426	-.1311
14.95	.59231	.00743	.5704	.1599	-.1373
15.95	.62513	.00722	.5991	.1788	-.1435
16.90	.65668	.00700	.6263	.1976	-.1496
17.94	.69087	.00674	.6552	.2192	-.1559

MODEL INVERTED

α,deg	C_N	C_A	C_L	C_D	C_m
5.79	.25657	.01015	.2542	.0360	-.0711
4.78	.21579	.01063	.2137	.0285	-.0609
3.78	.17365	.01106	.1725	.0225	-.0495
2.80	.12996	.01146	.1292	.0178	-.0379
1.78	.08501	.01190	.0846	.0145	-.0250
.79	.03963	.01226	.0395	.0128	-.0117
-.24	-.00479	.01238	-.0047	.0124	.0009
-1.25	-.05606	.01207	-.0558	.0133	.0157
-2.23	-.10168	.01164	-.1012	.0156	.0294
-3.20	-.14602	.01110	-.1452	.0192	.0419
-4.23	-.19066	.01060	-.1894	.0246	.0539
-5.27	-.23606	.01004	-.2341	.0317	.0657
-6.26	-.27568	.00954	-.2730	.0396	.0758
-7.18	-.31236	.00904	-.3088	.0480	.0842
-8.20	-.35302	.00850	-.3482	.0588	.0940
-9.24	-.39256	.00797	-.3862	.0709	.1027
-10.25	-.42937	.00747	-.4212	.0837	.1107
-11.22	-.46281	.00698	-.4526	.0969	.1173
-12.23	-.49776	.00652	-.4851	.1119	.1229
-13.25	-.52934	.00623	-.5138	.1274	.1272
-14.21	-.56017	.00597	-.5416	.1433	.1322
-15.22	-.59311	.00573	-.5708	.1613	.1370
-16.26	-.62791	.00540	-.6013	.1810	.1434
-17.28	-.66119	.00501	-.6299	.2011	.1500
-18.21	-.69195	.00466	-.6558	.2207	.1554

TABLE IV.- Continued

(b) $R = 2.0 \times 10^{6}$; $M = 2.0$ and 2.16

M = 2.0

MODEL UPRIGHT

α,deg	C_N	C_A	C_L	C_D	C_m
-6.31	-.24398	.00996	-.2414	.0367	.0646
-5.31	-.20784	.01036	-.2060	.0296	.0560
-4.27	-.16852	.01078	-.1672	.0233	.0460
-3.27	-.12984	.01117	-.1290	.0186	.0358
-2.27	-.09038	.01153	-.0898	.0151	.0251
-1.24	-.04876	.01183	-.0485	.0129	.0137
-.28	-.00973	.01196	-.0097	.0120	.0027
.76	.03295	.01205	.0328	.0125	-.0096
1.74	.07863	.01201	.0782	.0144	-.0222
2.75	.12064	.01186	.1199	.0176	-.0336
3.74	.15944	.01161	.1583	.0220	-.0437
4.75	.19906	.01128	.1974	.0277	-.0537
5.71	.23431	.01095	.2321	.0342	-.0622
6.73	.27117	.01060	.2681	.0423	-.0711
7.71	.30552	.01024	.3014	.0511	-.0785
8.73	.34117	.00994	.3357	.0616	-.0864
9.75	.37687	.00963	.3698	.0733	-.0940
10.73	.40864	.00933	.3998	.0853	-.1011
11.70	.44064	.00908	.4296	.0982	-.1079
12.70	.47286	.00874	.4594	.1125	-.1140
13.73	.50463	.00847	.4882	.1280	-.1200
14.74	.53452	.00825	.5148	.1440	-.1243
15.72	.56227	.00812	.5391	.1601	-.1281
16.70	.59224	.00791	.5650	.1778	-.1337
17.78	.62565	.00767	.5934	.1984	-.1403
18.71	.65376	.00749	.6168	.2168	-.1454
19.75	.68569	.00721	.6429	.2385	-.1513

MODEL INVERTED

α,deg	C_N	C_A	C_L	C_D	C_m
6.05	.24129	.01065	.2388	.0360	-.0641
5.04	.20456	.01100	.2028	.0289	-.0553
4.04	.16696	.01132	.1657	.0231	-.0457
3.03	.12756	.01157	.1268	.0183	-.0354
1.99	.08491	.01182	.0844	.0148	-.0241
1.01	.04547	.01196	.0453	.0128	-.0130
.00	.00429	.01202	.0043	.0120	-.0012
-.98	-.03781	.01195	-.0376	.0126	.0109
-2.00	-.08424	.01172	-.0838	.0147	.0236
-2.95	-.12195	.01148	-.1212	.0177	.0338
-3.95	-.16161	.01110	-.1605	.0222	.0444
-4.99	-.20115	.01072	-.1995	.0282	.0542
-5.99	-.23929	.01028	-.2369	.0352	.0636
-7.00	-.27596	.00983	-.2727	.0434	.0721
-7.98	-.31098	.00943	-.3067	.0525	.0801
-8.98	-.34478	.00902	-.3391	.0627	.0876
-10.00	-.37970	.00863	-.3724	.0745	.0949
-11.00	-.41263	.00821	-.4035	.0868	.1019
-11.97	-.44395	.00787	-.4327	.0998	.1086
-12.97	-.47630	.00745	-.4625	.1142	.1154
-14.01	-.50784	.00706	-.4910	.1298	.1205
-14.97	-.53588	.00678	-.5159	.1450	.1249
-16.00	-.56518	.00655	-.5415	.1620	.1284
-16.98	-.59474	.00622	-.5670	.1797	.1340
-18.01	-.62672	.00595	-.5942	.1994	.1400
-18.95	-.65484	.00557	-.6175	.2179	.1454
-19.97	-.68558	.00518	-.6426	.2390	.1512

M = 2.16

MODEL UPRIGHT

α,deg	C_N	C_A	C_L	C_D	C_m
-6.04	-.21556	.01031	-.2133	.0329	.0559
-5.01	-.18042	.01065	-.1788	.0264	.0476
-4.04	-.14698	.01097	-.1458	.0213	.0391
-3.03	-.11189	.01124	-.1111	.0171	.0300
-2.04	-.07524	.01151	-.0748	.0142	.0204
-1.02	-.03740	.01173	-.0372	.0124	.0104
-.03	.00023	.01184	.0002	.0118	.0001
.97	.03818	.01191	.0380	.0126	-.0106
1.96	.07913	.01193	.0787	.0146	-.0214
2.96	.11693	.01181	.1162	.0178	-.0312
4.01	.15449	.01166	.1533	.0224	-.0408
4.96	.18887	.01141	.1872	.0277	-.0494
5.98	.22389	.01115	.2215	.0344	-.0576
6.99	.25758	.01083	.2544	.0421	-.0654
7.98	.28899	.01056	.2847	.0506	-.0722
9.00	.32195	.01033	.3164	.0605	-.0791
9.98	.35337	.01008	.3463	.0712	-.0862
11.00	.38529	.00984	.3763	.0831	-.0930
12.00	.41612	.00960	.4050	.0959	-.0996
12.98	.44569	.00932	.4322	.1092	-.1057
13.99	.47763	.00907	.4613	.1243	-.1124
14.99	.50603	.00884	.4865	.1394	-.1177
15.99	.53411	.00867	.5111	.1554	-.1216
17.00	.56226	.00844	.5352	.1725	-.1266
18.02	.59296	.00820	.5613	.1912	-.1323
18.99	.62145	.00799	.5850	.2098	-.1380
19.97	.65025	.00772	.6085	.2294	-.1436

MODEL INVERTED

α,deg	C_N	C_A	C_L	C_D	C_m
5.76	.20948	.01092	.2073	.0319	-.0542
4.76	.17492	.01118	.1734	.0256	-.0459
3.79	.14150	.01143	.1404	.0208	-.0375
2.78	.10568	.01163	.1050	.0167	-.0283
1.77	.06865	.01176	.0683	.0139	-.0185
.77	.03082	.01182	.0307	.0122	-.0084
-.24	-.00718	.01182	-.0071	.0118	.0021
-1.25	-.04639	.01177	-.0461	.0128	.0128
-2.23	-.08619	.01163	-.0857	.0150	.0234
-3.21	-.12201	.01143	-.1212	.0182	.0329
-4.24	-.15984	.01113	-.1586	.0229	.0424
-5.22	-.19440	.01081	-.1926	.0284	.0509
-6.26	-.23023	.01045	-.2277	.0355	.0596
-7.23	-.26285	.01011	-.2595	.0431	.0670
-8.25	-.29636	.00971	-.2919	.0522	.0745
-9.23	-.32704	.00942	-.3213	.0617	.0810
-10.24	-.35909	.00909	-.3517	.0728	.0881
-11.24	-.38996	.00879	-.3808	.0846	.0947
-12.25	-.42123	.00842	-.4098	.0976	.1010
-13.24	-.45055	.00808	-.4367	.1111	.1069
-14.25	-.48222	.00775	-.4655	.1262	.1138
-15.23	-.51003	.00742	-.4902	.1411	.1187
-16.25	-.53775	.00715	-.5143	.1573	.1229
-17.23	-.56576	.00688	-.5383	.1742	.1275
-18.26	-.59503	.00659	-.5630	.1927	.1329
-19.24	-.62399	.00622	-.5871	.2115	.1386
-20.25	-.65416	.00577	-.6117	.2318	.1445

TABLE IV.- Concluded

(c) $R = 5.0 \times 10^6$; M = 2.0 and 2.16

M = 2.0

MODEL UPRIGHT

α,deg	C_N	C_A	C_L	C_D	C_m
-6.09	-.22996	.00883	-.2277	.0332	.0600
-5.24	-.20054	.00923	-.1989	.0275	.0527
-4.02	-.15569	.00983	-.1546	.0207	.0414
-3.10	-.12130	.01022	-.1206	.0168	.0324
-2.16	-.08521	.01059	-.0848	.0138	.0230
-1.01	-.03952	.01096	-.0393	.0117	.0106
-.35	-.01231	.01103	-.0122	.0111	.0029
.79	.03861	.01110	.0385	.0116	-.0111
2.00	.08942	.01093	.0890	.0140	-.0248
2.95	.12688	.01064	.1262	.0172	-.0346
3.86	.16125	.01034	.1602	.0212	-.0435
4.95	.20136	.00991	.1998	.0272	-.0536
5.90	.23627	.00950	.2340	.0337	-.0620

MODEL INVERTED

α,deg	C_N	C_A	C_L	C_D	C_m
5.94	.23381	.00933	.2316	.0335	-.0616
4.93	.19780	.00976	.1962	.0267	-.0528
3.83	.15717	.01020	.1561	.0207	-.0427
2.95	.12424	.01052	.1235	.0169	-.0341
1.89	.08291	.01083	.0825	.0136	-.0231
.78	.03681	.01105	.0367	.0115	-.0107
-.13	-.00137	.01110	-.0013	.0111	.0001
-1.03	-.04144	.01095	-.0412	.0117	.0110
-2.06	-.08428	.01072	-.0838	.0137	.0228
-3.10	-.12453	.01034	-.1238	.0171	.0334
-4.22	-.16681	.00987	-.1656	.0221	.0441
-5.07	-.19810	.00948	-.1965	.0270	.0520
-6.26	-.24029	.00889	-.2379	.0350	.0620

M = 2.16

MODEL UPRIGHT

α,deg	C_N	C_A	C_L	C_D	C_m
-6.97	-.24213	.00893	-.2393	.0382	.0603
-5.91	-.20808	.00938	-.2060	.0307	.0524
-4.96	-.17676	.00974	-.1753	.0250	.0449
-3.95	-.14206	.01009	-.1410	.0199	.0364
-2.97	-.10825	.01043	-.1076	.0160	.0280
-1.99	-.07314	.01074	-.0727	.0133	.0190
-.96	-.03544	.01096	-.0353	.0116	.0091
.13	.00811	.01112	.0081	.0111	-.0025
1.08	.04742	.01114	.0472	.0120	-.0130
2.02	.08258	.01103	.0821	.0139	-.0223
3.03	.11887	.01080	.1181	.0171	-.0315
4.08	.15529	.01051	.1541	.0215	-.0407
4.98	.18677	.01024	.1852	.0264	-.0484
6.09	.22449	.00987	.2222	.0336	-.0574
7.05	.25545	.00950	.2523	.0408	-.0647
8.09	.28853	.00910	.2844	.0496	-.0721

MODEL INVERTED

α,deg	C_N	C_A	C_L	C_D	C_m
7.72	.27332	.00915	.2696	.0458	-.0681
6.75	.24268	.00951	.2399	.0380	-.0611
5.72	.20927	.00986	.2072	.0307	-.0535
4.69	.17434	.01020	.1729	.0244	-.0453
3.65	.13857	.01050	.1376	.0193	-.0364
2.63	.10226	.01076	.1017	.0154	-.0273
1.70	.06880	.01094	.0684	.0130	-.0186
.65	.02977	.01105	.0296	.0114	-.0083
-.21	-.00498	.01108	-.0049	.0111	.0010
-1.35	-.05238	.01098	-.0521	.0122	.0136
-2.37	-.08998	.01073	-.0895	.0144	.0233
-3.35	-.12428	.01044	-.1235	.0177	.0321
-4.32	-.15835	.01012	-.1571	.0220	.0407
-5.36	-.19279	.00973	-.1910	.0277	.0492
-6.37	-.22717	.00931	-.2247	.0345	.0572
-7.39	-.25959	.00887	-.2563	.0422	.0648
-8.38	-.29105	.00841	-.2867	.0507	.0718

TABLE V.- FORCE COEFFICIENTS FOR ARROW WING WITH $(r/c)_{le} = 0.00470$

(a) $R = 2.0 \times 10^6$; $M = 1.6$ and 1.8

$M = 1.6$

MODEL UPRIGHT

α,deg	C_N	C_A	C_L	C_D	C_m
-6.08	-.29791	.00914	-.2953	.0407	.0778
-5.09	-.25273	.00987	-.2509	.0323	.0668
-4.07	-.20248	.01063	-.2012	.0250	.0542
-3.00	-.14894	.01137	-.1481	.0191	.0403
-2.04	-.10160	.01199	-.1011	.0156	.0271
-1.04	-.04996	.01266	-.0497	.0136	.0127
-.05	-.00265	.01302	-.0026	.0130	-.0006
.93	.04998	.01308	.0498	.0139	-.0144
1.97	.10493	.01297	.1044	.0166	-.0297
2.96	.15475	.01270	.1539	.0207	-.0432
3.95	.20445	.01227	.2031	.0263	-.0564
4.93	.25256	.01189	.2506	.0335	-.0685
5.93	.29894	.01156	.2962	.0424	-.0796
6.93	.34512	.01105	.3413	.0526	-.0897
7.99	.39403	.01055	.3887	.0652	-.1001
8.98	.43374	.01010	.4268	.0777	-.1066
9.97	.47144	.00989	.4626	.0914	-.1113
10.95	.50710	.00966	.4960	.1058	-.1161
11.96	.54522	.00940	.5314	.1222	-.1209
12.95	.58251	.00928	.5656	.1396	-.1264
13.97	.62264	.00900	.6021	.1590	-.1339
14.95	.65872	.00867	.6342	.1783	-.1403

MODEL INVERTED

α,deg	C_N	C_A	C_L	C_D	C_m
5.83	.29127	.01120	.2886	.0407	-.0782
4.89	.24715	.01158	.2453	.0326	-.0673
3.84	.19789	.01200	.1966	.0252	-.0547
2.86	.14879	.01234	.1480	.0198	-.0418
1.87	.09840	.01263	.0979	.0158	-.0281
.84	.04535	.01283	.0452	.0135	-.0133
-.14	-.00351	.01292	-.0035	.0129	-.0002
-1.16	-.05693	.01256	-.0567	.0137	.0148
-2.12	-.10774	.01200	-.1072	.0160	.0286
-3.17	-.16058	.01135	-.1597	.0202	.0432
-4.21	-.21337	.01066	-.2120	.0263	.0569
-5.15	-.25814	.00998	-.2562	.0331	.0683
-6.20	-.30798	.00927	-.3052	.0425	.0796
-7.15	-.34985	.00848	-.3461	.0519	.0888
-8.11	-.38983	.00784	-.3848	.0628	.0970
-9.17	-.43617	.00710	-.4295	.0765	.1058
-10.17	-.47588	.00648	-.4673	.0904	.1122
-11.16	-.51048	.00604	-.4997	.1047	.1152
-12.12	-.54683	.00561	-.5335	.1203	.1200
-13.18	-.58571	.00523	-.5691	.1387	.1253
-14.11	-.62040	.00476	-.6005	.1559	.1315
-15.17	-.66209	.00410	-.6379	.1772	.1387
-16.16	-.69738	.00346	-.6689	.1974	.1447

$M = 1.8$

MODEL UPRIGHT

α,deg	C_N	C_A	C_L	C_D	C_m
-6.04	-.26381	.01001	-.2613	.0377	.0664
-5.04	-.22334	.01048	-.2216	.0301	.0572
-4.02	-.17948	.01103	-.1783	.0236	.0466
-3.03	-.13647	.01145	-.1357	.0187	.0357
-2.05	-.09312	.01187	-.0926	.0152	.0245
-1.04	-.04740	.01217	-.0472	.0130	.0122
-.01	.00092	.01245	.0009	.0124	-.0008
.96	.04962	.01259	.0494	.0134	-.0144
1.97	.09679	.01265	.0963	.0160	-.0271
2.99	.14238	.01260	.1415	.0200	-.0388
4.01	.18677	.01249	.1854	.0255	-.0500
4.96	.22822	.01228	.2263	.0320	-.0599
5.98	.27063	.01205	.2679	.0402	-.0697
7.00	.31104	.01179	.3073	.0496	-.0784
8.00	.35011	.01152	.3451	.0601	-.0867
8.98	.38759	.01126	.3811	.0716	-.0944
9.98	.42430	.01089	.4160	.0842	-.1015
10.99	.46025	.01056	.4498	.0981	-.1082
11.94	.49368	.01025	.4809	.1122	-.1136
12.96	.52584	.01007	.5102	.1278	-.1171
13.98	.55598	.00984	.5371	.1438	-.1196
15.01	.59152	.00966	.5688	.1625	-.1251
15.98	.62345	.00937	.5968	.1806	-.1306
16.99	.65845	.00910	.6270	.2011	-.1369

MODEL INVERTED

α,deg	C_N	C_A	C_L	C_D	C_m
5.84	.26049	.01190	.2579	.0383	-.0671
4.83	.21984	.01215	.2180	.0306	-.0575
3.87	.17819	.01230	.1770	.0243	-.0479
2.87	.13473	.01239	.1339	.0191	-.0369
1.84	.08932	.01250	.0889	.0154	-.0250
.89	.04460	.01250	.0444	.0132	-.0130
-.14	-.00464	.01243	-.0046	.0124	.0004
-1.15	-.05441	.01220	-.0542	.0133	.0142
-2.12	-.09954	.01192	-.0990	.0156	.0266
-3.11	-.14334	.01158	-.1425	.0193	.0379
-4.17	-.19050	.01115	-.1892	.0250	.0495
-5.19	-.23342	.01063	-.2315	.0317	.0597
-6.16	-.27335	.01013	-.2707	.0394	.0688
-7.17	-.31301	.00960	-.3094	.0486	.0777
-8.13	-.34991	.00910	-.3451	.0585	.0854
-9.16	-.38975	.00856	-.3834	.0705	.0934
-10.13	-.42486	.00801	-.4168	.0826	.1003
-11.16	-.46147	.00738	-.4513	.0966	.1064
-12.13	-.49421	.00686	-.4817	.1106	.1118
-13.17	-.52857	.00632	-.5132	.1266	.1168
-14.17	-.56193	.00583	-.5434	.1432	.1213
-15.16	-.59210	.00541	-.5701	.1601	.1250
-16.13	-.62188	.00514	-.5960	.1777	.1287
-17.16	-.65897	.00468	-.6282	.1989	.1352

TABLE V.- Continued

(b) $R = 2.0 \times 10^6$; $M = 2.0$ and 2.16

M = 2.0

MODEL UPRIGHT

α,deg	C_N	C_A	C_L	C_D	C_m
-6.14	-.23893	.01048	-.2364	.0360	.0586
-5.14	-.20253	.01087	-.2007	.0290	.0504
-4.15	-.16581	.01122	-.1646	.0232	.0416
-3.07	-.12407	.01156	-.1233	.0182	.0314
-2.09	-.08543	.01182	-.0849	.0149	.0217
-1.14	-.04624	.01204	-.0460	.0130	.0118
-.13	-.00403	.01221	-.0040	.0122	.0004
.93	.04154	.01243	.0413	.0131	-.0120
1.88	.08304	.01262	.0826	.0153	-.0227
2.86	.12241	.01271	.1216	.0188	-.0326
3.89	.16299	.01272	.1618	.0237	-.0422
4.89	.20072	.01266	.1989	.0297	-.0511
5.89	.23777	.01251	.2352	.0368	-.0596
6.88	.27431	.01235	.2708	.0451	-.0673
7.90	.30942	.01217	.3048	.0546	-.0746
8.88	.34318	.01197	.3372	.0648	-.0810
9.90	.37712	.01177	.3695	.0764	-.0875
10.89	.41046	.01151	.4009	.0889	-.0938
11.89	.44281	.01130	.4310	.1023	-.0997
12.87	.47456	.01108	.4602	.1165	-.1057
13.93	.50683	.01079	.4893	.1325	-.1112
14.88	.53265	.01063	.5121	.1471	-.1134
15.87	.56241	.01042	.5381	.1638	-.1172
16.88	.59369	.01013	.5652	.1821	-.1226
17.89	.62450	.00985	.5913	.2012	-.1278
18.88	.65501	.00954	.6167	.2210	-.1332
19.89	.68608	.00927	.6420	.2421	-.1383

MODEL INVERTED

α,deg	C_N	C_A	C_L	C_D	C_m
5.96	.23603	.01214	.2335	.0366	-.0594
4.93	.19891	.01230	.1971	.0294	-.0508
3.97	.16270	.01238	.1615	.0236	-.0421
2.93	.12218	.01240	.1214	.0186	-.0325
1.95	.08447	.01240	.0840	.0153	-.0228
.94	.04249	.01231	.0423	.0130	-.0122
-.07	-.00051	.01221	-.0005	.0122	-.0005
-1.06	-.04238	.01213	-.0421	.0129	.0108
-2.04	-.08550	.01204	-.0850	.0151	.0221
-3.06	-.12666	.01181	-.1258	.0186	.0320
-4.04	-.16434	.01154	-.1631	.0231	.0412
-5.04	-.20206	.01120	-.2003	.0289	.0501
-6.05	-.23951	.01086	-.2370	.0360	.0585
-7.06	-.27566	.01048	-.2723	.0443	.0664
-8.08	-.31217	.01006	-.3077	.0538	.0737
-9.07	-.34658	.00964	-.3407	.0642	.0805
-10.07	-.37889	.00920	-.3715	.0753	.0866
-11.06	-.41178	.00875	-.4025	.0876	.0927
-12.05	-.44352	.00832	-.4320	.1008	.0984
-13.05	-.47603	.00787	-.4619	.1152	.1045
-14.07	-.50908	.00734	-.4920	.1309	.1109
-15.08	-.53879	.00688	-.5184	.1468	.1149
-16.05	-.56406	.00652	-.5403	.1622	.1175
-17.05	-.59376	.00614	-.5658	.1800	.1212
-18.09	-.62657	.00567	-.5938	.2000	.1265
-19.07	-.65514	.00520	-.6175	.2190	.1315
-20.07	-.68563	.00469	-.6424	.2397	.1366

M = 2.16

MODEL UPRIGHT

α,deg	C_N	C_A	C_L	C_D	C_m
-6.10	-.21900	.01092	-.2166	.0341	.0517
-5.06	-.18354	.01124	-.1818	.0274	.0438
-4.07	-.14961	.01150	-.1484	.0221	.0360
-3.07	-.11339	.01175	-.1126	.0178	.0277
-2.06	-.07601	.01196	-.0755	.0147	.0188
-1.05	-.03786	.01217	-.0376	.0129	.0090
-1.10	-.03981	.01214	-.0396	.0129	.0095
-.09	-.00172	.01232	-.0017	.0123	-.0001
.95	.03769	.01248	.0375	.0131	-.0102
1.92	.07759	.01266	.0771	.0153	-.0203
2.92	.11483	.01280	.1140	.0186	-.0294
3.91	.15060	.01285	.1494	.0231	-.0378
4.91	.18578	.01280	.1840	.0287	-.0458
5.91	.22092	.01269	.2184	.0354	-.0537
6.93	.25546	.01260	.2521	.0433	-.0610
7.95	.28944	.01249	.2849	.0524	-.0678
8.91	.31977	.01236	.3140	.0617	-.0739
9.94	.35263	.01219	.3452	.0729	-.0800
10.93	.38357	.01201	.3743	.0845	-.0860
11.91	.41415	.01187	.4028	.0971	-.0918
12.93	.44487	.01167	.4310	.1109	-.0976
13.92	.47520	.01149	.4585	.1255	-.1031
14.92	.50460	.01125	.4847	.1408	-.1080
15.95	.53401	.01101	.5104	.1574	-.1117
16.94	.56096	.01072	.5335	.1737	-.1158
17.92	.58967	.01050	.5578	.1914	-.1203
18.94	.62083	.01024	.5839	.2112	-.1257

MODEL INVERTED

α,deg	C_N	C_A	C_L	C_D	C_m
5.90	.21731	.01240	.2149	.0347	-.0526
4.94	.18401	.01251	.1822	.0283	-.0452
3.89	.14685	.01256	.1457	.0225	-.0369
2.91	.11214	.01256	.1114	.0182	-.0288
1.91	.07484	.01249	.0744	.0150	-.0197
.89	.03672	.01240	.0365	.0130	-.0098
-.08	-.00069	.01234	-.0007	.0123	-.0005
-1.10	-.03955	.01225	-.0393	.0130	.0093
-2.11	-.08069	.01216	-.0802	.0151	.0197
-3.07	-.11618	.01199	-.1154	.0182	.0284
-4.09	-.15254	.01178	-.1513	.0226	.0370
-5.12	-.18944	.01151	-.1877	.0284	.0453
-6.10	-.22286	.01123	-.2204	.0348	.0527
-7.10	-.25708	.01092	-.2538	.0426	.0599
-8.13	-.29091	.01057	-.2865	.0516	.0670
-9.11	-.32285	.01023	-.3172	.0612	.0733
-10.10	-.35368	.00987	-.3465	.0717	.0792
-11.12	-.38482	.00946	-.3758	.0835	.0849
-12.12	-.41656	.00906	-.4054	.0964	.0907
-13.12	-.44633	.00866	-.4327	.1097	.0964
-14.10	-.47579	.00827	-.4595	.1239	.1018
-15.12	-.50595	.00783	-.4864	.1395	.1071
-16.12	-.53348	.00745	-.5104	.1553	.1101
-17.11	-.56066	.00708	-.5338	.1717	.1141
-18.12	-.59054	.00660	-.5592	.1899	.1190
-19.12	-.62041	.00617	-.5842	.2091	.1240
-20.12	-.64886	.00568	-.6073	.2285	.1291

TABLE V.- Concluded

(c) $R = 5.0 \times 10^6$; M = 2.0 and 2.16

M = 2.0

MODEL UPRIGHT

α,deg	C_N	C_A	C_L	C_D	C_m
-6.06	-.23310	.00928	-.2308	.0338	.0557
-4.98	-.19460	.00981	-.1930	.0267	.0472
-4.14	-.16464	.01021	-.1635	.0221	.0402
-3.00	-.12094	.01064	-.1202	.0169	.0301
-2.09	-.08522	.01096	-.0848	.0141	.0213
-1.20	-.04931	.01119	-.0491	.0122	.0122
.02	.00284	.01145	.0028	.0114	-.0015
.74	.03364	.01153	.0335	.0120	-.0094
1.70	.07528	.01170	.0749	.0139	-.0201
2.82	.11988	.01172	.1192	.0176	-.0311
3.80	.15771	.01162	.1566	.0220	-.0399
4.97	.20202	.01146	.2003	.0289	-.0500
5.99	.23898	.01117	.2365	.0361	-.0579
6.99	.27415	.01086	.2708	.0441	-.0653

MODEL INVERTED

α,deg	C_N	C_A	C_L	C_D	C_m
5.95	.23440	.01086	.2320	.0351	-.0572
4.86	.19588	.01117	.1942	.0277	-.0488
3.74	.15358	.01141	.1525	.0214	-.0390
2.98	.12451	.01155	.1237	.0180	-.0322
1.88	.08131	.01151	.0809	.0142	-.0216
1.08	.04840	.01154	.0482	.0124	-.0131
-.12	-.00320	.01142	-.0032	.0114	.0002
-1.09	-.04515	.01129	-.0449	.0121	.0111
-2.11	-.08817	.01113	-.0877	.0144	.0219
-3.05	-.12530	.01087	-.1245	.0175	.0309
-4.05	-.16292	.01050	-.1618	.0220	.0399
-5.06	-.20048	.01006	-.1988	.0277	.0484
-6.03	-.23578	.00957	-.2335	.0343	.0562

M = 2.16

MODEL UPRIGHT

α,deg	C_N	C_A	C_L	C_D	C_m
-6.80	-.24236	.00936	-.2395	.0380	.0552
-5.85	-.21173	.00974	-.2096	.0313	.0487
-4.83	-.17721	.01013	-.1757	.0250	.0413
-3.90	-.14474	.01048	-.1437	.0203	.0340
-2.92	-.10995	.01076	-.1093	.0163	.0261
-1.89	-.07234	.01102	-.0719	.0134	.0170
-.89	-.03384	.01123	-.0337	.0118	.0077
.17	.00709	.01143	.0071	.0115	-.0026
1.15	.04742	.01158	.0472	.0125	-.0124
2.11	.08435	.01166	.0839	.0148	-.0214
3.10	.12043	.01172	.1196	.0182	-.0300
4.10	.15569	.01168	.1545	.0228	-.0381
5.11	.19109	.01155	.1893	.0285	-.0461
6.09	.22416	.01136	.2217	.0351	-.0532
7.12	.25824	.01109	.2549	.0430	-.0605

MODEL INVERTED

α,deg	C_N	C_A	C_L	C_D	C_m
6.72	.24224	.01112	.2393	.0394	-.0566
5.73	.21054	.01134	.2084	.0323	-.0498
4.70	.17555	.01152	.1740	.0259	-.0423
3.72	.14174	.01162	.1407	.0208	-.0348
2.78	.10786	.01166	.1072	.0169	-.0270
1.69	.06832	.01163	.0679	.0136	-.0176
.73	.03063	.01156	.0305	.0120	-.0084
-.11	-.00240	.01151	-.0024	.0115	-.0001
-1.31	-.05147	.01138	-.0512	.0126	.0119
-2.22	-.08528	.01121	-.0848	.0145	.0203
-3.38	-.12753	.01095	-.1267	.0184	.0302
-4.25	-.15807	.01069	-.1568	.0224	.0373
-5.21	-.19086	.01036	-.1891	.0277	.0448
-6.28	-.22711	.00993	-.2247	.0347	.0525
-7.27	-.26002	.00948	-.2567	.0423	.0594

TABLE VI.- FORCE COEFFICIENTS FOR MODIFIED ARROW WING WITH SHARP LEADING EDGE

(a) $R = 2.0 \times 10^6$; M = 1.6 and 1.8

M = 1.6

MODEL UPRIGHT

α,deg	C_N	C_A	C_L	C_D	C_m
-5.85	-.29671	.00857	-.2943	.0388	.0855
-4.86	-.24812	.00943	-.2464	.0304	.0728
-3.85	-.19872	.01029	-.1976	.0236	.0593
-2.80	-.14529	.01127	-.1446	.0184	.0441
-1.86	-.09845	.01213	-.0980	.0153	.0297
-.81	-.04754	.01284	-.0474	.0135	.0143
.13	-.00283	.01310	-.0029	.0131	.0007
1.09	.04524	.01278	.0450	.0136	-.0130
2.13	.09737	.01192	.0969	.0155	-.0283
3.17	.15061	.01081	.1498	.0191	-.0443
4.12	.19942	.00980	.1982	.0241	-.0585
5.16	.25298	.00867	.2512	.0314	-.0727
6.12	.29870	.00769	.2962	.0395	-.0849
7.14	.34826	.00668	.3447	.0499	-.0968
8.17	.39394	.00590	.3891	.0618	-.1074
9.14	.43431	.00521	.4280	.0741	-.1146
10.18	.47650	.00471	.4682	.0888	-.1205
11.15	.51404	.00443	.5035	.1037	-.1260
12.18	.55336	.00441	.5400	.1210	-.1311
13.13	.58974	.00418	.5734	.1381	-.1370
14.12	.62915	.00378	.6092	.1572	-.1447
15.14	.66886	.00332	.6448	.1779	-.1522

MODEL INVERTED

α,deg	C_N	C_A	C_L	C_D	C_m
6.14	.29563	.00747	.2931	.0390	-.0845
5.09	.24438	.00853	.2427	.0302	-.0713
4.07	.19354	.00967	.1924	.0234	-.0569
3.07	.14287	.01078	.1421	.0184	-.0421
2.11	.09558	.01177	.0951	.0153	-.0278
1.06	.04185	.01267	.0416	.0134	-.0121
.10	-.00034	.01300	-.0004	.0130	.0004
-.86	-.05127	.01289	-.0511	.0137	.0156
-1.90	-.10270	.01216	-.1022	.0156	.0307
-2.94	-.15746	.01125	-.1567	.0193	.0470
-3.88	-.20364	.01038	-.2025	.0242	.0605
-4.87	-.25376	.00947	-.2520	.0310	.0738
-5.90	-.30237	.00865	-.2999	.0397	.0865
-7.91	-.39184	.00729	-.3871	.0611	.1055
-9.91	-.47418	.00657	-.4660	.0880	.1185
-11.94	-.55432	.00633	-.5410	.1209	.1310
-13.91	-.63208	.00565	-.6122	.1575	.1455
-14.95	-.67221	.00525	-.6481	.1785	.1528

M = 1.8

MODEL UPRIGHT

α,deg	C_N	C_A	C_L	C_D	C_m
-5.79	-.26171	.00914	-.2595	.0355	.0719
-4.76	-.21786	.00985	-.2163	.0279	.0608
-3.76	-.17376	.01053	-.1727	.0219	.0492
-2.76	-.12958	.01124	-.1289	.0175	.0369
-1.77	-.08535	.01194	-.0849	.0146	.0245
-.77	-.04055	.01250	-.0404	.0130	.0119
.23	.00265	.01259	.0026	.0126	-.0003
1.26	.04998	.01230	.0497	.0134	-.0136
2.24	.09311	.01159	.0926	.0152	-.0260
3.21	.13628	.01075	.1355	.0184	-.0380
4.25	.18480	.00982	.1836	.0235	-.0512
5.27	.22957	.00905	.2278	.0301	-.0628
6.19	.26854	.00834	.2661	.0373	-.0728
7.22	.31177	.00758	.3083	.0467	-.0829
8.23	.35404	.00686	.3494	.0575	-.0923
9.23	.39277	.00619	.3867	.0691	-.1010
10.24	.43116	.00562	.4233	.0822	-.1087
11.20	.46510	.00506	.4553	.0953	-.1156
12.26	.50376	.00457	.4913	.1114	-.1226
13.20	.53688	.00427	.5217	.1268	-.1278
14.23	.57183	.00390	.5533	.1443	-.1344
15.25	.60475	.00369	.5825	.1627	-.1383
16.27	.63594	.00381	.6094	.1818	-.1413
17.21	.66638	.00367	.6355	.2007	-.1463

MODEL INVERTED

α,deg	C_N	C_A	C_L	C_D	C_m
5.97	.25673	.00835	.2545	.0350	-.0698
4.96	.21269	.00911	.2111	.0275	-.0590
4.01	.17148	.00992	.1704	.0219	-.0476
2.98	.12452	.01086	.1238	.0173	-.0350
1.98	.07944	.01171	.0790	.0145	-.0224
.98	.03541	.01235	.0352	.0130	-.0098
-.01	-.00531	.01259	-.0053	.0126	.0021
-1.03	-.05405	.01246	-.0538	.0134	.0157
-2.00	-.09725	.01186	-.0968	.0152	.0277
-3.00	-.14220	.01116	-.1414	.0186	.0407
-4.02	-.18870	.01047	-.1875	.0237	.0528
-5.03	-.23391	.00981	-.2321	.0303	.0646
-6.03	-.27720	.00916	-.2747	.0382	.0754
-8.02	-.35822	.00802	-.3536	.0579	.0940
-10.03	-.43508	.00702	-.4272	.0827	.1101
-11.99	-.50368	.00633	-.4914	.1109	.1232
-14.03	-.57119	.00617	-.5527	.1445	.1311
-15.98	-.63527	.00593	-.6091	.1806	.1418
-16.99	-.67072	.00578	-.6398	.2015	.1482

TABLE VI.- Concluded

(b) $R = 2.0 \times 10^{6}$; M = 2.0 and 2.16

M = 2.0

MODEL UPRIGHT

α,deg	C_N	C_A	C_L	C_D	C_m
-6.05	-.24637	.00954	-.2440	.0355	.0645
-5.07	-.20790	.01001	-.2062	.0283	.0555
-4.05	-.16755	.01055	-.1664	.0223	.0454
-3.02	-.12674	.01111	-.1260	.0178	.0347
-2.04	-.08767	.01168	-.0872	.0148	.0241
-1.04	-.04854	.01220	-.0483	.0131	.0134
-.04	-.00769	.01237	-.0077	.0124	.0025
.95	.03025	.01224	.0300	.0127	-.0077
1.95	.07318	.01180	.0727	.0143	-.0193
2.97	.11502	.01107	.1143	.0170	-.0303
3.98	.15665	.01039	.1556	.0212	-.0414
4.94	.19436	.00973	.1928	.0264	-.0508
5.94	.23376	.00911	.2316	.0333	-.0604
6.94	.27115	.00851	.2681	.0412	-.0690
7.93	.30859	.00796	.3045	.0504	-.0770
8.96	.34502	.00741	.3397	.0610	-.0849
9.91	.37806	.00691	.3712	.0719	-.0920
10.94	.41248	.00641	.4038	.0846	-.0991
11.90	.44582	.00600	.4350	.0978	-.1056
12.93	.47956	.00563	.4661	.1128	-.1121
13.96	.51320	.00524	.4968	.1289	-.1185
14.92	.54256	.00495	.5230	.1445	-.1241
15.95	.57553	.00464	.5521	.1626	-.1298
16.92	.60556	.00437	.5781	.1804	-.1356
17.96	.63529	.00428	.6030	.1999	-.1392

MODEL INVERTED

α,deg	C_N	C_A	C_L	C_D	C_m
6.26	.24253	.00868	.2401	.0351	-.0629
5.30	.20626	.00932	.2045	.0283	-.0537
4.26	.16507	.00998	.1639	.0222	-.0436
3.25	.12442	.01071	.1236	.0178	-.0331
2.31	.08519	.01144	.0847	.0149	-.0226
1.31	.04613	.01203	.0458	.0131	-.0120
.29	.00694	.01233	.0069	.0124	-.0014
-.71	-.03368	.01234	-.0335	.0128	.0095
-1.70	-.07670	.01201	-.0763	.0143	.0212
-2.74	-.11865	.01141	-.1180	.0171	.0326
-3.73	-.15910	.01086	-.1581	.0212	.0427
-4.69	-.19777	.01036	-.1963	.0265	.0524
-5.70	-.23721	.00987	-.2351	.0334	.0616
-7.71	-.31190	.00894	-.3079	.0507	.0787
-9.71	-.38207	.00810	-.3752	.0724	.0931
-11.71	-.44909	.00745	-.4382	.0984	.1069
-13.72	-.51459	.00690	-.4983	.1287	.1194
-15.71	-.57618	.00647	-.5529	.1623	.1304
-17.74	-.63588	.00651	-.6037	.2000	.1382

M = 2.16

MODEL UPRIGHT

α,deg	C_N	C_A	C_L	C_D	C_m
-5.75	-.21501	.00990	-.2129	.0314	.0542
-4.80	-.18219	.01029	-.1807	.0255	.0461
-3.79	-.14567	.01072	-.1446	.0203	.0376
-2.76	-.10777	.01123	-.1071	.0164	.0281
-1.77	-.07059	.01174	-.0702	.0139	.0187
-.79	-.03505	.01207	-.0349	.0126	.0097
.27	.00352	.01216	.0035	.0122	-.0005
1.23	.03802	.01197	.0378	.0128	-.0094
2.27	.07919	.01148	.0787	.0146	-.0204
3.21	.11464	.01093	.1138	.0173	-.0291
4.27	.15322	.01034	.1520	.0217	-.0388
5.27	.19046	.00980	.1888	.0273	-.0477
6.22	.22420	.00931	.2219	.0335	-.0557
7.24	.25946	.00880	.2563	.0414	-.0638
8.23	.29324	.00833	.2890	.0502	-.0712
9.25	.32773	.00788	.3222	.0605	-.0784
10.25	.35998	.00747	.3529	.0714	-.0851
11.24	.39111	.00706	.3822	.0831	-.0913
12.25	.42319	.00670	.4121	.0963	-.0979
13.21	.45365	.00640	.4402	.1099	-.1043
14.23	.48548	.00611	.4691	.1252	-.1104
15.26	.51673	.00583	.4970	.1416	-.1168
16.25	.54713	.00554	.5237	.1584	-.1225
17.25	.57690	.00527	.5494	.1761	-.1286
18.23	.60598	.00500	.5740	.1943	-.1341
19.25	.63349	.00494	.5965	.2135	-.1373
20.24	.66077	.00478	.6183	.2331	-.1414

MODEL INVERTED

α,deg	C_N	C_A	C_L	C_D	C_m
5.98	.21251	.00922	.2104	.0313	-.0527
4.97	.17701	.00976	.1755	.0251	-.0443
4.01	.14203	.01030	.1410	.0202	-.0358
3.01	.10543	.01091	.1047	.0164	-.0268
1.99	.06781	.01154	.0674	.0139	-.0168
.99	.03077	.01196	.0306	.0125	-.0076
-.00	-.00444	.01214	-.0044	.0121	.0015
-1.02	-.04211	.01207	-.0419	.0128	.0115
-2.02	-.08211	.01169	-.0816	.0146	.0216
-2.99	-.11876	.01123	-.1180	.0174	.0309
-4.02	-.15680	.01077	-.1557	.0217	.0406
-5.05	-.19477	.01035	-.1931	.0275	.0494
-6.02	-.22903	.00997	-.2267	.0339	.0575
-8.00	-.29622	.00926	-.2920	.0504	.0725
-10.01	-.36130	.00857	-.3543	.0712	.0859
-12.04	-.42687	.00803	-.4158	.0969	.0994
-14.01	-.48779	.00762	-.4714	.1255	.1122
-16.02	-.54905	.00721	-.5258	.1584	.1243
-18.04	-.60807	.00689	-.5760	.1949	.1346
-20.00	-.66316	.00673	-.6209	.2332	.1426

TABLE VII.- FORCE COEFFICIENTS FOR MODIFIED ARROW WING WITH $(r/c)_{le} = 0.00235$

(a) $R = 2.0 \times 10^6$; $M = 1.6$ and 1.8

M = 1.6

MODEL UPRIGHT

α,deg	C_N	C_A	C_L	C_D	C_m
-6.04	-.29831	.00835	-.2958	.0397	.0851
-5.08	-.25180	.00925	-.2500	.0315	.0733
-4.06	-.20241	.01011	-.2012	.0244	.0595
-3.07	-.15147	.01099	-.1507	.0191	.0453
-2.07	-.10087	.01191	-.1004	.0155	.0299
-1.05	-.04936	.01272	-.0491	.0136	.0141
-.10	-.00203	.01312	-.0020	.0131	-.0002
1.00	.05789	.01300	.0577	.0140	-.0175
1.95	.10644	.01246	.1060	.0161	-.0318
2.93	.15671	.01192	.1559	.0199	-.0471
4.01	.21266	.01123	.2113	.0261	-.0624
4.94	.25865	.01068	.2568	.0329	-.0745
5.97	.30947	.00994	.3068	.0420	-.0886
6.97	.35567	.00928	.3519	.0524	-.0992
7.96	.39819	.00871	.3931	.0638	-.1089
8.99	.44070	.00822	.4340	.0770	-.1157
9.97	.47824	.00795	.4696	.0907	-.1204
10.96	.51610	.00797	.5052	.1059	-.1241
11.95	.55436	.00774	.5408	.1223	-.1305
12.97	.59544	.00740	.5786	.1408	-.1382
13.97	.63293	.00703	.6125	.1596	-.1453
14.95	.67021	.00664	.6458	.1793	-.1522

MODEL INVERTED

α,deg	C_N	C_A	C_L	C_D	C_m
5.91	.30344	.00964	.3008	.0408	-.0871
4.86	.25098	.01042	.2492	.0317	-.0735
3.92	.20664	.01097	.2054	.0251	-.0609
2.89	.15215	.01170	.1514	.0193	-.0459
1.90	.10208	.01233	.1016	.0157	-.0309
.89	.05100	.01280	.0508	.0136	-.0153
-.10	-.00001	.01310	.0000	.0131	-.0006
-1.09	-.05119	.01275	-.0509	.0137	.0146
-2.15	-.10799	.01195	-.1075	.0160	.0314
-3.12	-.15707	.01112	-.1562	.0196	.0461
-4.10	-.20618	.01030	-.2049	.0250	.0601
-5.11	-.25661	.00942	-.2547	.0322	.0740
-6.10	-.30530	.00849	-.3027	.0409	.0868
-8.10	-.39684	.00671	-.3919	.0626	.1088
-10.14	-.47946	.00525	-.4711	.0895	.1226
-12.12	-.55220	.00482	-.5389	.1206	.1299
-14.14	-.63051	.00369	-.6105	.1576	.1440
-15.12	-.66771	.00310	-.6438	.1772	.1513

M = 1.8

MODEL UPRIGHT

α,deg	C_N	C_A	C_L	C_D	C_m
-6.01	-.26239	.00928	-.2600	.0367	.0714
-5.00	-.22014	.00995	-.2184	.0291	.0611
-4.02	-.17853	.01056	-.1774	.0230	.0498
-2.99	-.13297	.01119	-.1322	.0181	.0377
-2.00	-.08817	.01178	-.0877	.0149	.0252
-1.00	-.04315	.01229	-.0429	.0130	.0123
-.00	.00280	.01254	.0028	.0125	-.0010
.99	.05060	.01252	.0504	.0134	-.0149
2.01	.09941	.01225	.0989	.0157	-.0284
2.99	.14527	.01193	.1445	.0195	-.0412
3.99	.18770	.01153	.1864	.0246	-.0528
4.99	.23142	.01111	.2296	.0312	-.0642
5.98	.27392	.01070	.2713	.0392	-.0746
6.98	.31475	.01020	.3112	.0484	-.0848
8.02	.35631	.00975	.3515	.0594	-.0935
8.99	.39191	.00937	.3856	.0705	-.1013
10.01	.43250	.00888	.4244	.0840	-.1099
11.01	.46858	.00852	.4583	.0979	-.1167
11.98	.50042	.00823	.4878	.1120	-.1217
13.00	.53326	.00801	.5178	.1278	-.1256
13.99	.56534	.00788	.5467	.1443	-.1295
15.03	.60066	.00766	.5781	.1632	-.1355
16.02	.63437	.00740	.6077	.1822	-.1413

MODEL INVERTED

α,deg	C_N	C_A	C_L	C_D	C_m
5.83	.26379	.01054	.2614	.0373	-.0723
4.87	.22249	.01098	.2208	.0298	-.0619
3.85	.17951	.01142	.1783	.0234	-.0508
2.83	.13379	.01182	.1330	.0184	-.0387
1.88	.09130	.01218	.0909	.0152	-.0261
.84	.04313	.01244	.0429	.0131	-.0127
-.15	-.00201	.01251	-.0020	.0125	.0003
-1.15	-.05090	.01230	-.0506	.0133	.0146
-2.15	-.09752	.01182	-.0970	.0155	.0278
-3.17	-.14434	.01126	-.1435	.0192	.0404
-4.16	-.18718	.01069	-.1859	.0242	.0521
-5.16	-.23168	.01006	-.2298	.0309	.0637
-6.14	-.27187	.00942	-.2693	.0385	.0738
-7.17	-.31451	.00874	-.3110	.0479	.0841
-8.18	-.35531	.00803	-.3505	.0585	.0931
-10.16	-.42933	.00678	-.4214	.0824	.1089
-12.20	-.50144	.00557	-.4889	.1114	.1223
-14.17	-.56361	.00500	-.5452	.1428	.1291
-16.19	-.63142	.00419	-.6052	.1800	.1407

TABLE VII.- Concluded

(b) $R = 2.0 \times 10^6$; $M = 2.0$ and 2.16

M = 2.0

MODEL UPRIGHT

α,deg	C_N	C_A	C_L	C_D	C_m
-6.27	-.24445	.00976	-.2419	.0364	.0646
-5.24	-.20692	.01028	-.2051	.0291	.0549
-4.25	-.16850	.01078	-.1672	.0232	.0452
-3.26	-.13045	.01124	-.1296	.0186	.0350
-2.26	-.08997	.01166	-.0894	.0152	.0244
-1.27	-.05066	.01198	-.0504	.0131	.0136
-.24	-.00631	.01224	-.0063	.0123	.0015
.75	.03468	.01230	.0345	.0128	-.0103
1.75	.08014	.01228	.0797	.0147	-.0222
2.74	.11957	.01213	.1189	.0178	-.0327
3.76	.16136	.01188	.1602	.0224	-.0435
4.76	.20051	.01164	.1988	.0282	-.0534
5.76	.23945	.01130	.2371	.0353	-.0631
6.76	.27654	.01098	.2733	.0434	-.0716
7.76	.31227	.01065	.3080	.0527	-.0795
8.75	.34725	.01031	.3416	.0630	-.0867
9.75	.38131	.01000	.3741	.0744	-.0942
10.76	.41524	.00971	.4061	.0870	-.1011
11.73	.44756	.00938	.4363	.1002	-.1078
12.73	.48061	.00909	.4668	.1148	-.1143
13.74	.51222	.00884	.4955	.1303	-.1198
14.74	.54339	.00861	.5233	.1466	-.1252
15.76	.57318	.00848	.5493	.1639	-.1285
16.75	.60381	.00830	.5758	.1820	-.1335
17.75	.63402	.00806	.6014	.2010	-.1388
18.73	.66440	.00779	.6267	.2208	-.1444

MODEL INVERTED

α,deg	C_N	C_A	C_L	C_D	C_m
6.09	.24574	.01089	.2432	.0369	-.0658
5.12	.20976	.01123	.2079	.0299	-.0566
4.09	.17060	.01155	.1693	.0237	-.0464
3.11	.13246	.01184	.1316	.0190	-.0363
2.08	.09037	.01209	.0899	.0154	-.0252
1.09	.05010	.01226	.0499	.0132	-.0142
.09	.00880	.01229	.0088	.0123	-.0026
-.90	-.03340	.01223	-.0332	.0128	.0091
-1.89	-.07759	.01201	-.0772	.0146	.0212
-2.91	-.11861	.01164	-.1179	.0176	.0322
-3.90	-.15878	.01124	-.1576	.0220	.0425
-4.92	-.19871	.01080	-.1971	.0278	.0527
-5.92	-.23660	.01032	-.2343	.0347	.0619
-6.91	-.27436	.00979	-.2712	.0427	.0707
-7.91	-.30970	.00928	-.3055	.0518	.0789
-9.91	-.37956	.00822	-.3725	.0734	.0932
-11.91	-.44606	.00726	-.4350	.0992	.1071
-13.89	-.50936	.00637	-.4929	.1285	.1187
-15.92	-.57062	.00557	-.5472	.1618	.1275
-17.92	-.63146	.00481	-.5994	.1988	.1380

M = 2.16

MODEL UPRIGHT

α,deg	C_N	C_A	C_L	C_D	C_m
-6.02	-.21670	.01036	-.2144	.0330	.0545
-5.04	-.18317	.01076	-.1815	.0268	.0463
-4.03	-.14673	.01116	-.1456	.0214	.0375
-3.03	-.11087	.01151	-.1101	.0174	.0285
-2.03	-.07387	.01182	-.0734	.0144	.0190
-1.02	-.03592	.01209	-.0357	.0127	.0091
-.02	.00249	.01224	.0025	.0122	-.0007
.98	.04051	.01232	.0403	.0130	-.0109
2.00	.08158	.01230	.0811	.0151	-.0214
2.96	.11826	.01221	.1175	.0183	-.0308
3.97	.15511	.01203	.1539	.0228	-.0400
4.99	.19207	.01182	.1903	.0285	-.0491
5.98	.22689	.01157	.2244	.0351	-.0573
6.97	.26093	.01132	.2576	.0429	-.0652
7.97	.29464	.01107	.2903	.0518	-.0724
8.97	.32698	.01077	.3213	.0616	-.0792
9.99	.35993	.01056	.3526	.0728	-.0861
10.96	.39109	.01030	.3820	.0845	-.0927
11.98	.42331	.01006	.4120	.0977	-.0993
12.97	.45408	.00978	.4403	.1115	-.1056
13.99	.48650	.00958	.4698	.1269	-.1122
14.99	.51568	.00938	.4957	.1424	-.1177
16.00	.54512	.00915	.5215	.1590	-.1224
16.99	.57274	.00897	.5451	.1759	-.1267
17.98	.60201	.00879	.5699	.1942	-.1312
18.99	.63097	.00855	.5939	.2134	-.1364
19.98	.66111	.00832	.6185	.2337	-.1420

MODEL INVERTED

α,deg	C_N	C_A	C_L	C_D	C_m
5.87	.21918	.01133	.2169	.0337	-.0555
4.86	.18351	.01160	.1819	.0271	-.0470
3.88	.14835	.01183	.1472	.0218	-.0384
2.85	.11095	.01203	.1102	.0175	-.0291
1.86	.07452	.01217	.0741	.0146	-.0198
.86	.03683	.01225	.0366	.0128	-.0099
-.13	-.00048	.01224	-.0005	.0122	.0001
-1.14	-.04026	.01215	-.0400	.0130	.0103
-2.16	-.08102	.01196	-.0805	.0150	.0206
-3.13	-.11754	.01167	-.1167	.0181	.0301
-4.16	-.15547	.01133	-.1542	.0226	.0395
-5.14	-.19062	.01097	-.1889	.0280	.0481
-6.15	-.22554	.01056	-.2231	.0347	.0567
-7.16	-.26038	.01013	-.2571	.0425	.0647
-8.17	-.29444	.00967	-.2901	.0514	.0723
-10.13	-.35766	.00880	-.3505	.0716	.0849
-12.15	-.42076	.00799	-.4097	.0964	.0980
-14.15	-.48232	.00718	-.4659	.1248	.1105
-16.14	-.54255	.00635	-.5194	.1570	.1222
-18.16	-.59962	.00567	-.5680	.1923	.1304
-20.16	-.65849	.00475	-.6165	.2314	.1411

TABLE VIII.- FORCE COEFFICIENTS FOR MODIFIED ARROW WING WITH $(r/c)_{le} = 0.00470$

(a) $R = 2.0 \times 10^6$; $M = 1.6$ and 1.8

$M = 1.6$

MODEL UPRIGHT

α,deg	C_N	C_A	C_L	C_D	C_m
-6.03	-.29963	.00980	-.2969	.0412	.0843
-5.10	-.25666	.01053	-.2547	.0333	.0730
-4.02	-.20281	.01132	-.2015	.0255	.0593
-3.01	-.15279	.01212	-.1519	.0201	.0448
-2.03	-.10296	.01268	-.1024	.0163	.0303
-1.06	-.05209	.01317	-.0518	.0141	.0149
-.04	-.00056	.01356	-.0005	.0136	-.0003
.96	.05335	.01352	.0531	.0144	-.0163
1.92	.10469	.01330	.1042	.0168	-.0318
2.96	.15914	.01288	.1583	.0211	-.0471
3.96	.20958	.01249	.2082	.0269	-.0613
4.95	.25811	.01189	.2561	.0341	-.0739
5.98	.30750	.01137	.3046	.0433	-.0866
6.95	.35213	.01060	.3483	.0531	-.0976
7.96	.39782	.00994	.3926	.0649	-.1080
8.95	.43811	.00919	.4313	.0772	-.1162
9.99	.48069	.00854	.4719	.0918	-.1233
10.95	.51788	.00804	.5069	.1063	-.1287
12.00	.55547	.00783	.5417	.1231	-.1319
12.98	.59071	.00758	.5739	.1401	-.1364
13.98	.62967	.00704	.6093	.1589	-.1433
14.95	.66328	.00653	.6391	.1775	-.1499

MODEL INVERTED

α,deg	C_N	C_A	C_L	C_D	C_m
5.91	.29860	.01103	.2959	.0417	-.0850
4.91	.25028	.01159	.2484	.0330	-.0727
3.92	.20284	.01216	.2015	.0260	-.0595
2.92	.15227	.01260	.1514	.0203	-.0455
1.92	.10167	.01300	.1012	.0164	-.0309
.89	.04844	.01332	.0482	.0141	-.0146
-.09	-.00167	.01345	-.0016	.0135	-.0003
-1.10	-.05903	.01320	-.0588	.0143	.0168
-2.10	-.11047	.01274	-.1099	.0168	.0323
-3.04	-.15872	.01216	-.1579	.0206	.0464
-4.14	-.21412	.01142	-.2127	.0268	.0615
-5.09	-.25974	.01071	-.2578	.0337	.0737
-6.02	-.30435	.00993	-.3016	.0418	.0851
-8.10	-.39807	.00818	-.3929	.0642	.1064
-10.08	-.48038	.00658	-.4718	.0906	.1238
-12.11	-.55342	.00576	-.5399	.1218	.1290
-14.05	-.62454	.00483	-.6047	.1563	.1413

$M = 1.8$

MODEL UPRIGHT

α,deg	C_N	C_A	C_L	C_D	C_m
-6.04	-.26536	.01072	-.2628	.0386	.0714
-5.06	-.22420	.01127	-.2223	.0310	.0612
-4.03	-.18171	.01179	-.1804	.0245	.0501
-3.02	-.13704	.01222	-.1362	.0194	.0385
-2.02	-.09201	.01257	-.0915	.0158	.0260
-1.00	-.04624	.01282	-.0460	.0136	.0129
-.02	.00106	.01302	.0011	.0130	-.0006
.98	.05026	.01311	.0500	.0140	-.0146
1.97	.09708	.01305	.0966	.0164	-.0279
3.01	.14343	.01291	.1426	.0204	-.0407
4.01	.18824	.01272	.1869	.0259	-.0525
4.97	.22937	.01246	.2274	.0323	-.0633
6.00	.27276	.01204	.2700	.0405	-.0738
6.95	.30992	.01161	.3062	.0490	-.0830
7.99	.35194	.01111	.3470	.0599	-.0921
8.96	.38814	.01058	.3817	.0709	-.0999
9.98	.42555	.01003	.4174	.0836	-.1079
10.98	.46231	.00952	.4520	.0974	-.1153
11.96	.49673	.00897	.4841	.1117	-.1225
13.00	.53278	.00843	.5172	.1281	-.1278
13.96	.56151	.00806	.5430	.1433	-.1305
14.93	.59092	.00784	.5689	.1599	-.1331
15.94	.62565	.00747	.5995	.1790	-.1391
16.99	.66060	.00695	.6297	.1997	-.1456

MODEL INVERTED

α,deg	C_N	C_A	C_L	C_D	C_m
5.92	.26578	.01189	.2631	.0392	-.0722
4.84	.22027	.01228	.2185	.0308	-.0608
3.92	.18115	.01258	.1799	.0249	-.0509
2.86	.13378	.01273	.1330	.0194	-.0385
1.87	.09012	.01294	.0896	.0159	-.0261
.90	.04443	.01302	.0442	.0137	-.0132
-.13	-.00231	.01303	-.0023	.0130	.0001
-1.11	-.05260	.01295	-.0523	.0140	.0150
-2.11	-.10015	.01269	-.0996	.0164	.0284
-3.08	-.14475	.01233	-.1439	.0201	.0402
-4.10	-.18823	.01195	-.1869	.0254	.0518
-5.08	-.22977	.01145	-.2279	.0317	.0624
-6.14	-.27471	.01082	-.2720	.0401	.0734
-7.08	-.31227	.01030	-.3086	.0487	.0826
-8.13	-.35346	.00963	-.3486	.0595	.0917
-10.08	-.42574	.00842	-.4177	.0828	.1074
-12.13	-.50013	.00709	-.4875	.1120	.1225
-14.10	-.56101	.00611	-.5426	.1426	.1290
-16.06	-.62384	.00527	-.5981	.1776	.1377
-18.16	-.69452	.00403	-.6587	.2202	.1506

(b) $R = 2.0 \times 10^6$; M = 2.0 and 2.16

M = 2.0

MODEL UPRIGHT

α,deg	C_N	C_A	C_L	C_D	C_m
-6.19	-.24028	.01122	-.2377	.0370	.0624
-5.25	-.20673	.01164	-.2048	.0305	.0543
-4.23	-.16860	.01200	-.1673	.0244	.0444
-3.17	-.12661	.01230	-.1257	.0193	.0340
-2.17	-.08706	.01253	-.0865	.0158	.0233
-1.18	-.04714	.01267	-.0469	.0136	.0124
-.18	-.00527	.01282	-.0052	.0128	.0010
.81	.03566	.01293	.0355	.0134	-.0103
1.84	.08092	.01303	.0805	.0156	-.0226
2.81	.12119	.01305	.1204	.0190	-.0332
3.82	.16052	.01299	.1593	.0236	-.0434
4.84	.20003	.01283	.1982	.0297	-.0532
5.79	.23538	.01263	.2329	.0363	-.0622
6.81	.27431	.01235	.2709	.0448	-.0710
7.79	.30820	.01200	.3037	.0537	-.0790
8.82	.34400	.01158	.3382	.0642	-.0866
9.79	.37751	.01122	.3701	.0753	-.0936
10.76	.40877	.01081	.3996	.0869	-.1002
11.81	.44490	.01037	.4334	.1012	-.1077
12.77	.47537	.00997	.4614	.1148	-.1139
13.80	.50695	.00951	.4900	.1302	-.1190
14.83	.53840	.00910	.5181	.1466	-.1238
15.79	.56545	.00869	.5417	.1622	-.1272
16.80	.59574	.00835	.5679	.1802	-.1319
17.81	.62723	.00797	.5947	.1994	-.1375
18.83	.65874	.00755	.6211	.2197	-.1432

MODEL INVERTED

α,deg	C_N	C_A	C_L	C_D	C_m
6.07	.24226	.01212	.2396	.0377	-.0641
5.04	.20430	.01236	.2024	.0303	-.0549
4.05	.16607	.01259	.1648	.0243	-.0452
3.10	.13016	.01269	.1293	.0197	-.0357
2.08	.08898	.01278	.0885	.0160	-.0249
1.06	.04735	.01281	.0471	.0137	-.0135
.06	.00621	.01279	.0062	.0128	-.0020
-.96	-.03811	.01279	-.0379	.0134	.0100
-1.93	-.08082	.01274	-.0803	.0155	.0218
-2.93	-.12023	.01258	-.1194	.0187	.0324
-3.92	-.15928	.01234	-.1581	.0232	.0426
-4.91	-.19742	.01201	-.1957	.0288	.0521
-5.91	-.23550	.01164	-.2330	.0358	.0613
-7.96	-.31044	.01072	-.3060	.0536	.0786
-9.99	-.37958	.00967	-.3722	.0754	.0931
-11.97	-.44625	.00870	-.4347	.1011	.1071
-13.97	-.50961	.00761	-.4927	.1304	.1195
-15.96	-.56582	.00677	-.5421	.1621	.1257
-17.95	-.62691	.00580	-.5946	.1987	.1365
-19.98	-.68900	.00463	-.6459	.2398	.1477

M = 2.16

MODEL UPRIGHT

α,deg	C_N	C_A	C_L	C_D	C_m
-6.04	-.21888	.01173	-.2164	.0347	.0546
-5.05	-.18534	.01206	-.1836	.0283	.0463
-4.09	-.15117	.01236	-.1499	.0231	.0381
-3.04	-.11350	.01260	-.1127	.0186	.0289
-2.05	-.07673	.01275	-.0762	.0155	.0194
-1.00	-.03720	.01289	-.0370	.0135	.0092
-.01	.00063	.01301	.0006	.0130	-.0005
.97	.03833	.01310	.0381	.0137	-.0102
1.96	.07839	.01320	.0779	.0159	-.0205
2.98	.11606	.01321	.1152	.0192	-.0302
3.96	.15190	.01317	.1506	.0236	-.0392
4.98	.18863	.01306	.1868	.0294	-.0483
5.94	.22210	.01292	.2196	.0358	-.0563
6.97	.25846	.01267	.2550	.0439	-.0645
8.00	.29278	.01237	.2882	.0530	-.0721
8.98	.32407	.01207	.3182	.0625	-.0790
9.97	.35626	.01176	.3488	.0733	-.0856
10.98	.38872	.01144	.3794	.0853	-.0924
11.98	.41970	.01113	.4083	.0980	-.0991
12.97	.45091	.01077	.4370	.1117	-.1058
13.92	.47910	.01035	.4625	.1253	-.1109
14.95	.50984	.00993	.4900	.1411	-.1167
15.96	.53906	.00952	.5157	.1574	-.1213
16.95	.56687	.00916	.5396	.1740	-.1255
17.96	.59587	.00885	.5641	.1921	-.1301
18.99	.62654	.00842	.5897	.2118	-.1353
19.94	.65420	.00799	.6122	.2307	-.1404

MODEL INVERTED

α,deg	C_N	C_A	C_L	C_D	C_m
5.93	.21837	.01264	.2159	.0351	-.0550
4.93	.18348	.01278	.1817	.0285	-.0466
3.94	.14876	.01291	.1475	.0231	-.0380
2.91	.11141	.01298	.1106	.0186	-.0289
1.89	.07358	.01299	.0731	.0154	-.0193
.91	.03662	.01299	.0364	.0136	-.0098
-.07	.00003	.01297	.0000	.0130	-.0002
-1.08	-.03904	.01292	-.0388	.0137	.0100
-2.09	-.08047	.01289	-.0799	.0158	.0203
-3.10	-.11784	.01273	-.1170	.0191	.0301
-4.08	-.15325	.01256	-.1520	.0234	.0388
-5.09	-.18934	.01222	-.1875	.0290	.0476
-6.10	-.22502	.01190	-.2225	.0357	.0562
-8.12	-.29398	.01113	-.2895	.0526	.0719
-10.11	-.35771	.01031	-.3503	.0730	.0855
-12.10	-.41962	.00944	-.4083	.0972	.0983
-14.08	-.48084	.00853	-.4643	.1253	.1103
-16.12	-.54000	.00751	-.5167	.1571	.1203
-18.10	-.59521	.00662	-.5637	.1912	.1287
-20.08	-.65387	.00551	-.6122	.2297	.1392

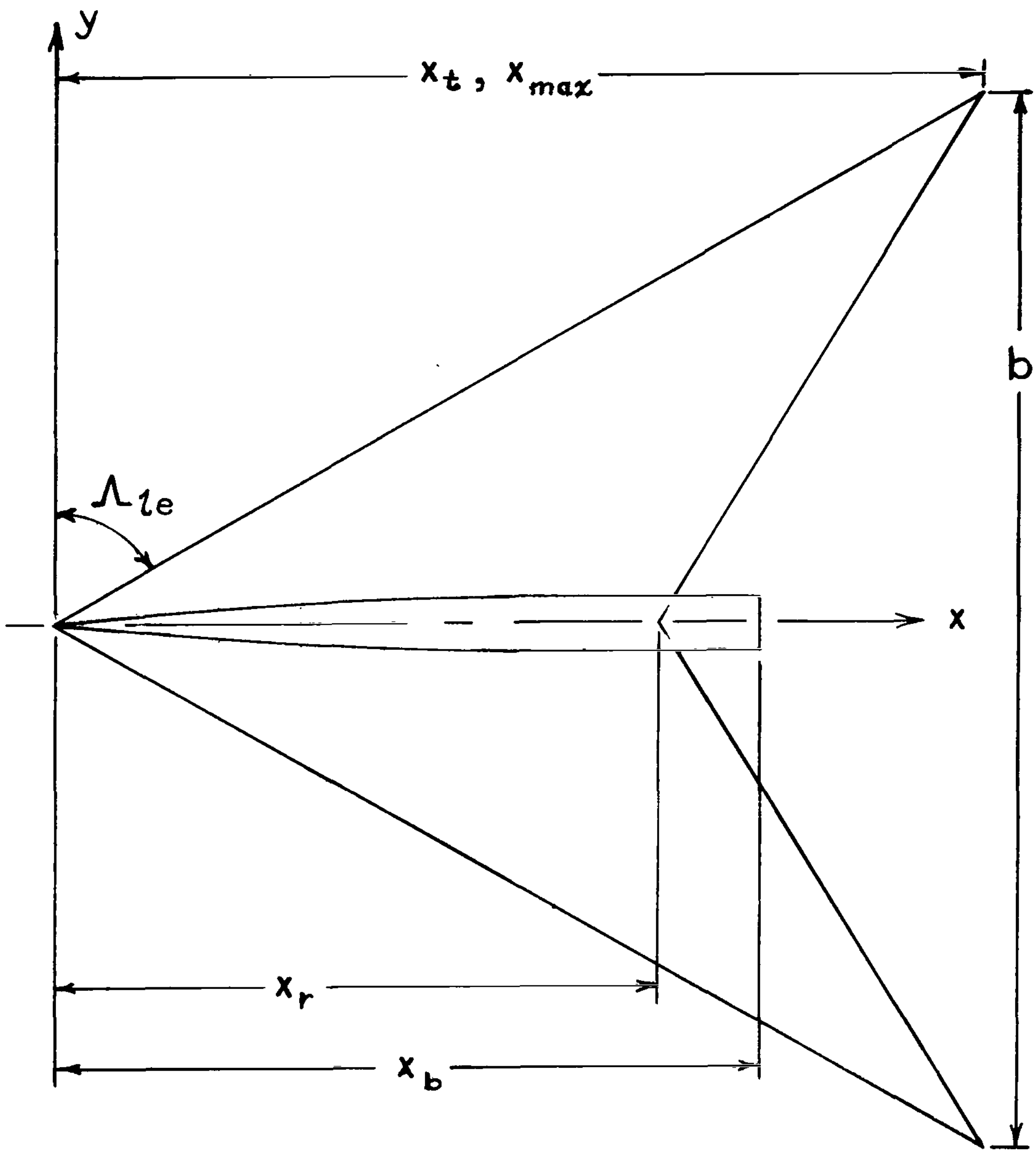

(a) Reference arrow wing.

Figure 1.- Wind-tunnel model descriptions.

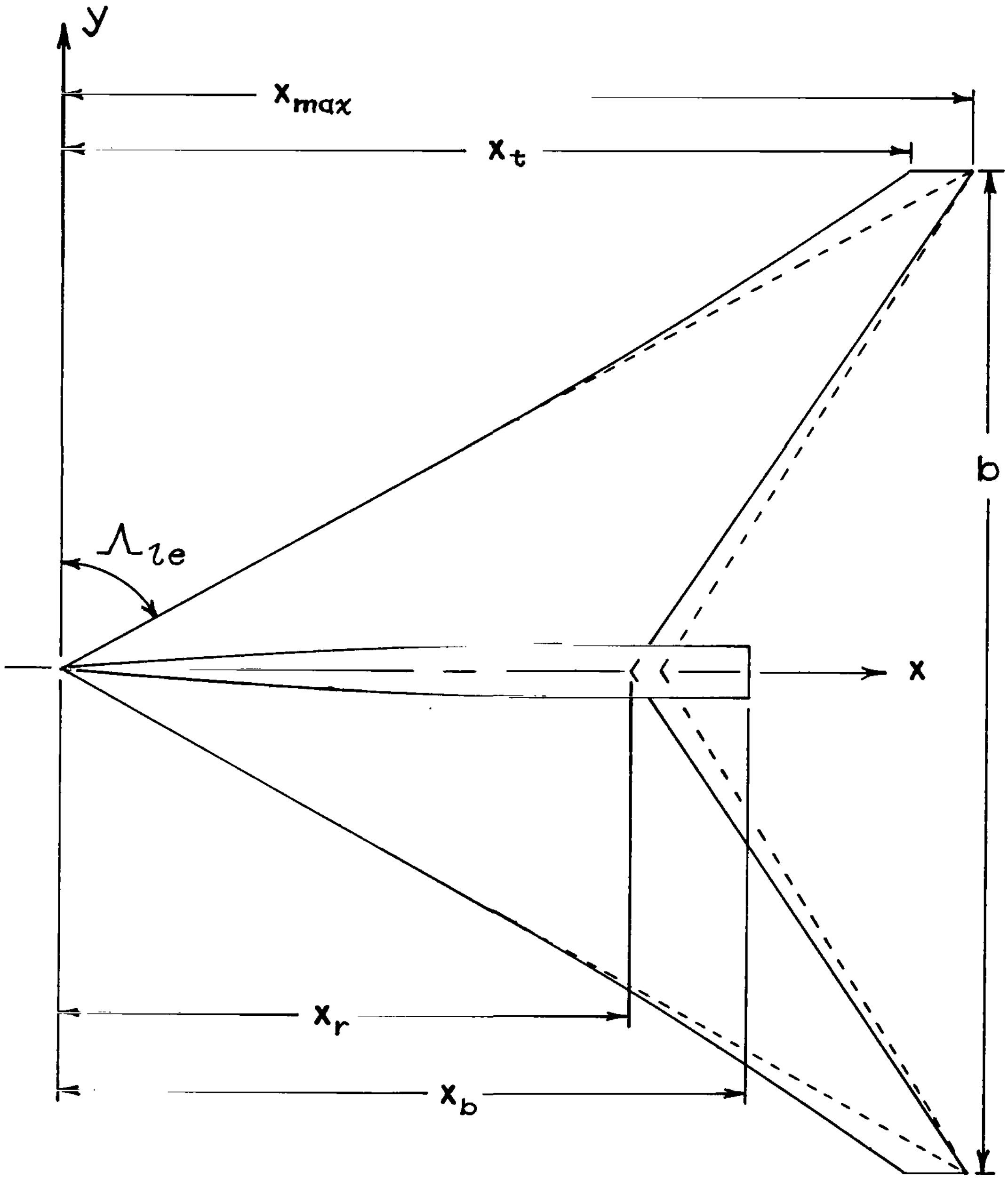

(b) Modified arrow wing.

Figure 1.- Continued.

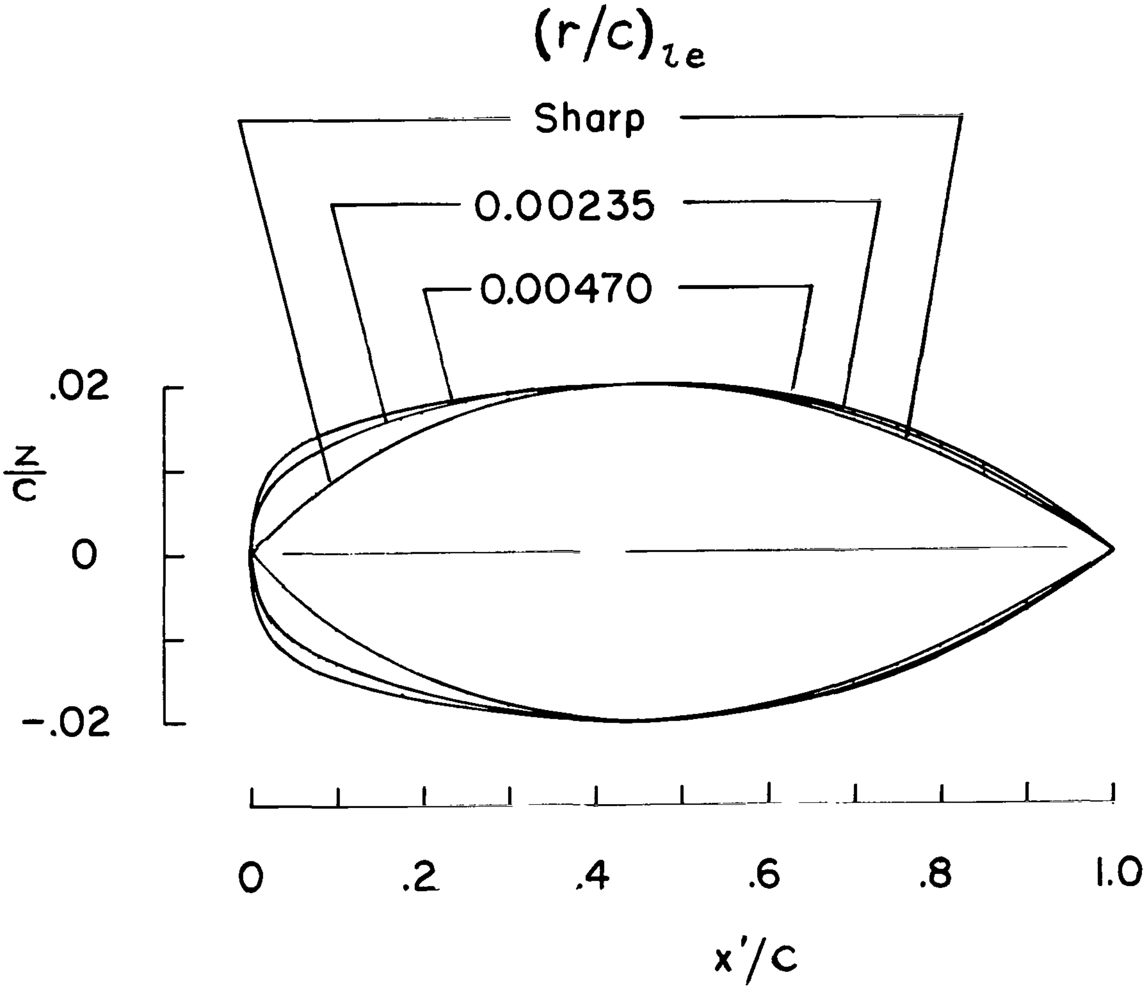

(c) Airfoil description.

Figure 1.- Concluded.

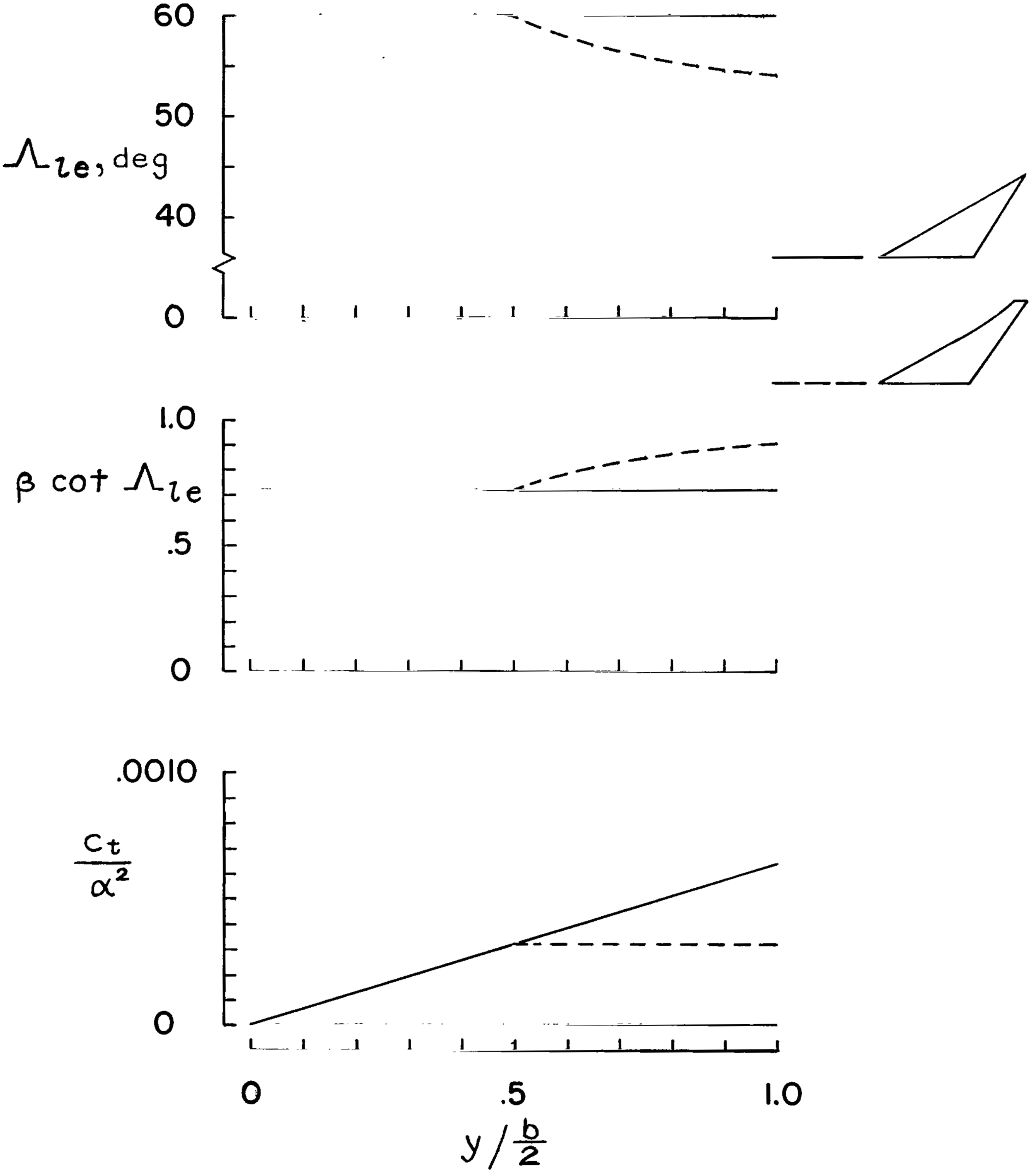

Figure 2.- Comparison of planforms and full leading-edge thrust variation on arrow and modified arrow wings at $M = 1.6$.

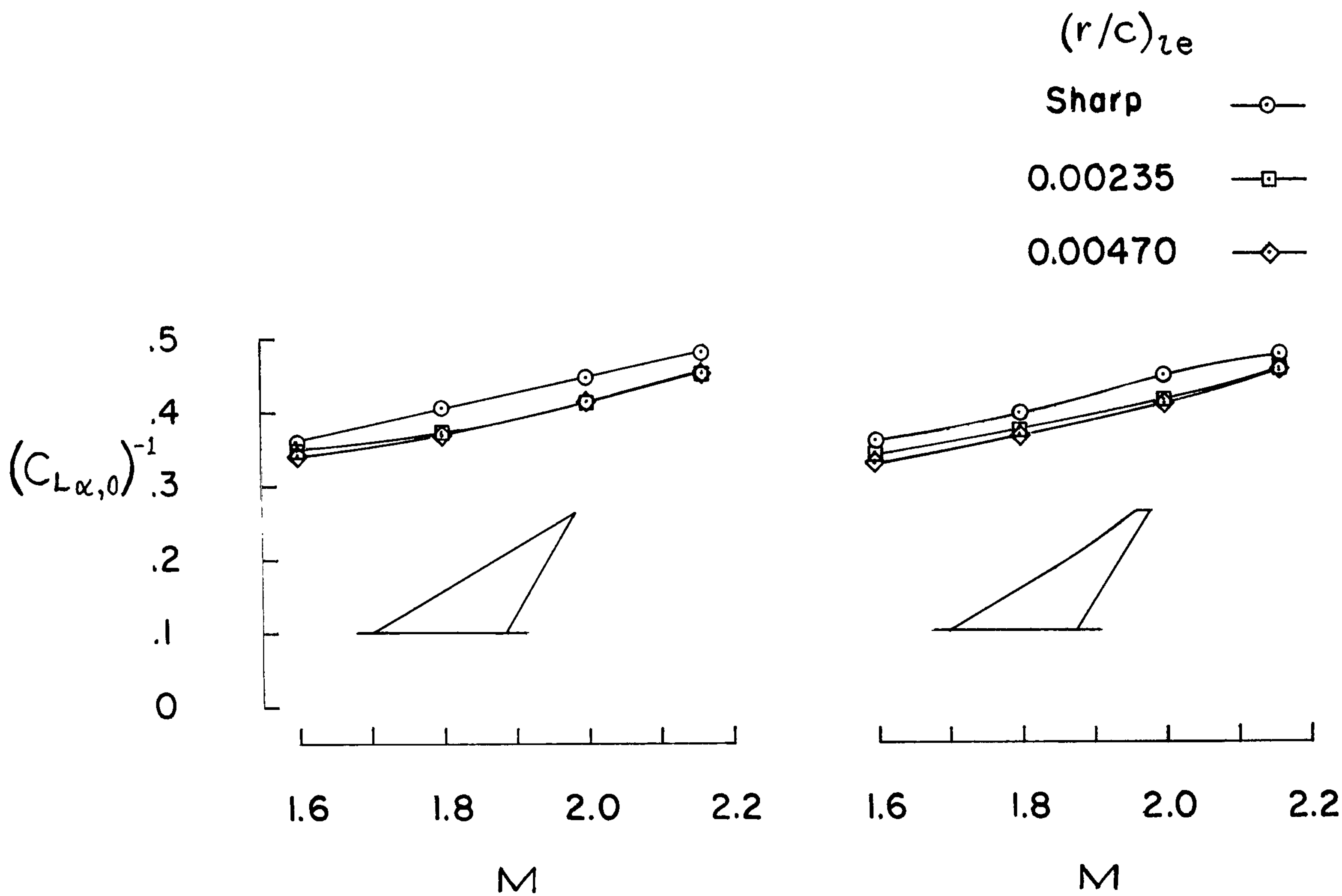

Figure 3.- Experimental values of $\left(C_{L_{\alpha,0}}\right)^{-1}$ for $R = 2.0 \times 10^6$.

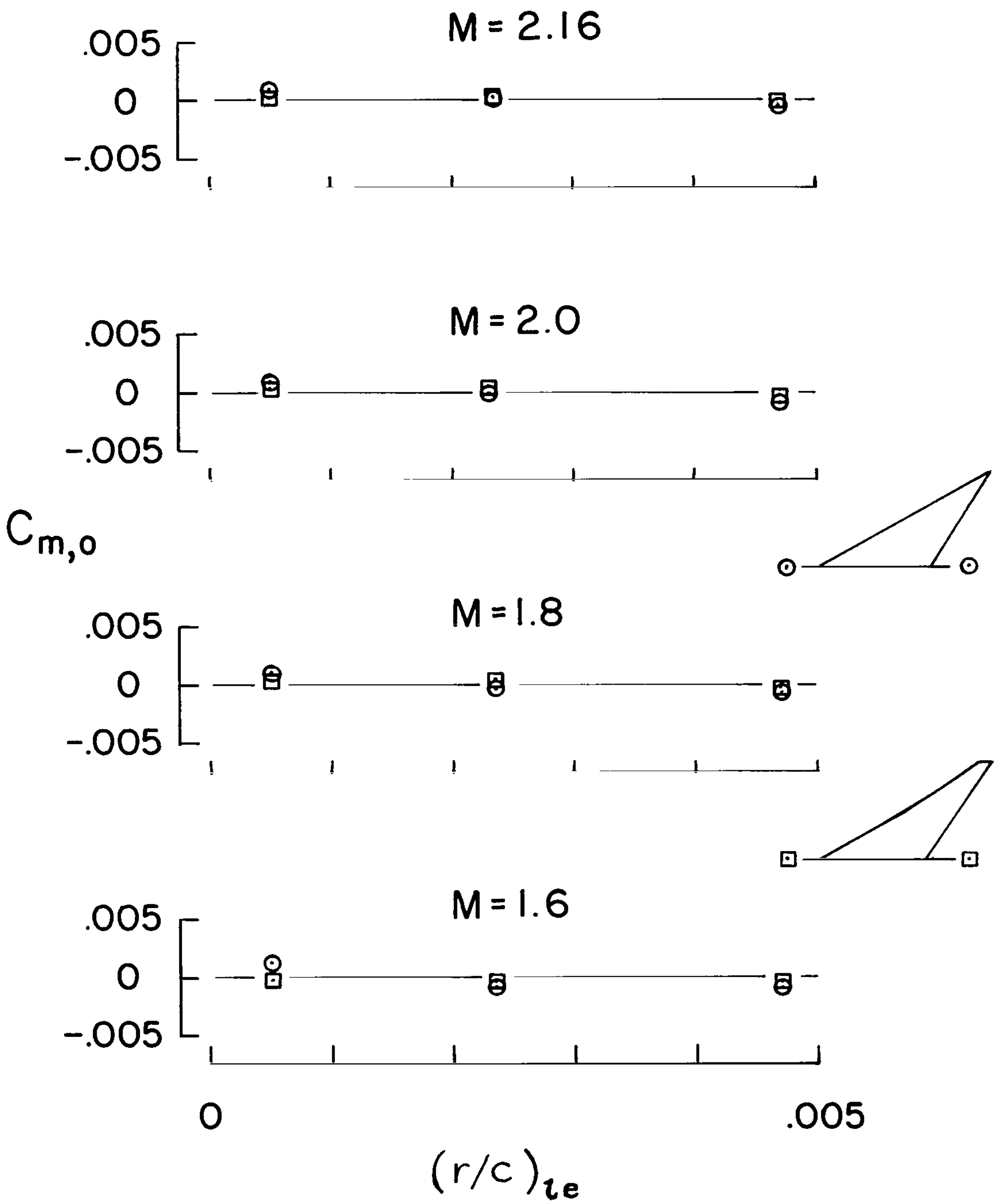

Figure 4.- Experimental values of $C_{m,o}$ for $R = 2.0 \times 10^6$.

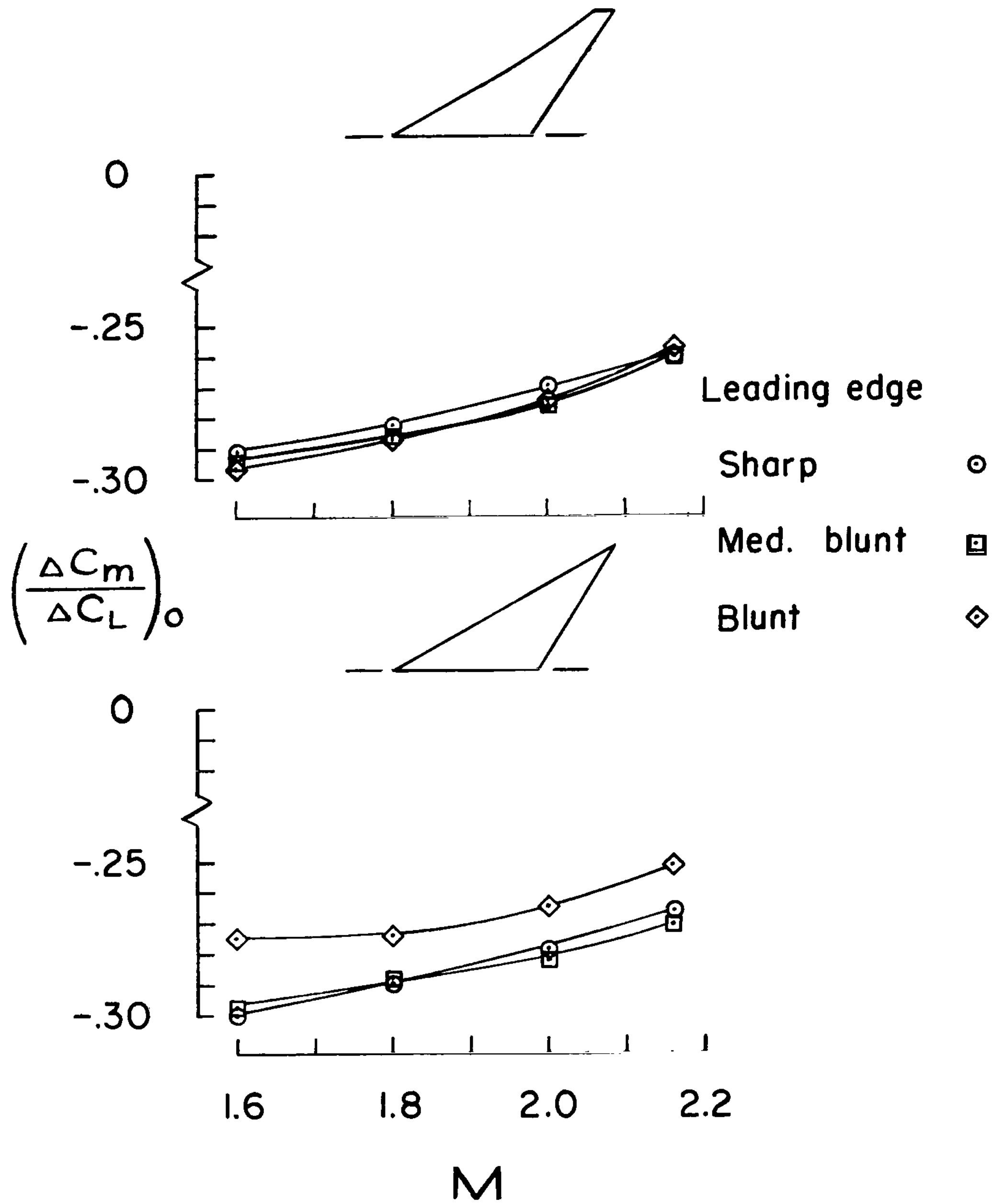

(a) Mach number effects.

Figure 5.- Effects of planform, bluntness, and Mach number on $(\Delta C_m/\Delta C_L)_o$ at $R = 2.0 \times 10^6$.

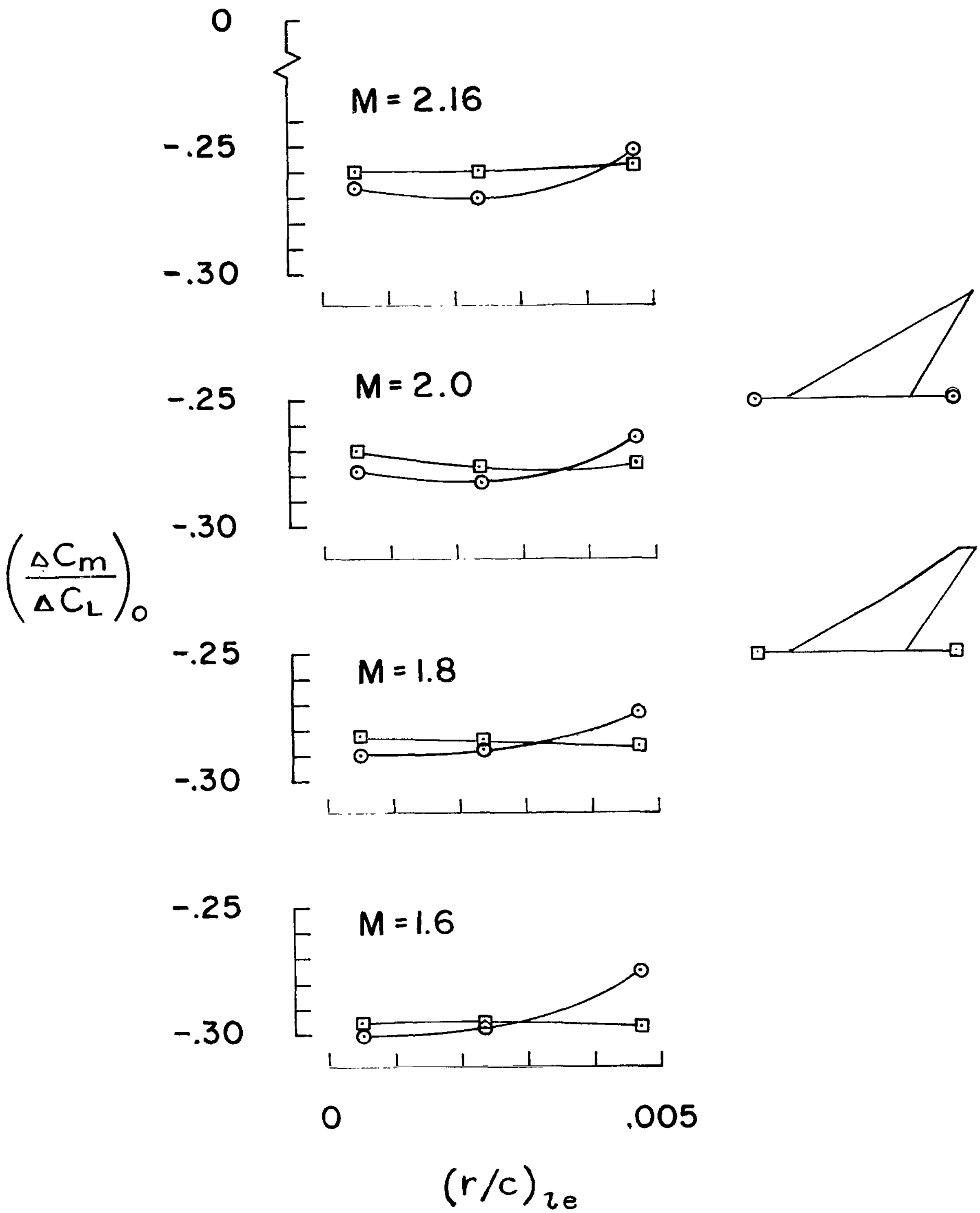

(b) Bluntness effects.

Figure 5.- Concluded.

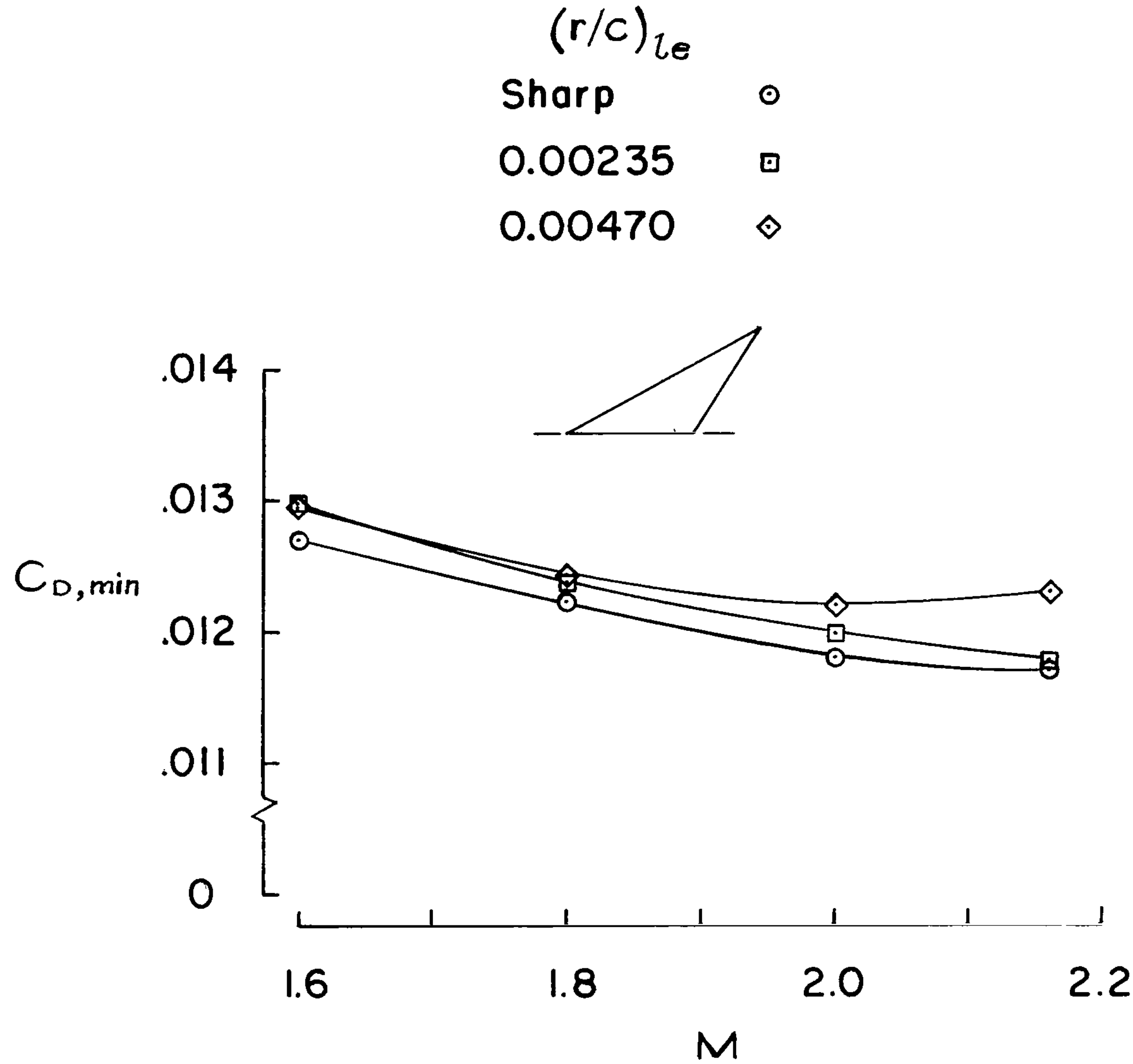

(a) Arrow wing.

Figure 6.- Effect of planform and leading-edge bluntness on $C_{D,min}$ at $R = 2.0 \times 10^6$.

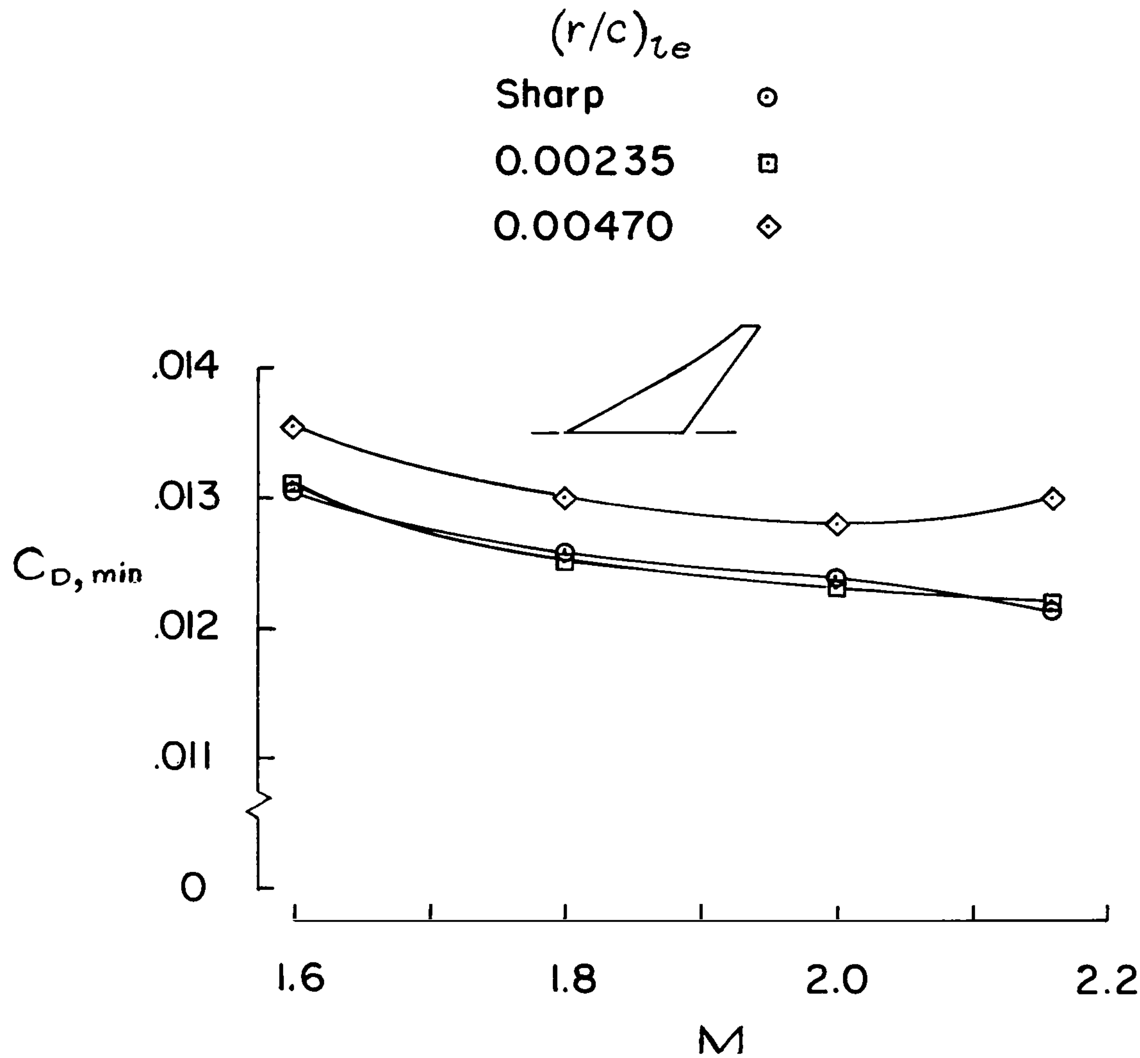

(b) Modified arrow wing.

Figure 6.- Continued.

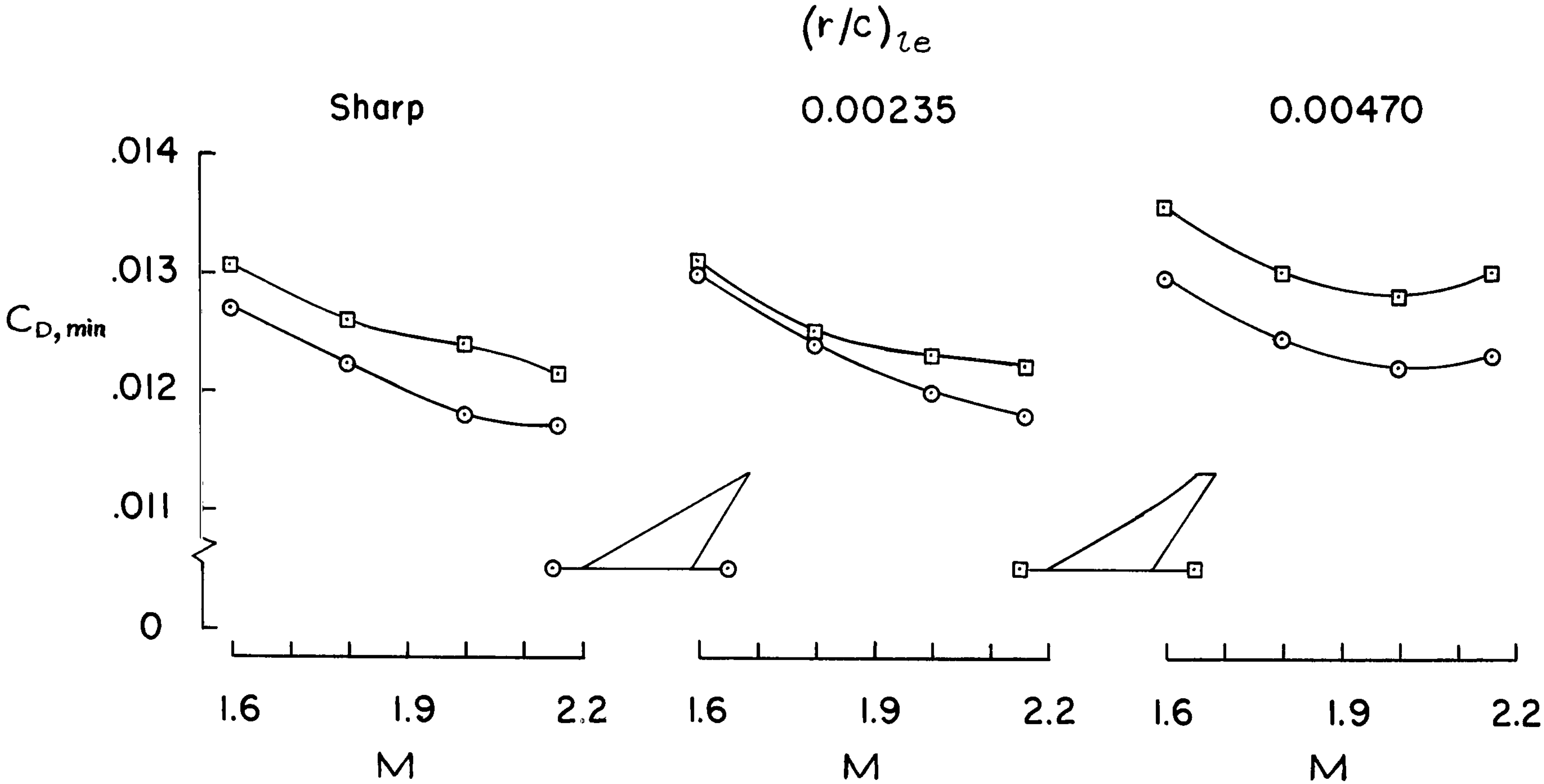

(c) Comparison of $C_{D,min}$ for arrow and modified arrow wings.

Figure 6.- Concluded.

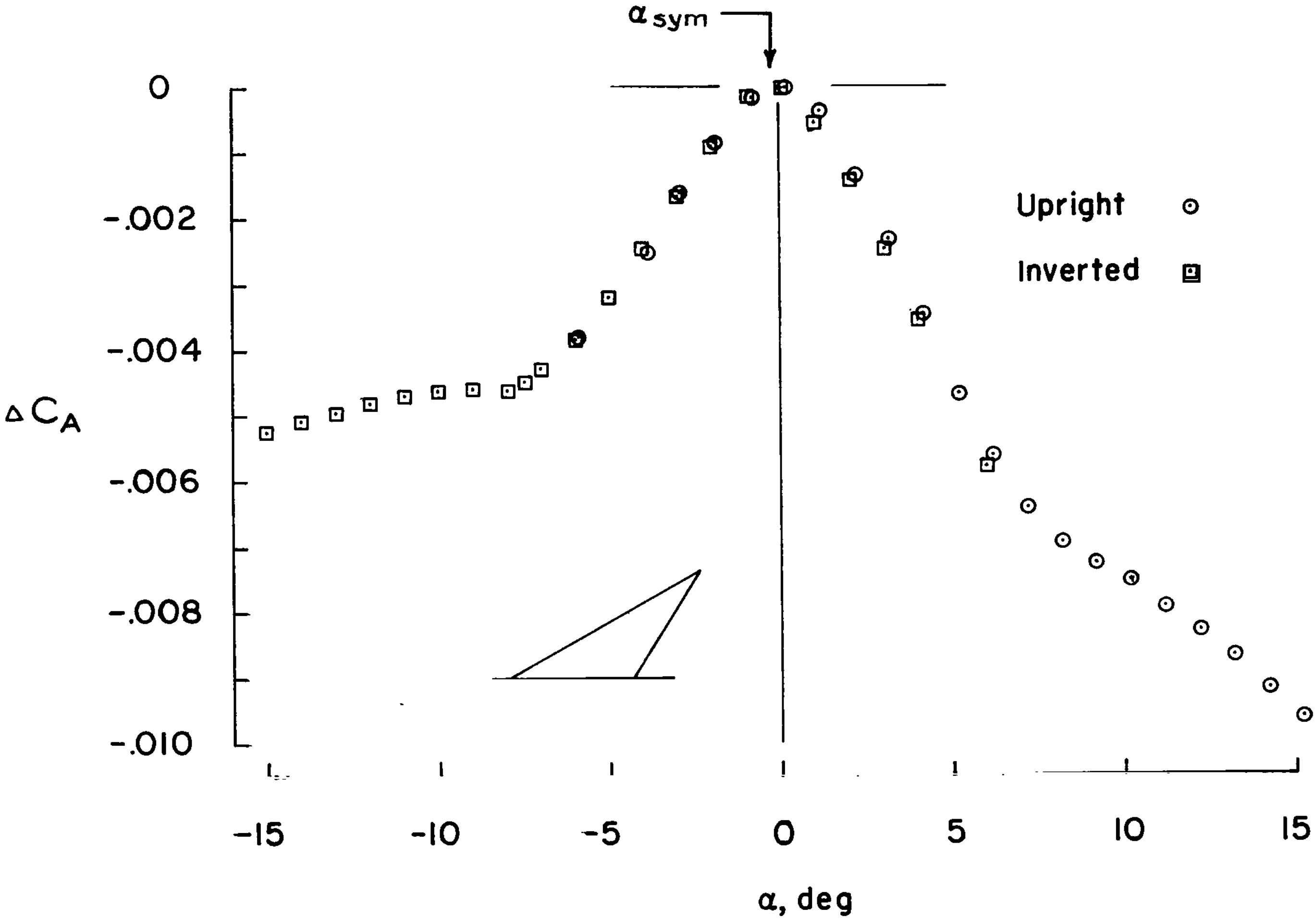

(a) Sharp leading edge at $M = 1.6$ and $R = 2.0 \times 10^6$.

Figure 7.- Samples of experimental ΔC_A plotted against α for arrow wings.

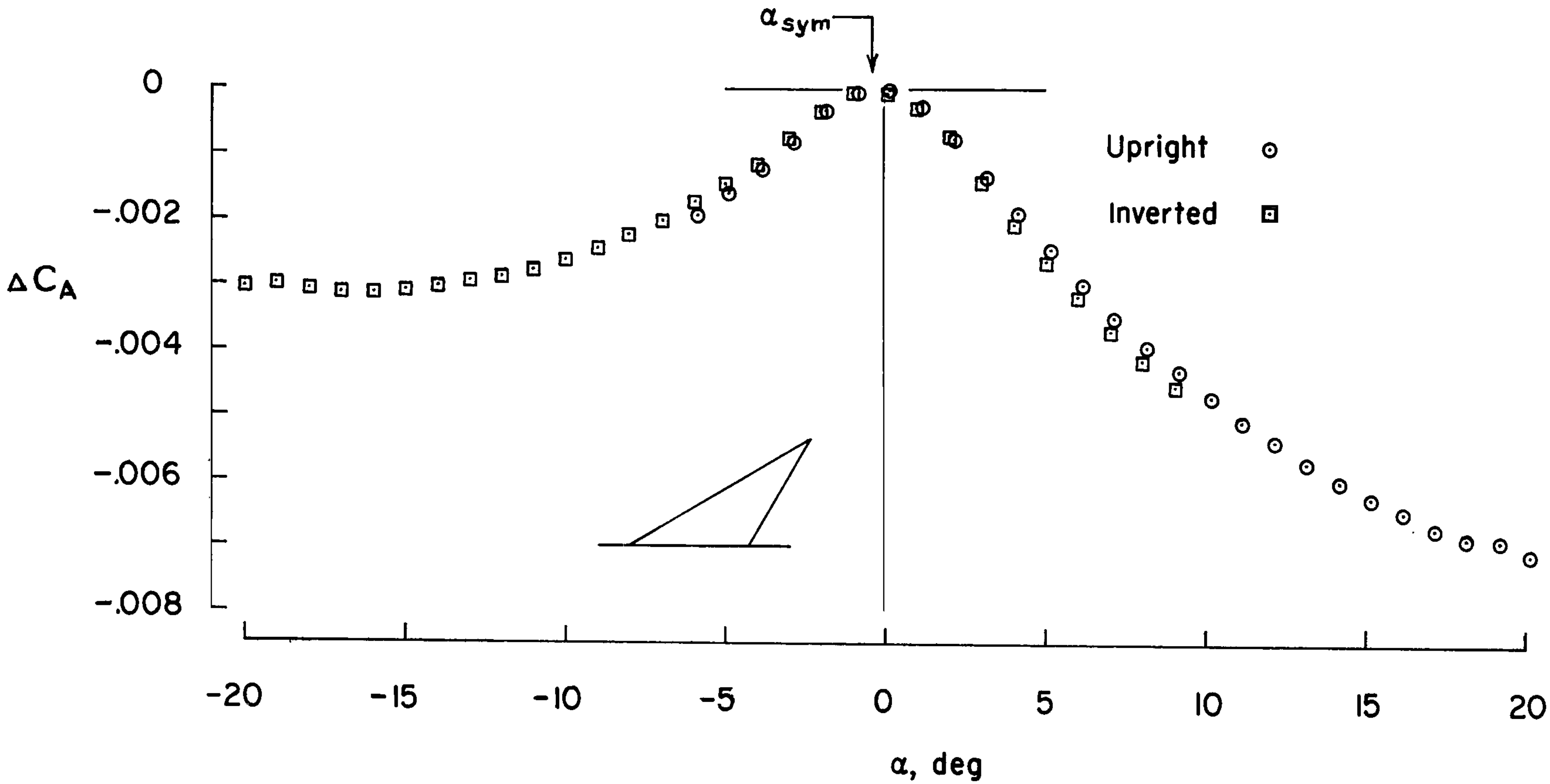

(b) Sharp leading edge at M = 2.16 and R = 2.0 × 10^6.

Figure 7.- Continued.

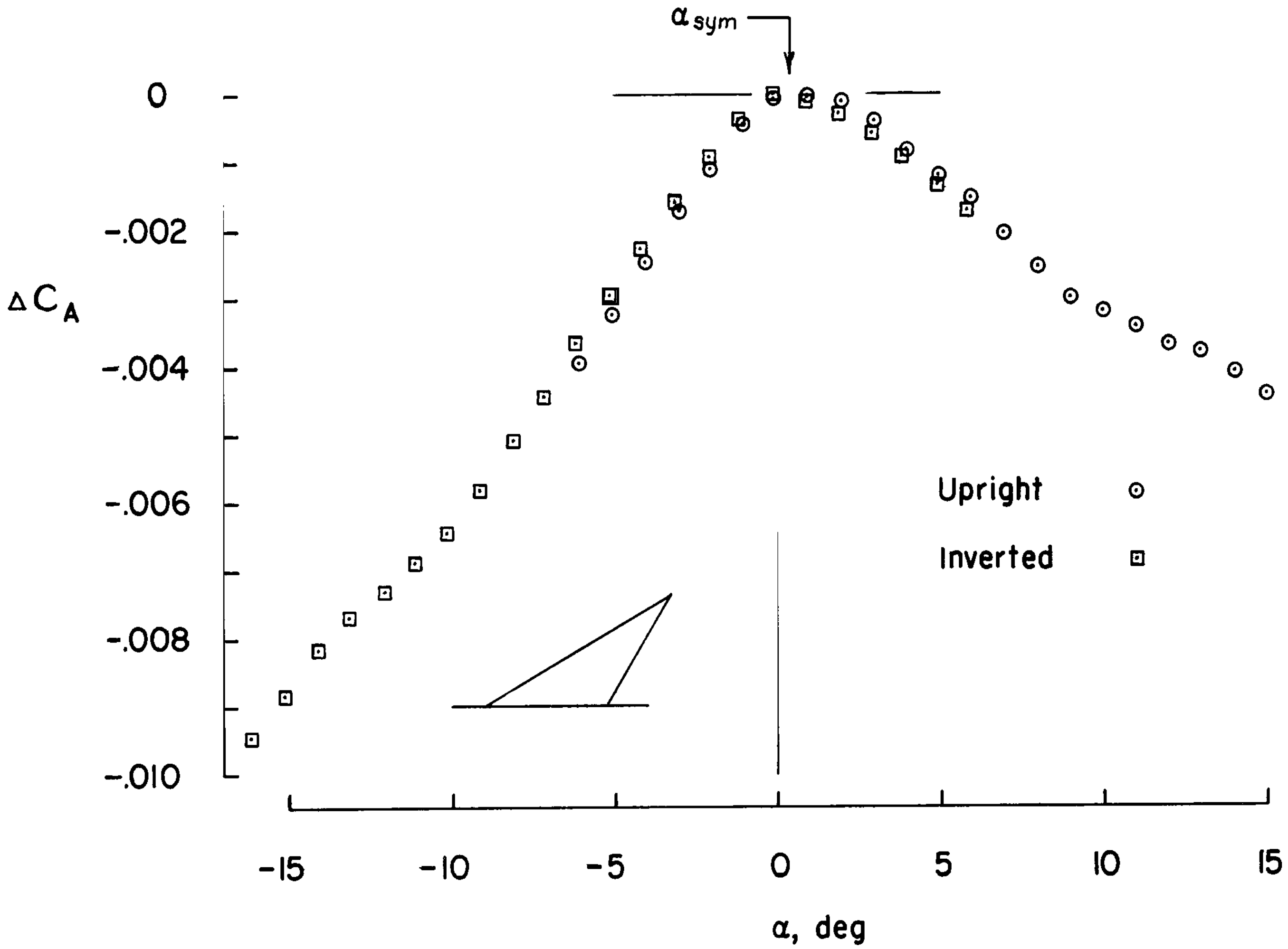

(c) $(r/c)_{le} = 0.00470$ at $M = 1.6$ and $R = 2.0 \times 10^6$.

Figure 7.- Continued.

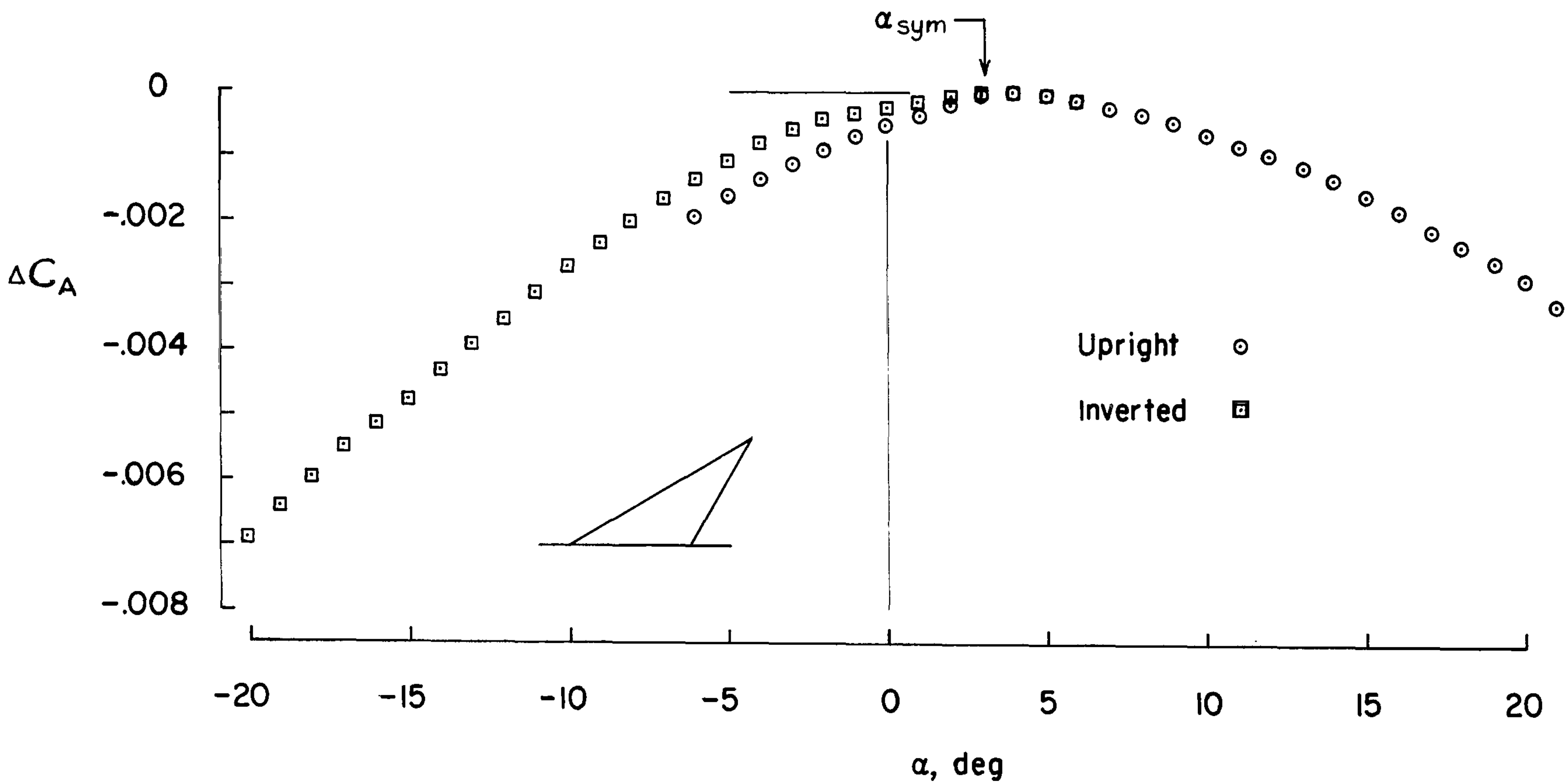

(d) $(r/c)_{le} = 0.00470$ at $M = 2.16$ and $R = 2.0 \times 10^6$.

Figure 7.- Concluded.

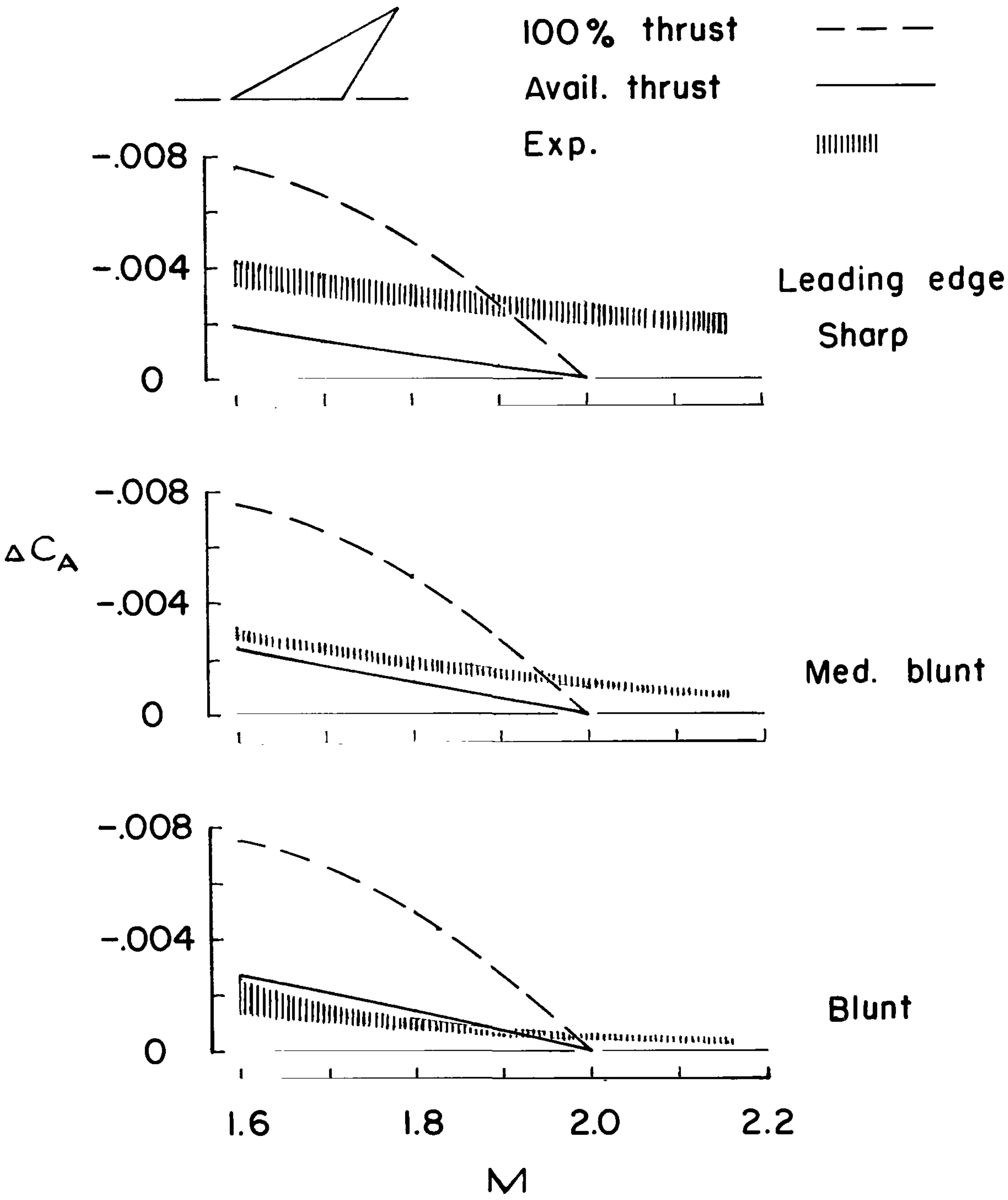

Figure 8.- Comparison of full and available leading-edge thrust theory with experiment for $\Delta\alpha = 5.0°$ and $R = 2.0 \times 10^6$.

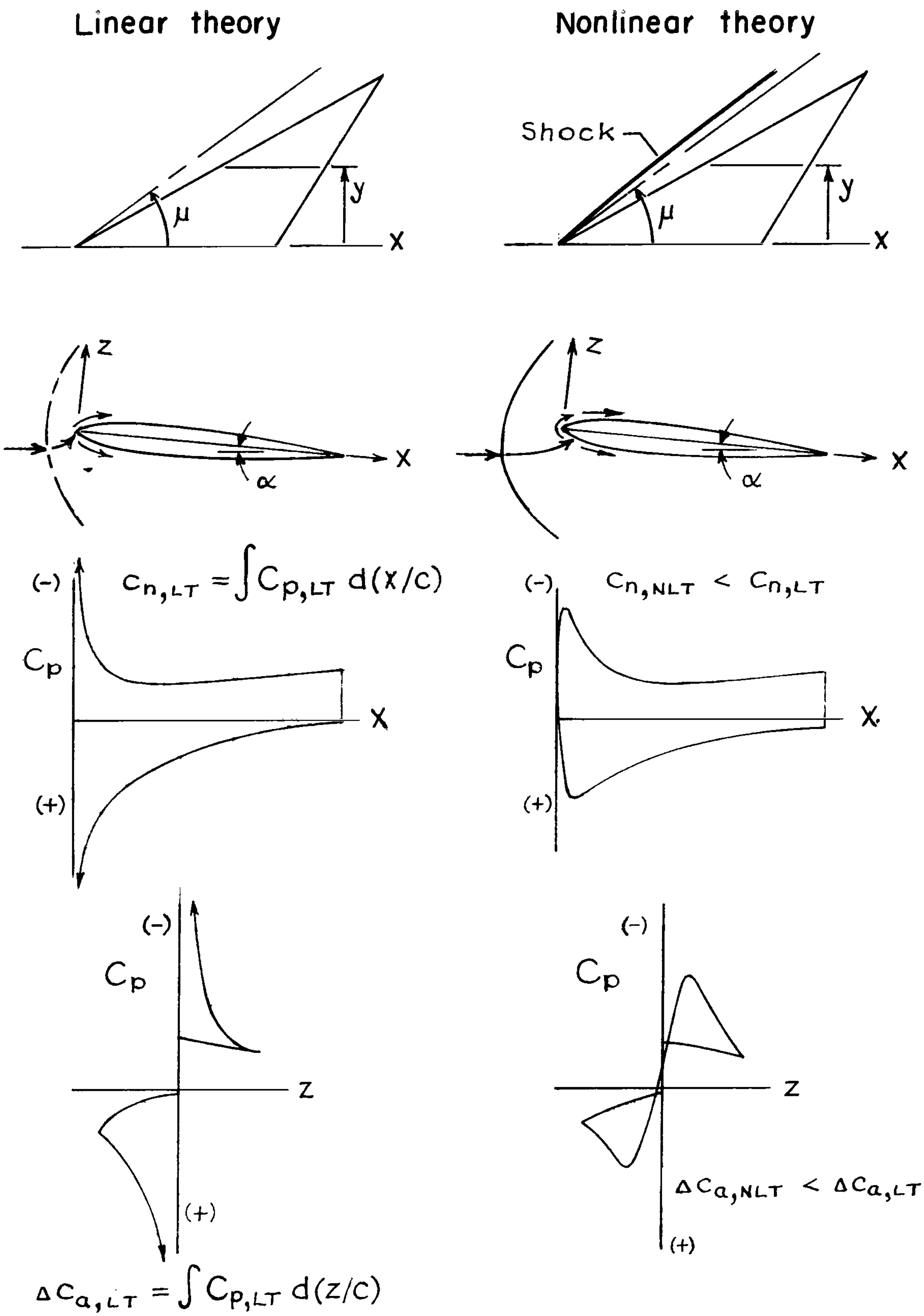

Figure 9.- Comparison of linear and nonlinear theory flow models.

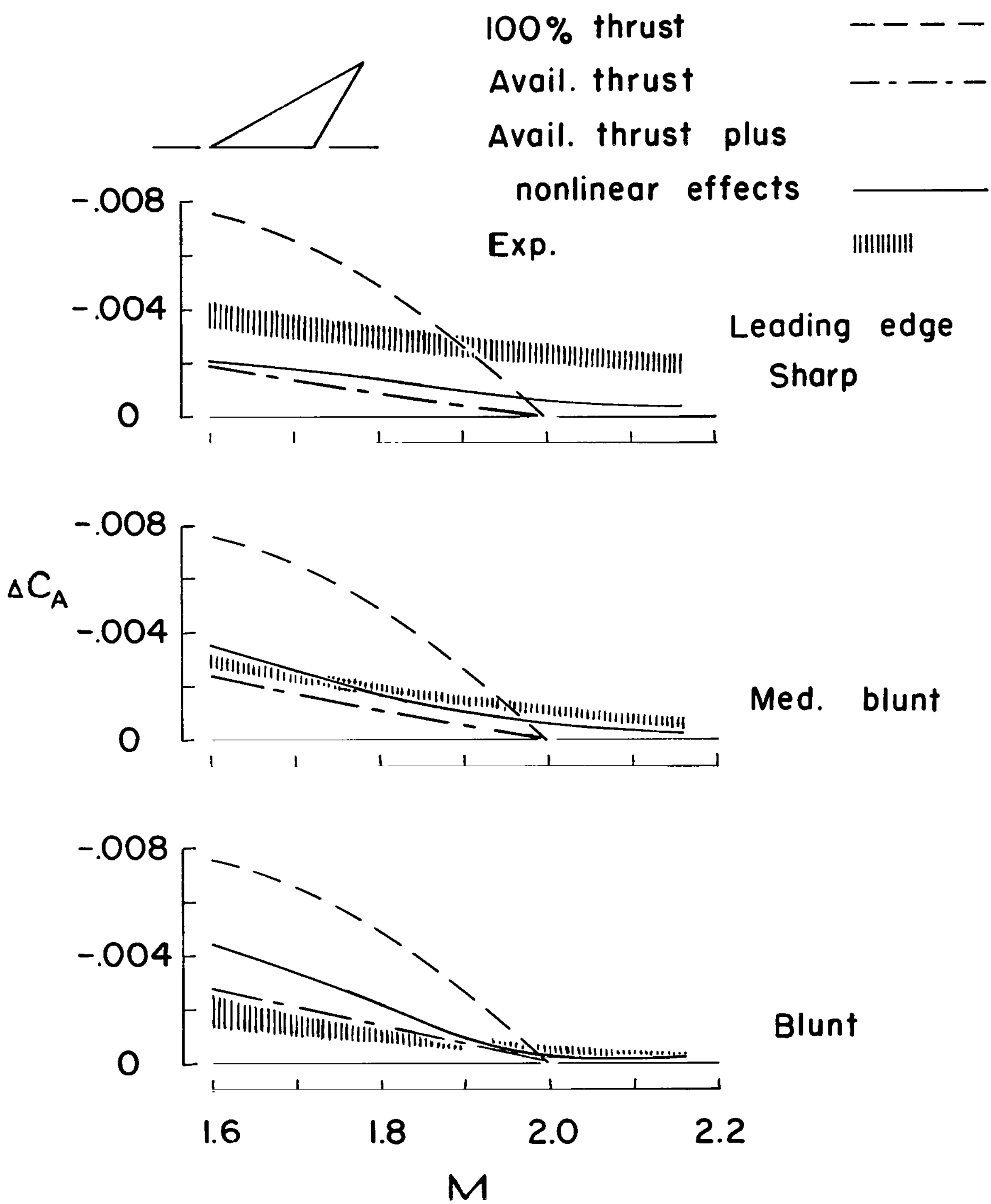

Figure 10.- Comparison of theoretical and experimental ΔC_A at $\Delta\alpha = 5.0°$ and $R = 2.0 \times 10^6$ with nonlinear corrections included.

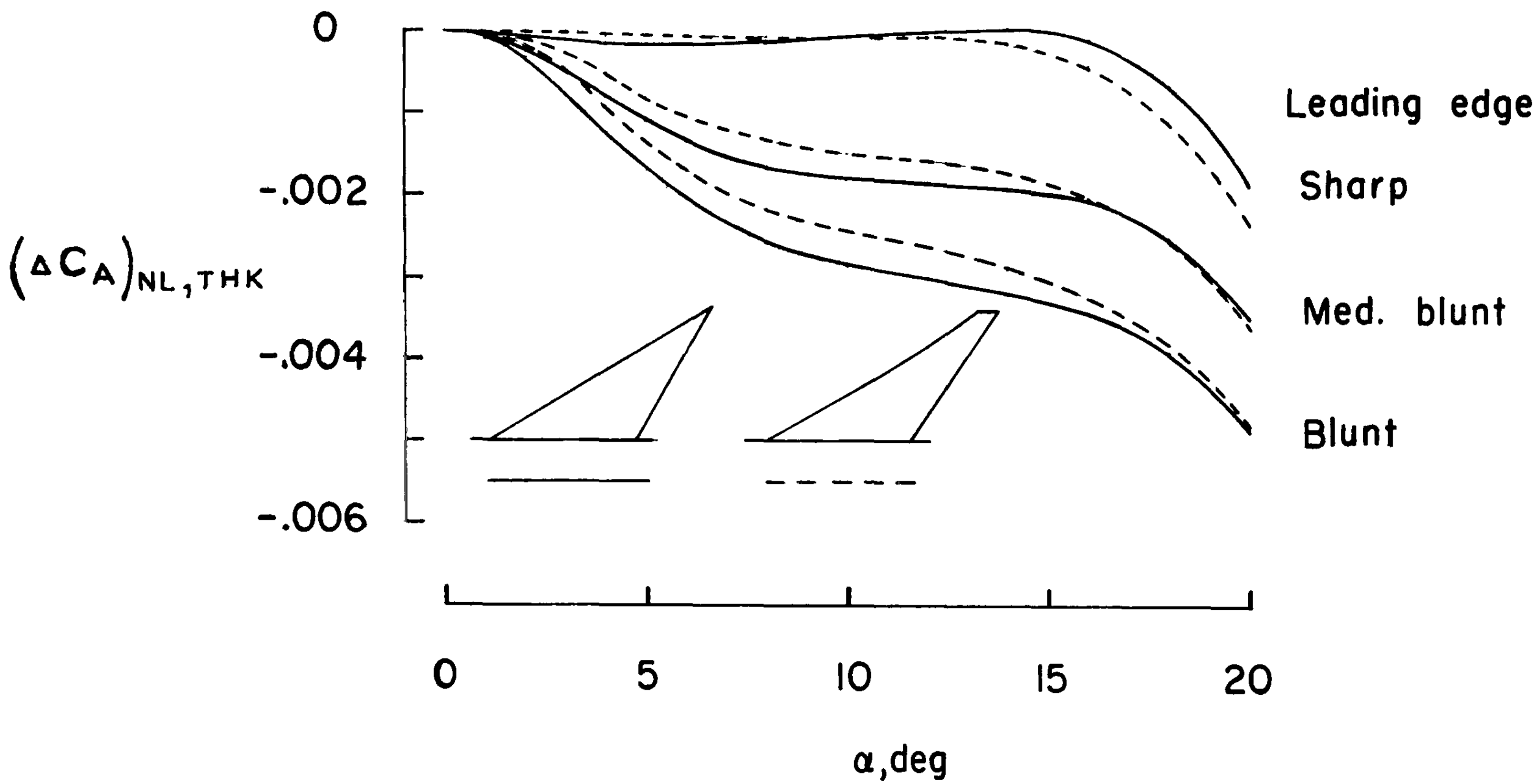

Figure 11.- Theoretical values of $(\Delta C_A)_{NL,THK}$ at $M = 1.6$ and $R = 2.0 \times 10^6$.

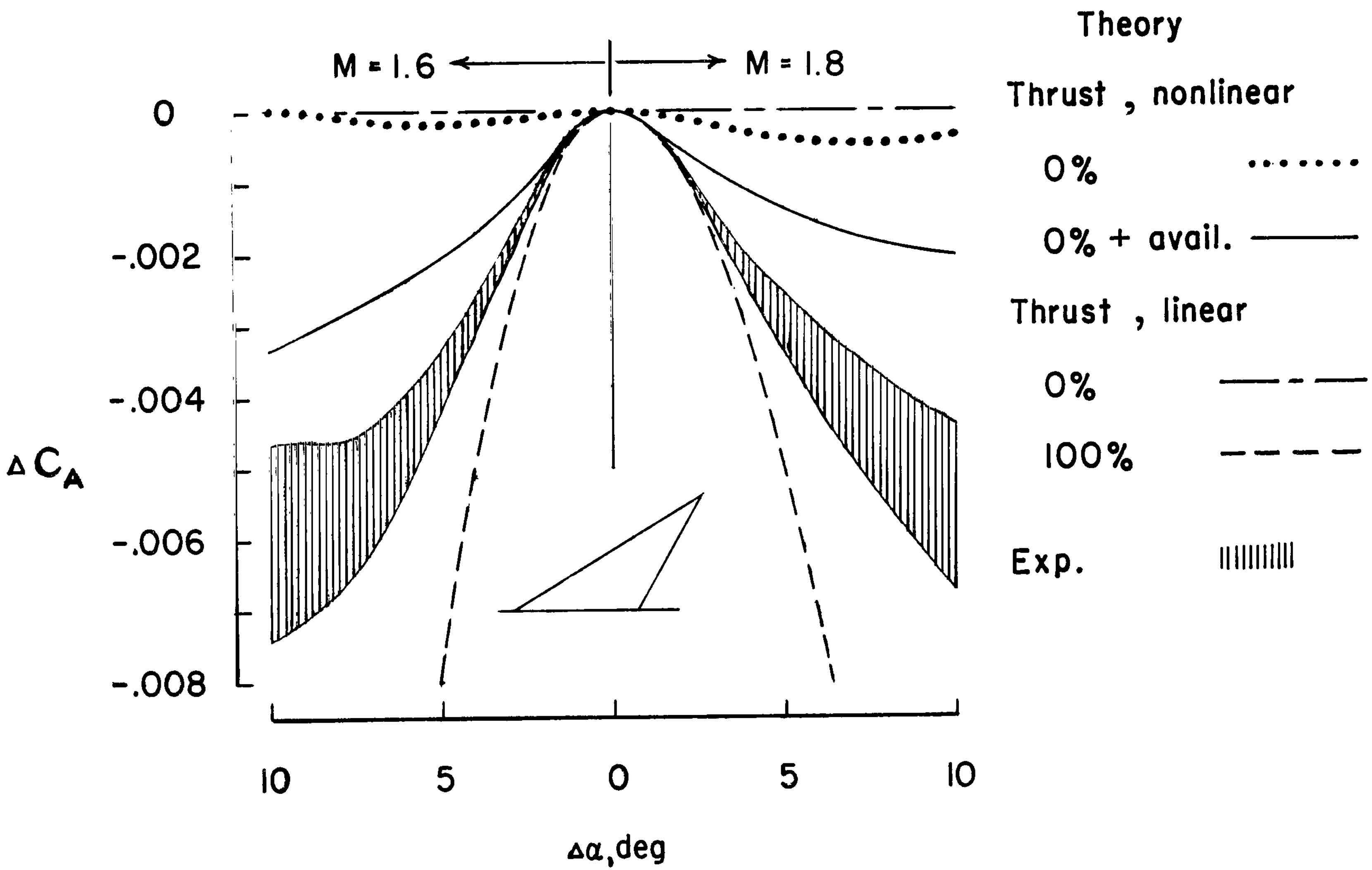

(a) Arrow wing; sharp leading edge; M = 1.6 and 1.8.

Figure 12.- Comparison of theoretical and experimental ΔC_A for $R = 2.0 \times 10^6$.

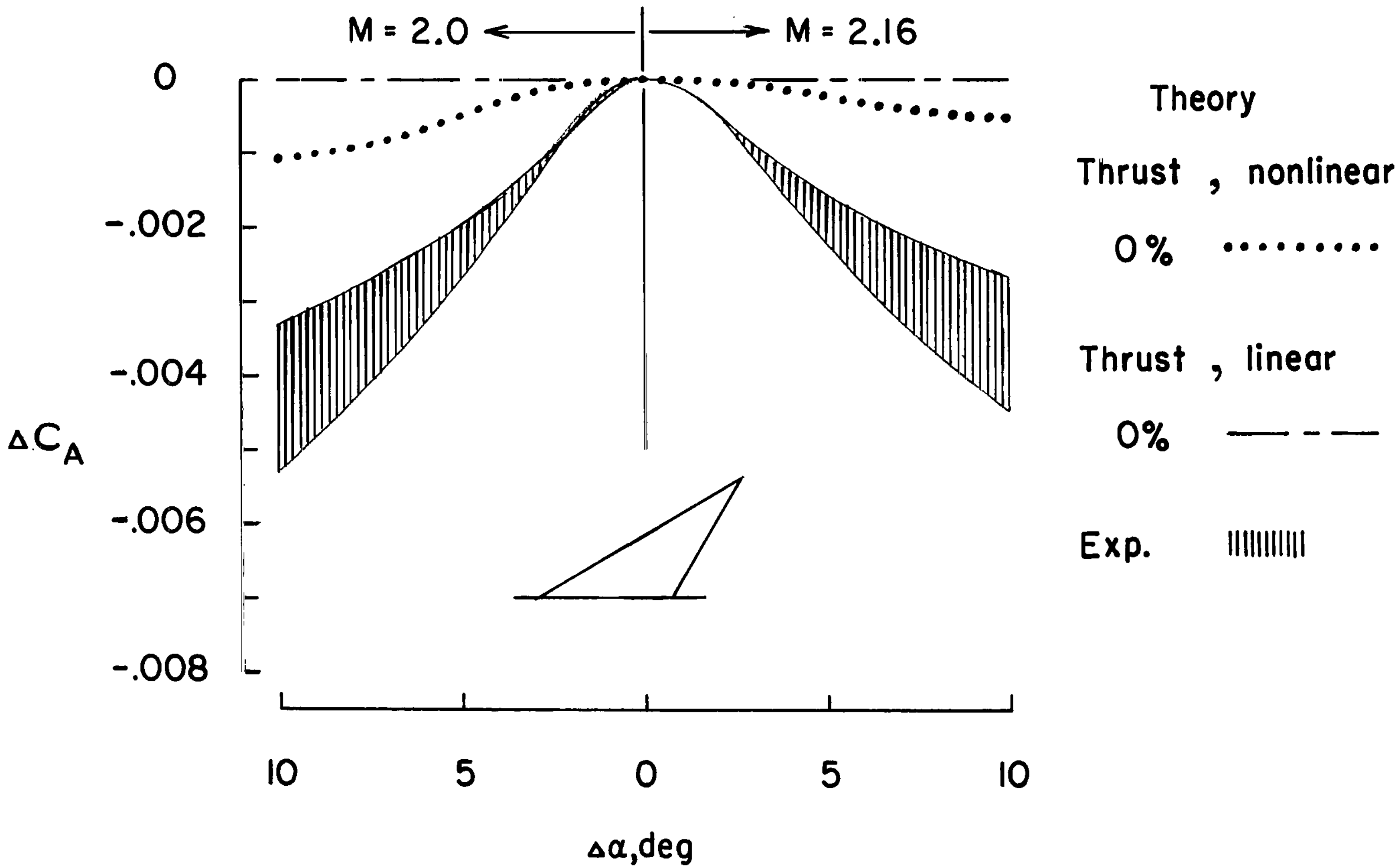

(b) Arrow wing; sharp leading edge; M = 2.0 and 2.16.

Figure 12.- Concluded.

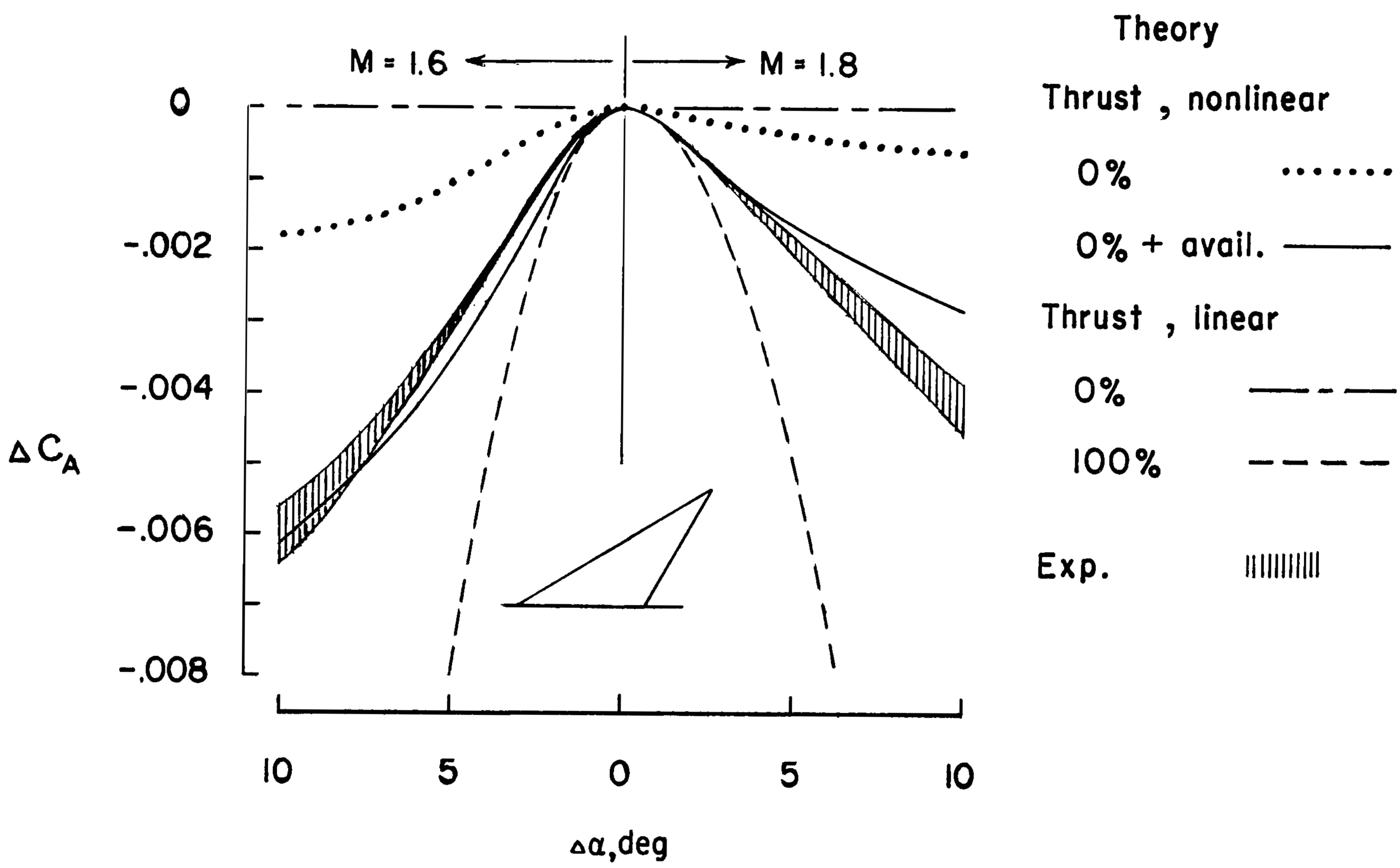

(a) Arrow wing; $(r/c)_{le} = 0.00235$; M = 1.6 and 1.8.

Figure 13.- Comparison of theoretical and experimental ΔC_A for $R = 2.0 \times 10^6$.

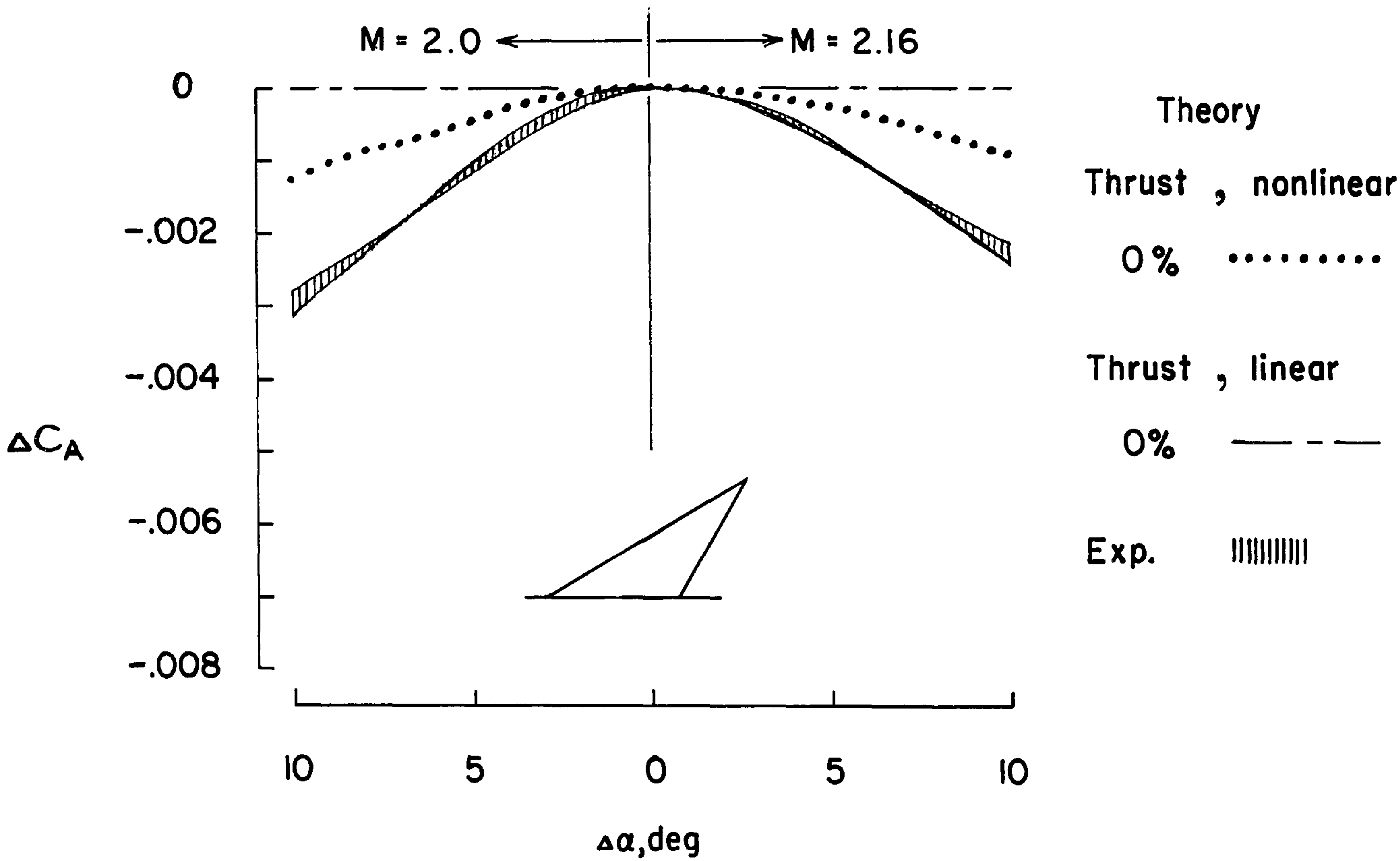

(b) Arrow wing; $(r/c)_{le} = 0.00235$; M = 2.0 and 2.16.

Figure 13.- Concluded.

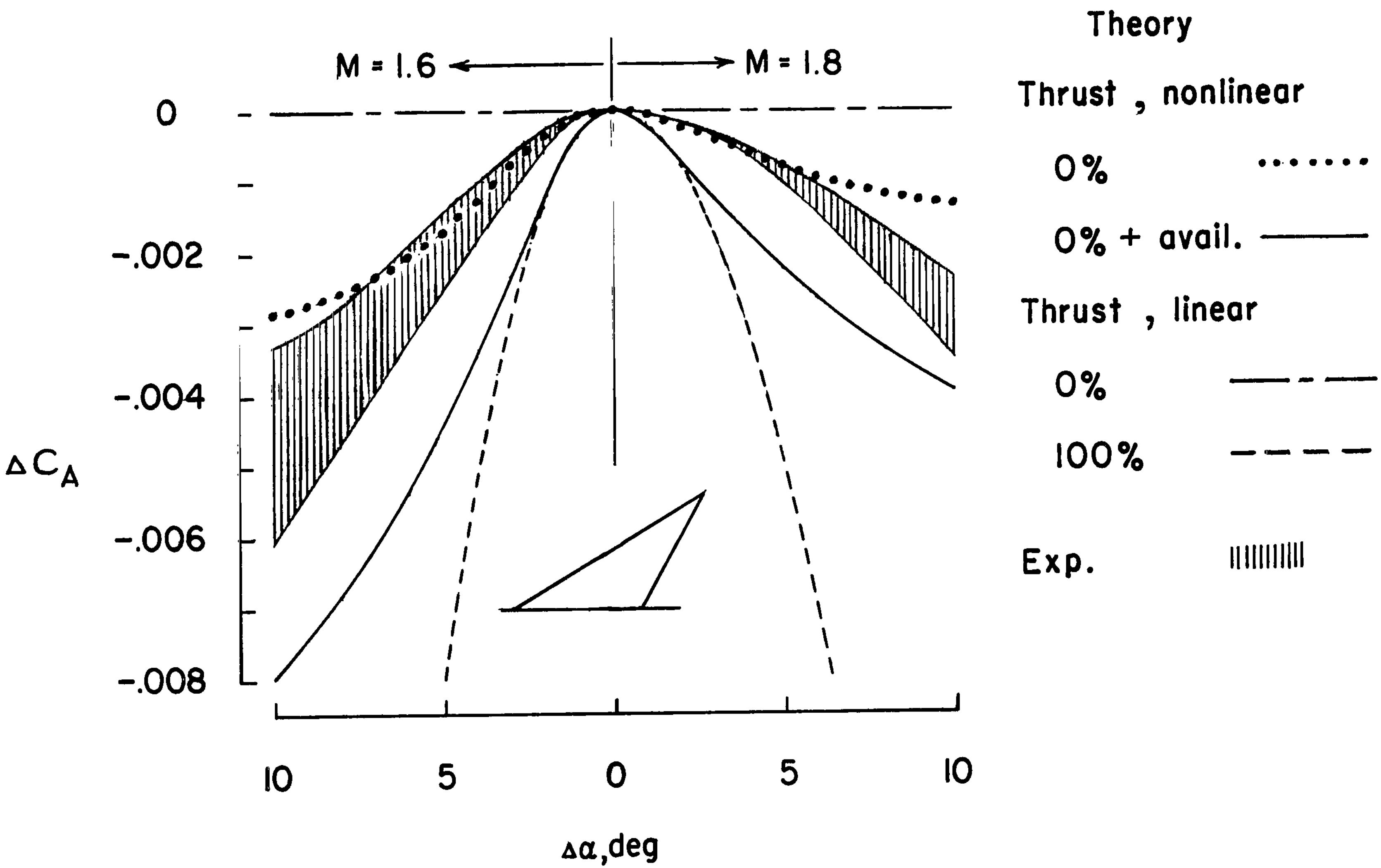

(a) Arrow wing; $(r/c)_{le} = 0.00470$; M = 1.6 and 1.8.

Figure 14.- Comparison of theoretical and experimental ΔC_A for $R = 2.0 \times 10^6$.

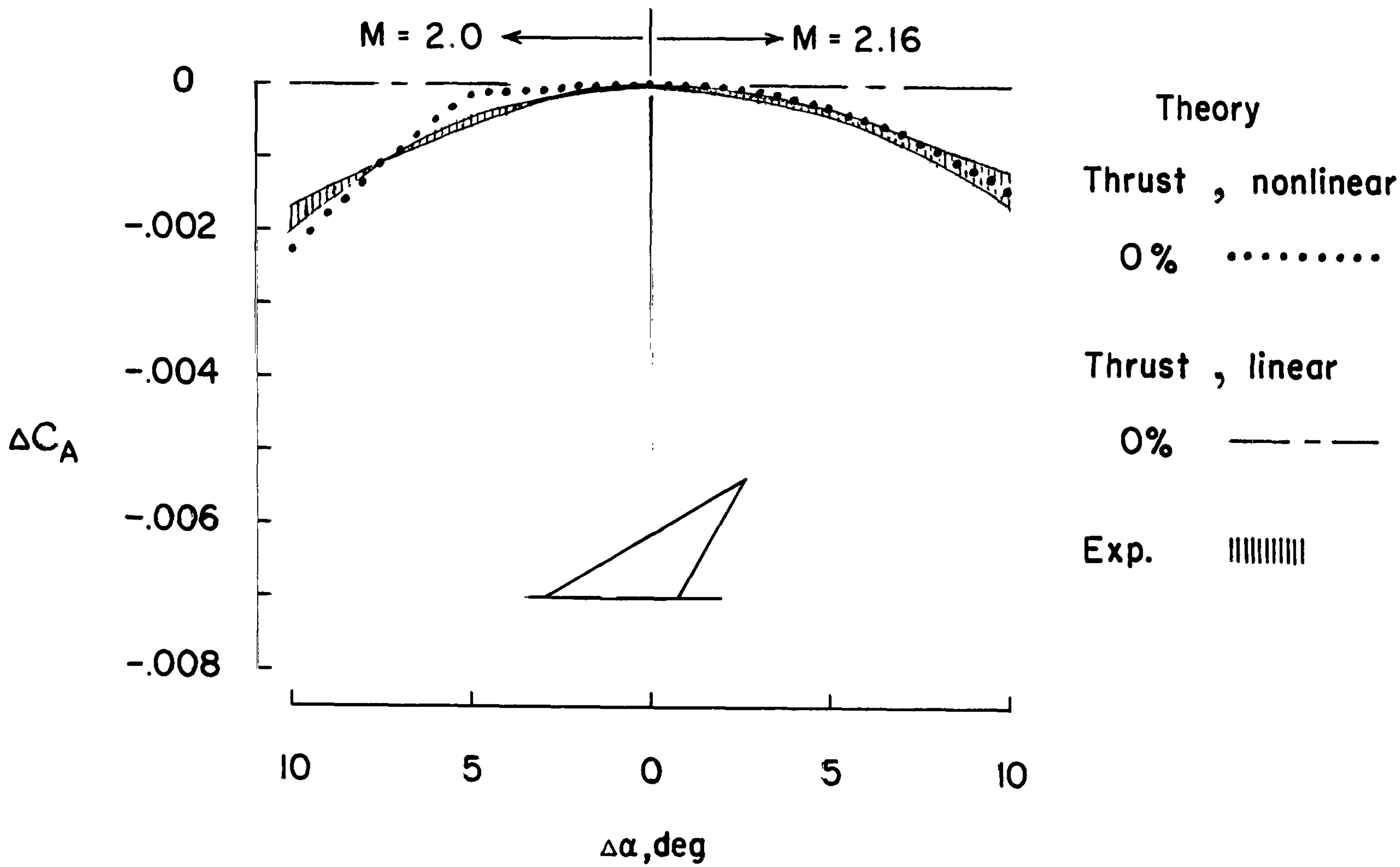

(b) Arrow wing; $(r/c)_{le}$ = 0.00470; M = 2.0 and 2.16.

Figure 14.- Concluded.

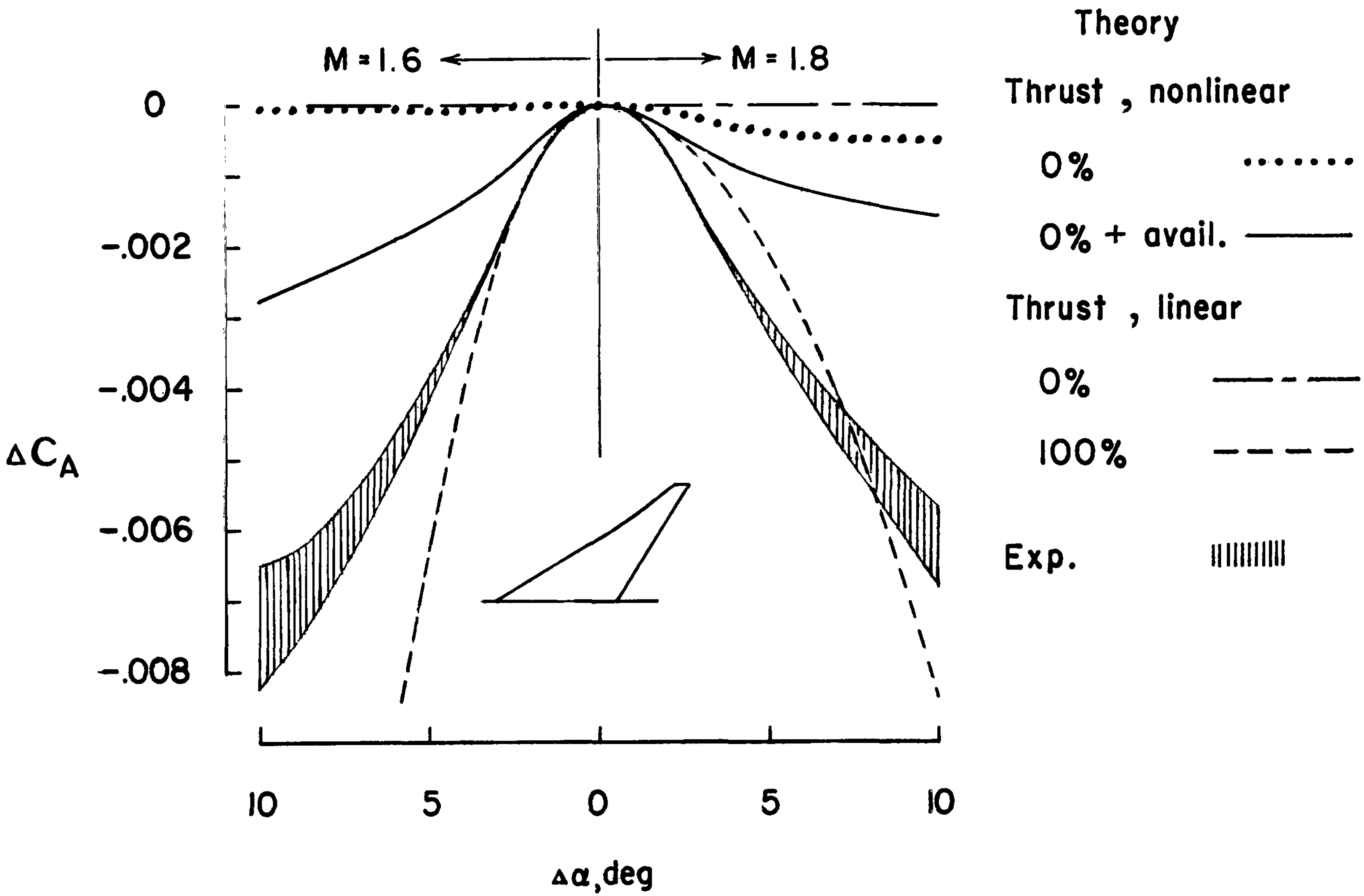

(a) Modified arrow wing; sharp leading edge; M = 1.6 and 1.8.

Figure 15.- Comparison of theoretical and experimental ΔC_A for $R = 2.0 \times 10^6$.

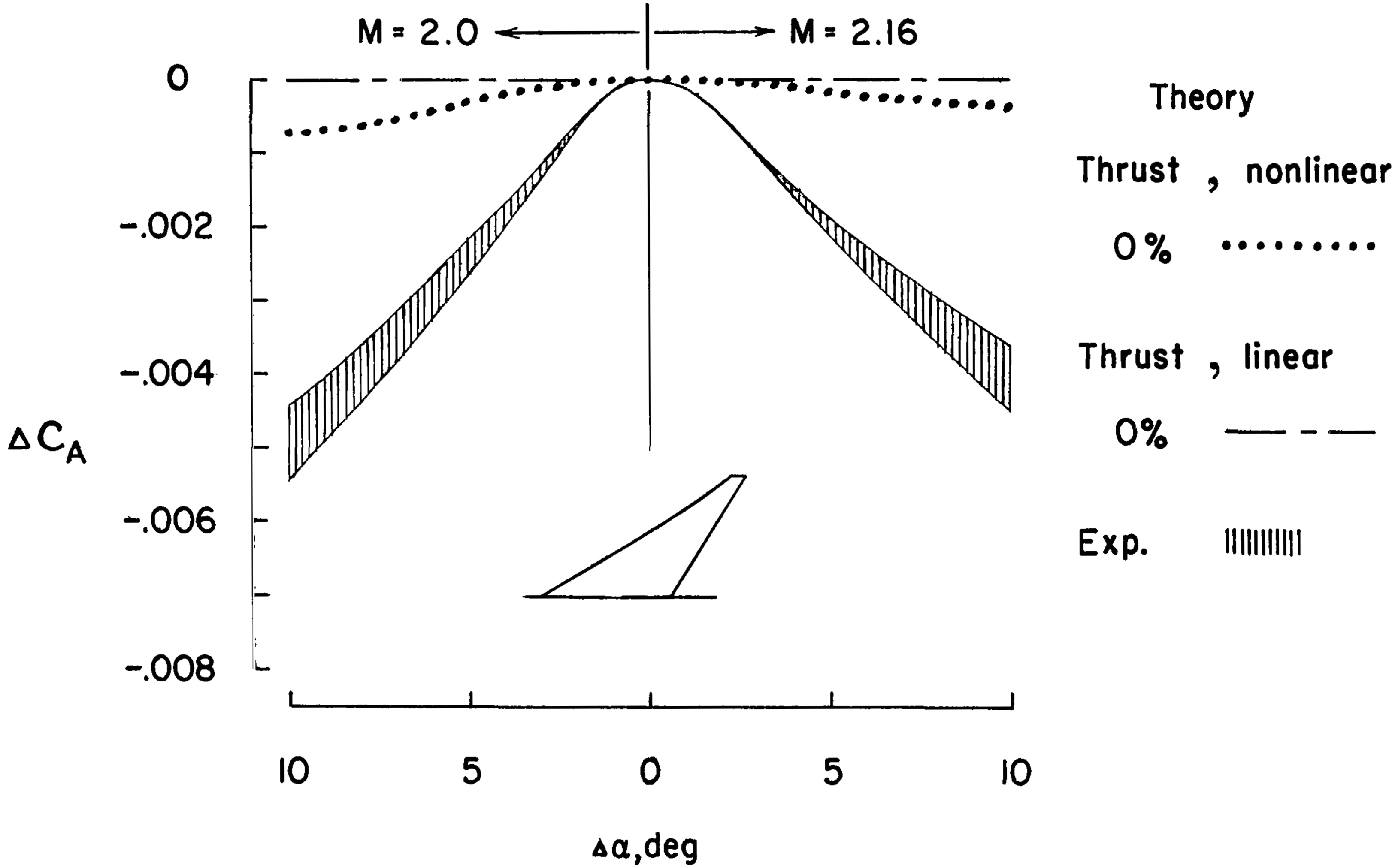

(b) Modified arrow wing; sharp leading edge; M = 2.0 and 2.16.

Figure 15.- Concluded.

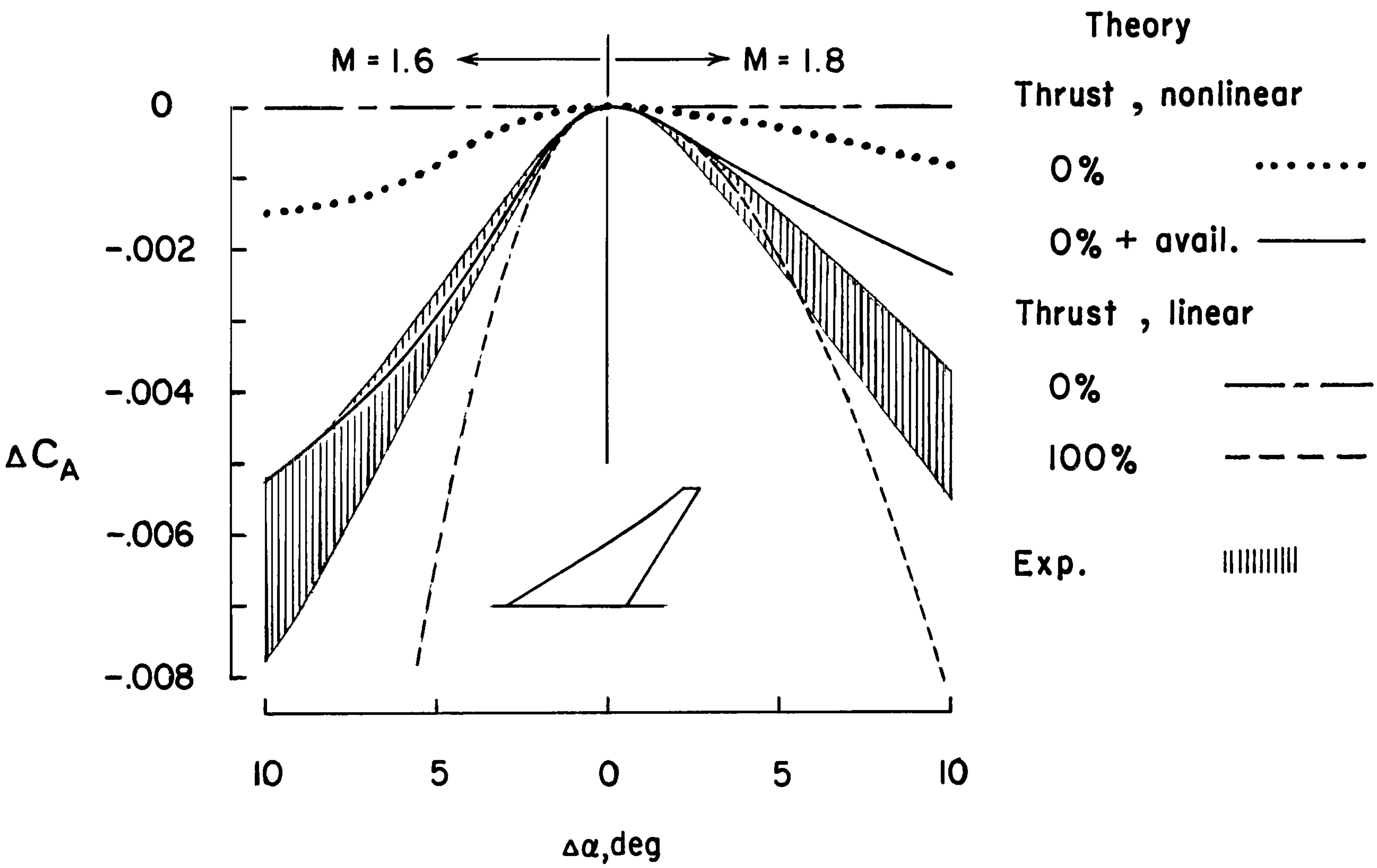

(a) Modified arrow wing; $(r/c)_{le} = 0.00235$; M = 1.6 and 1.8.

Figure 16.- Comparison of theoretical and experimental ΔC_A for $R = 2.0 \times 10^6$.

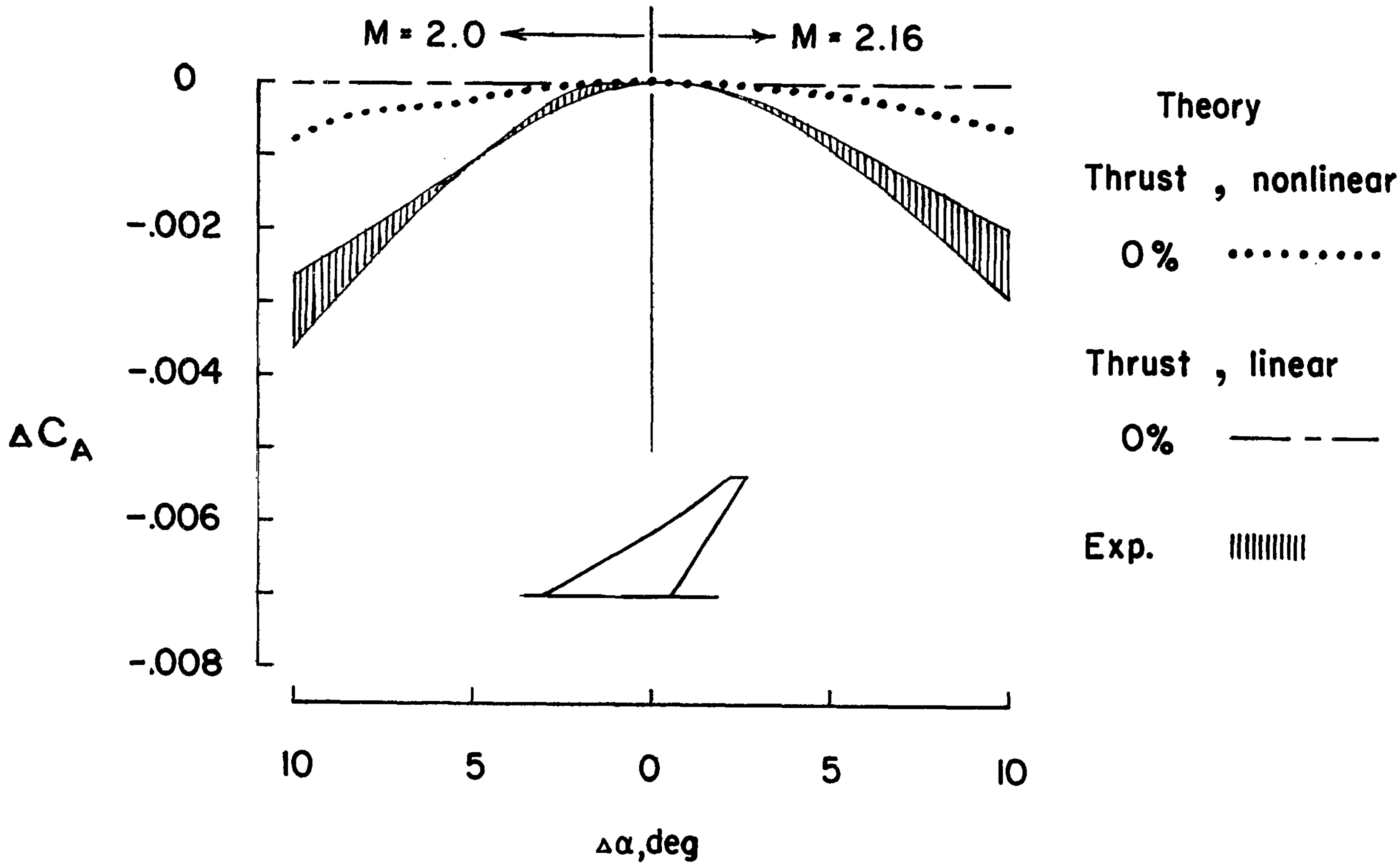

(b) Modified arrow wing; $(r/c)_{le} = 0.00235$; M = 2.0 and 2.16.

Figure 16.- Concluded.

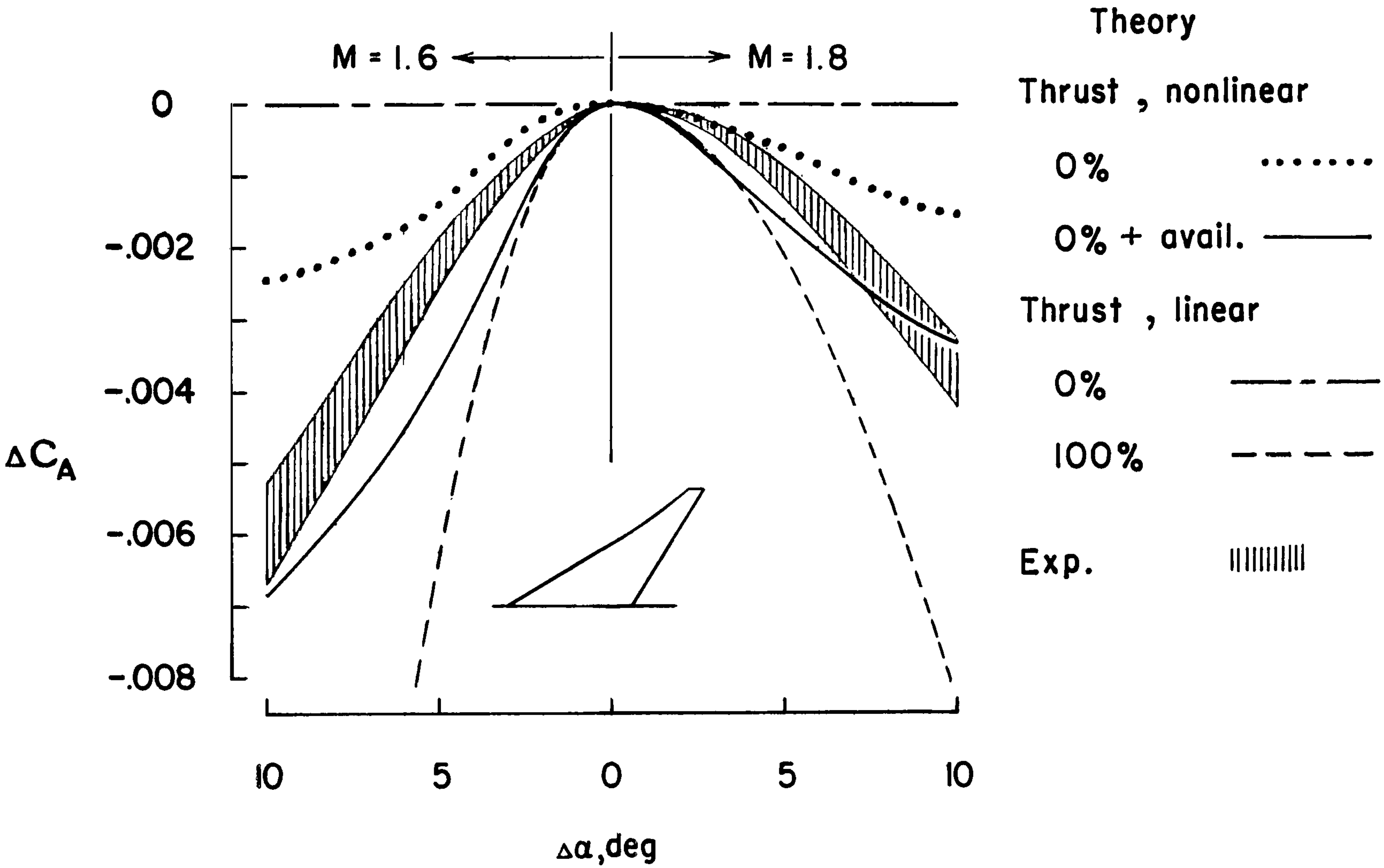

(a) Modified arrow wing; $(r/c)_{le} = 0.00470$; M = 1.6 and 1.8.

Figure 17.- Comparison of theoretical and experimental ΔC_A for $R = 2.0 \times 10^6$.

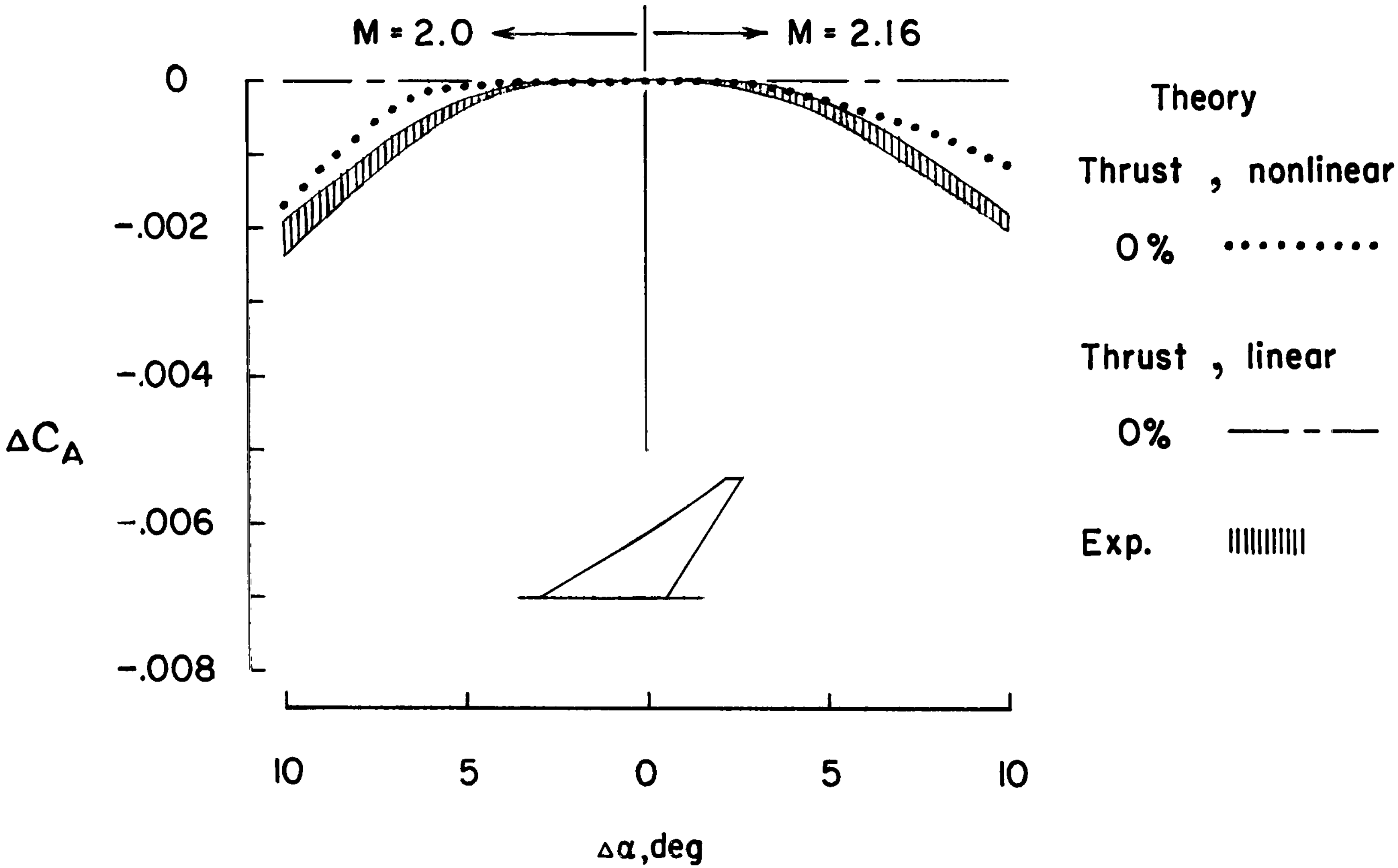

(b) Modified arrow wing; $(r/c)_{le} = 0.00470$; M = 2.0 and 2.16.

Figure 17.- Concluded.

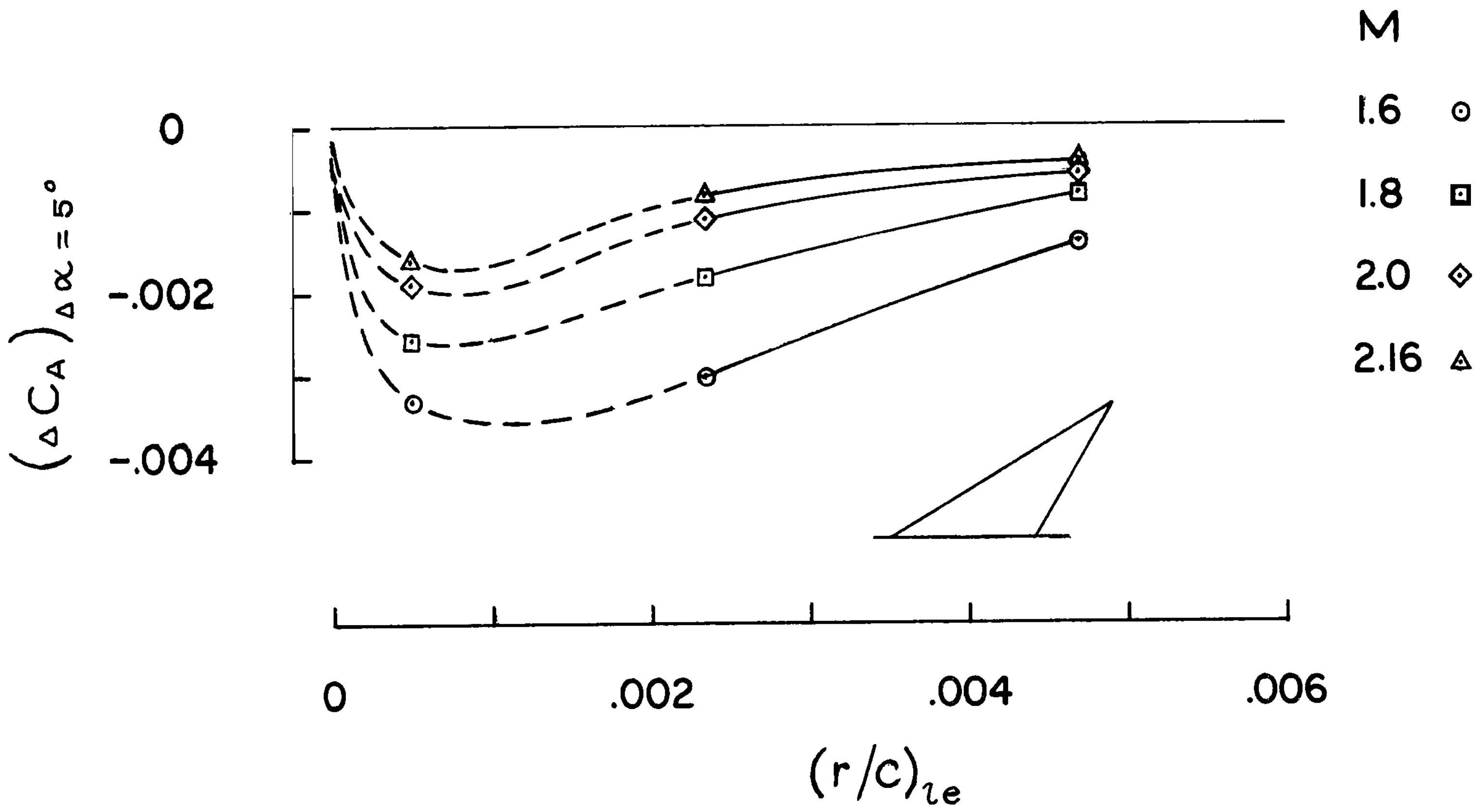

(a) Arrow wing at $R = 2.0 \times 10^6$.

Figure 18.- Effect of leading-edge bluntness on ΔC_A.

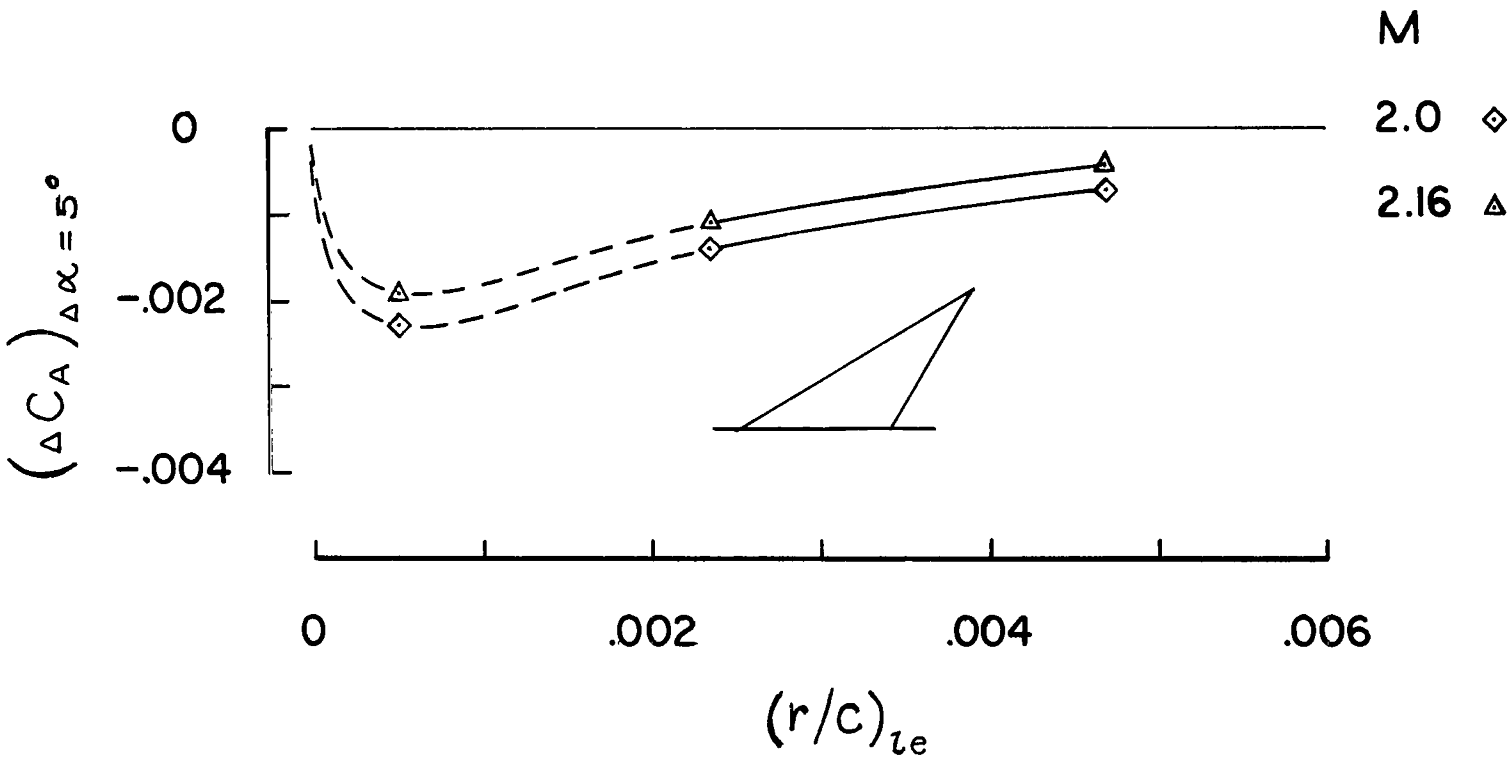

(b) Arrow wing at $R = 5.0 \times 10^6$.

Figure 18.- Continued.

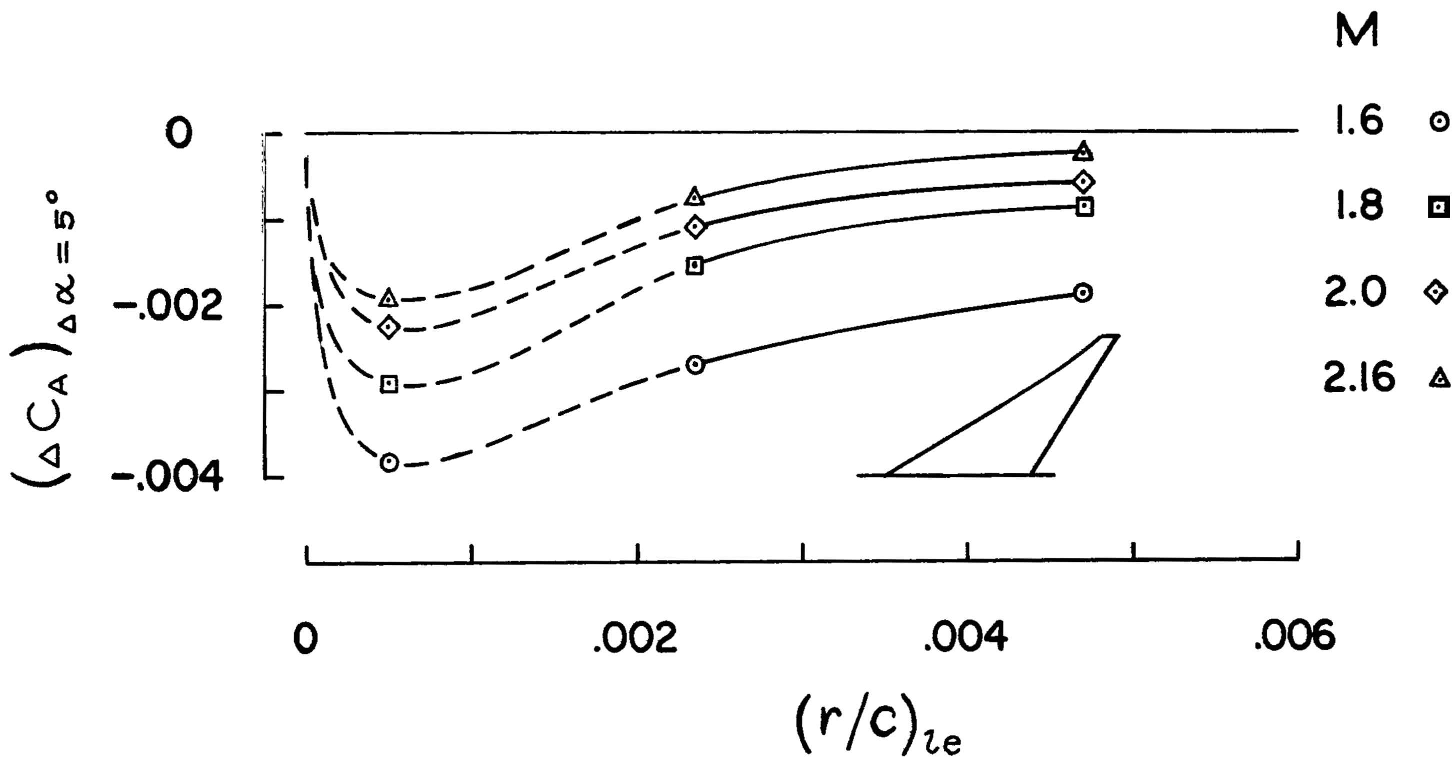

(c) Modified arrow wing at $R = 2.0 \times 10^6$.

Figure 18.- Concluded.

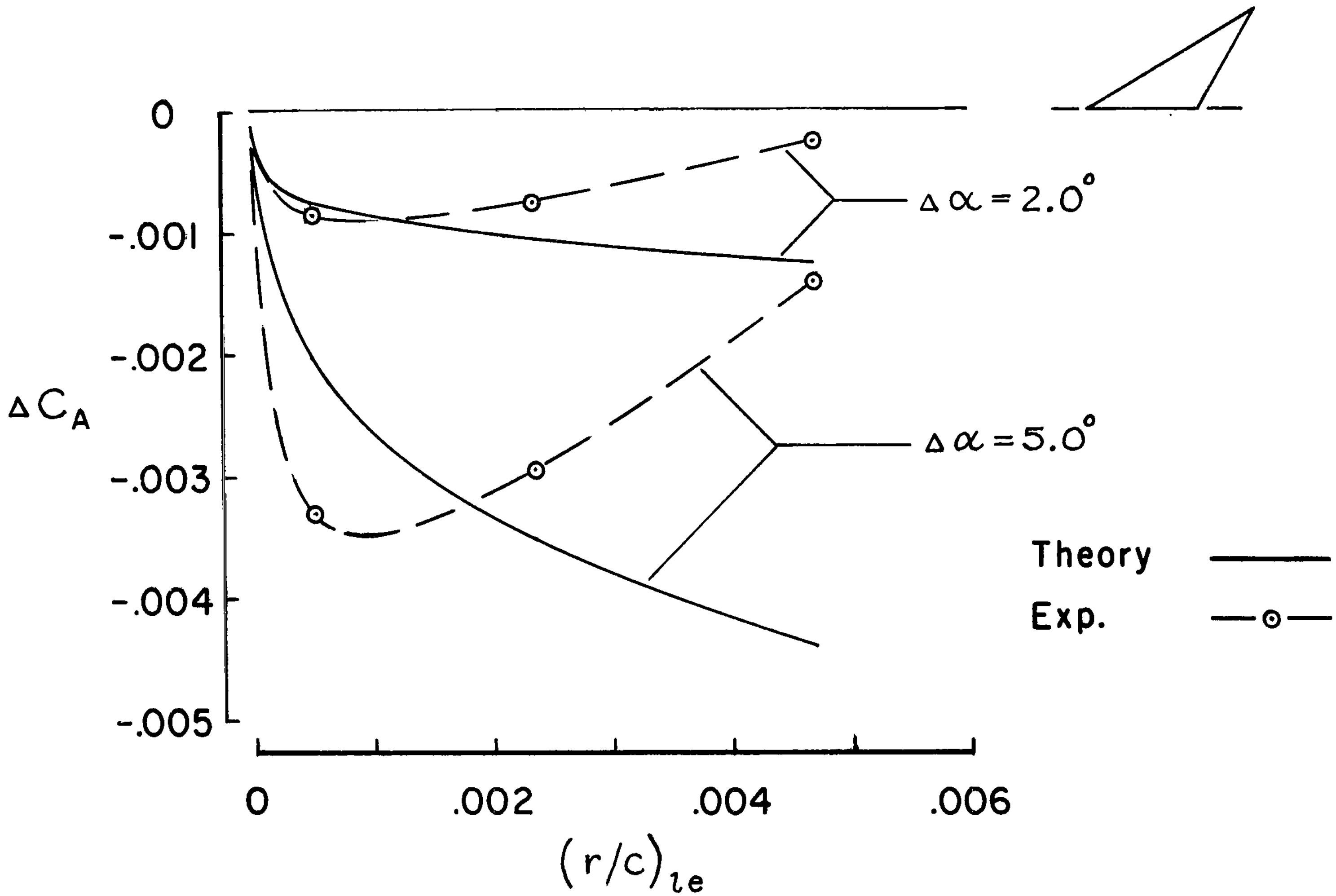

Figure 19.- Comparison of theory and experiment for arrow wing at $M = 1.6$ and $R = 2.0 \times 10^6$.

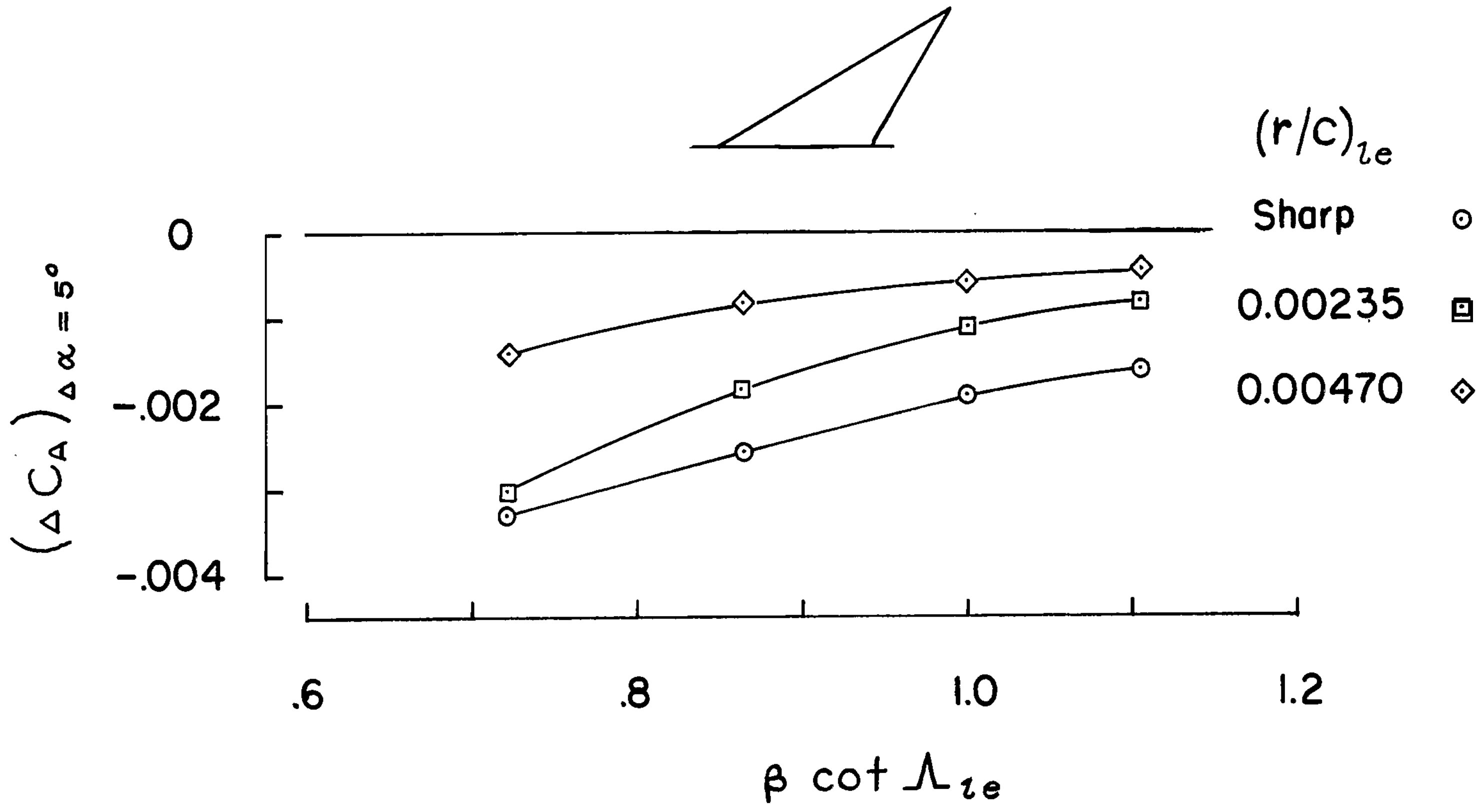

Figure 20.- Effect of sweep parameter $\beta \cot \Lambda_{le}$ on ΔC_A at $R = 2.0 \times 10^6$.

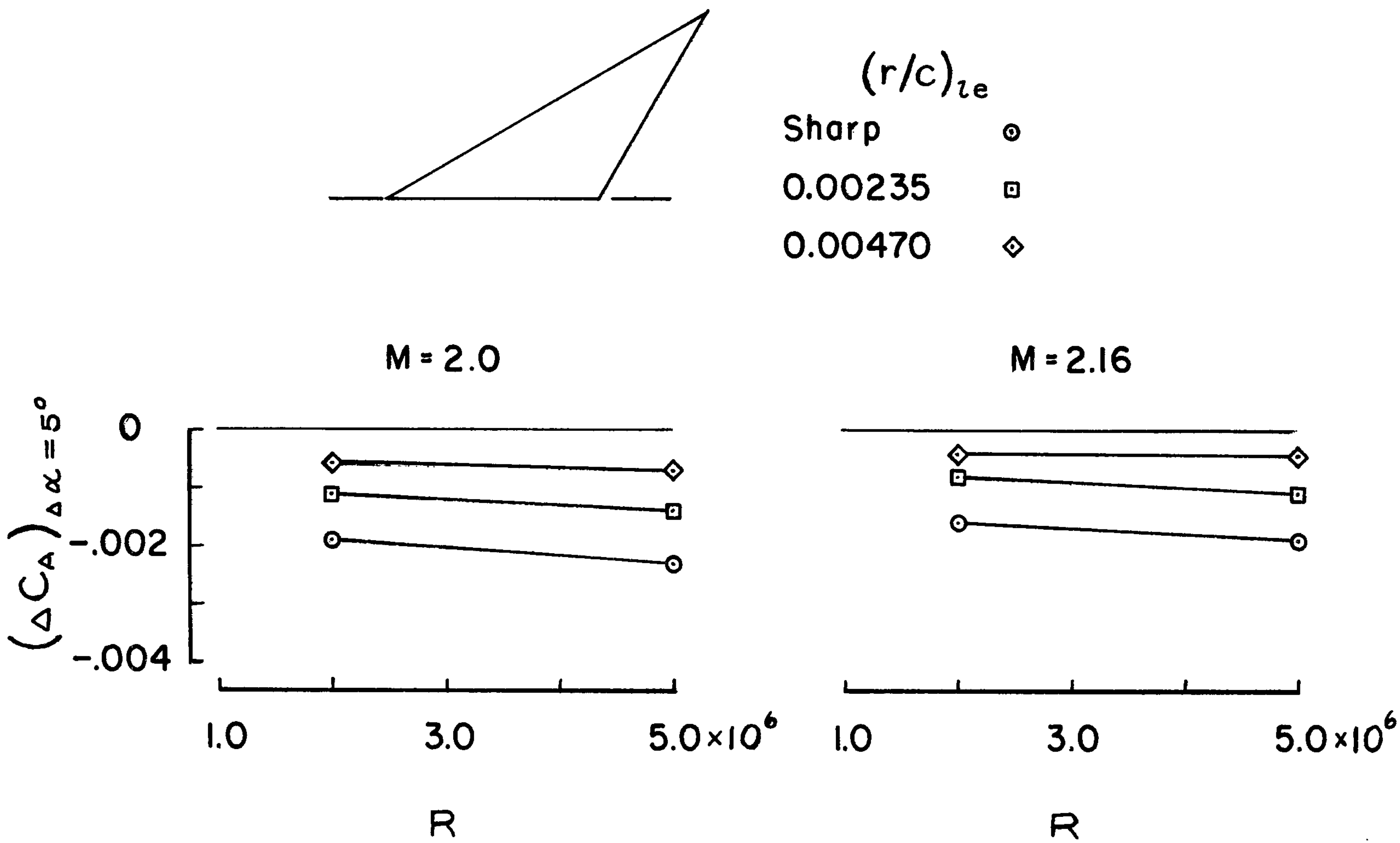

Figure 21.- Effect of Reynolds number on ΔC_A for arrow wings.

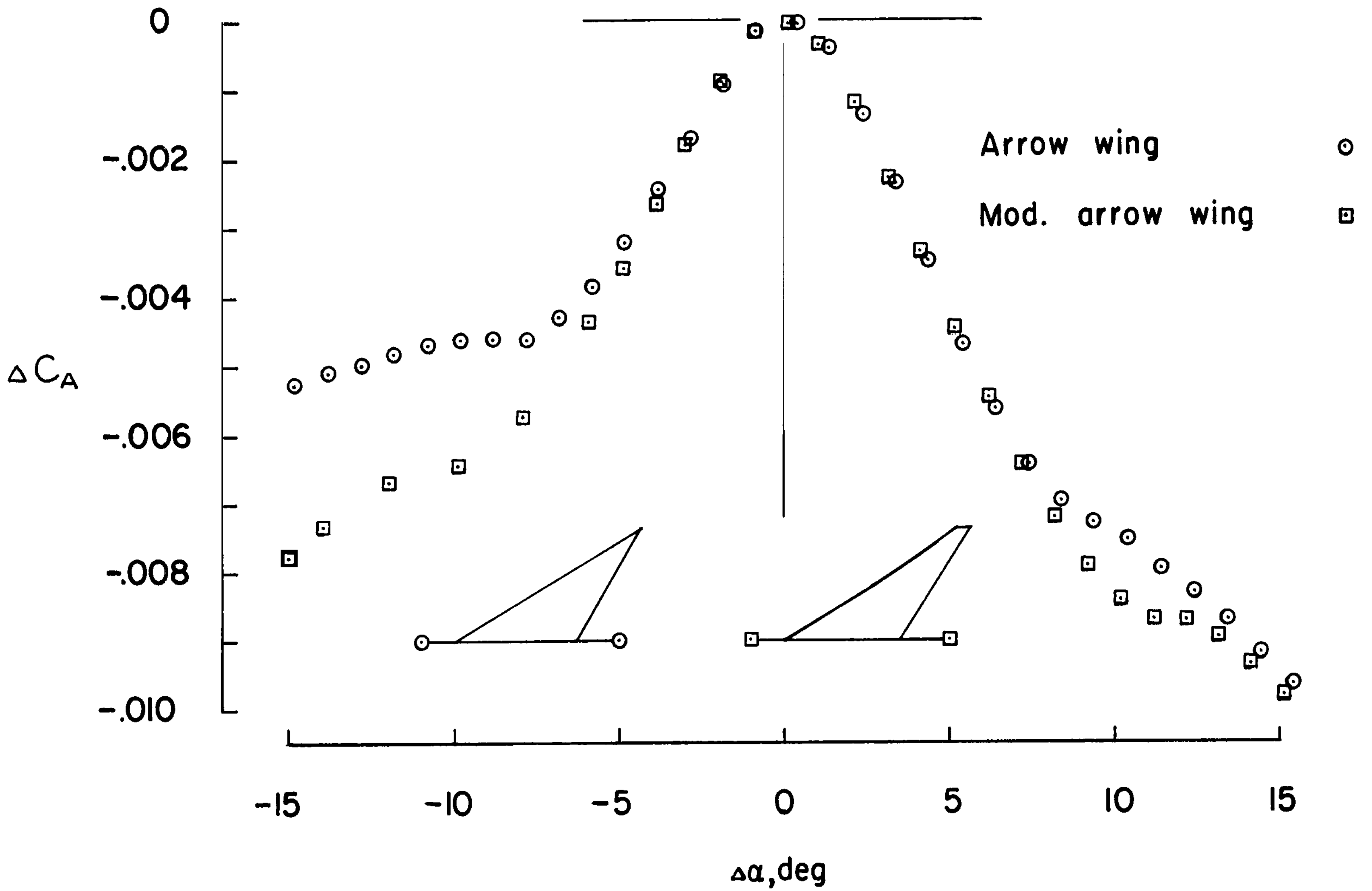

(a) Sharp leading edge.

Figure 22.- Effect of planform on ΔC_A at $M = 1.6$ and $R = 2.0 \times 10^6$.

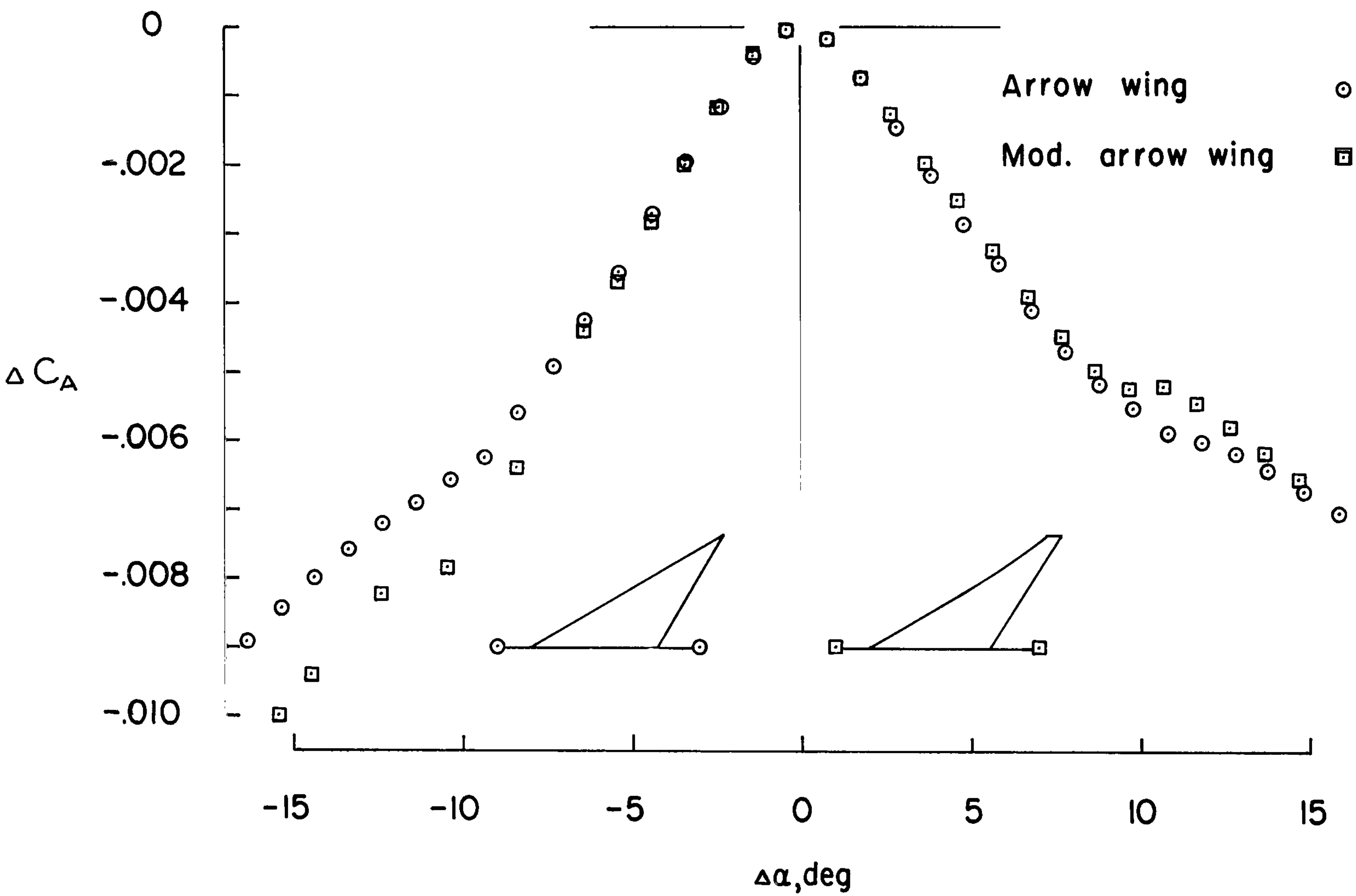

(b) $(r/c)_{le} = 0.00235$.

Figure 22.- Continued.

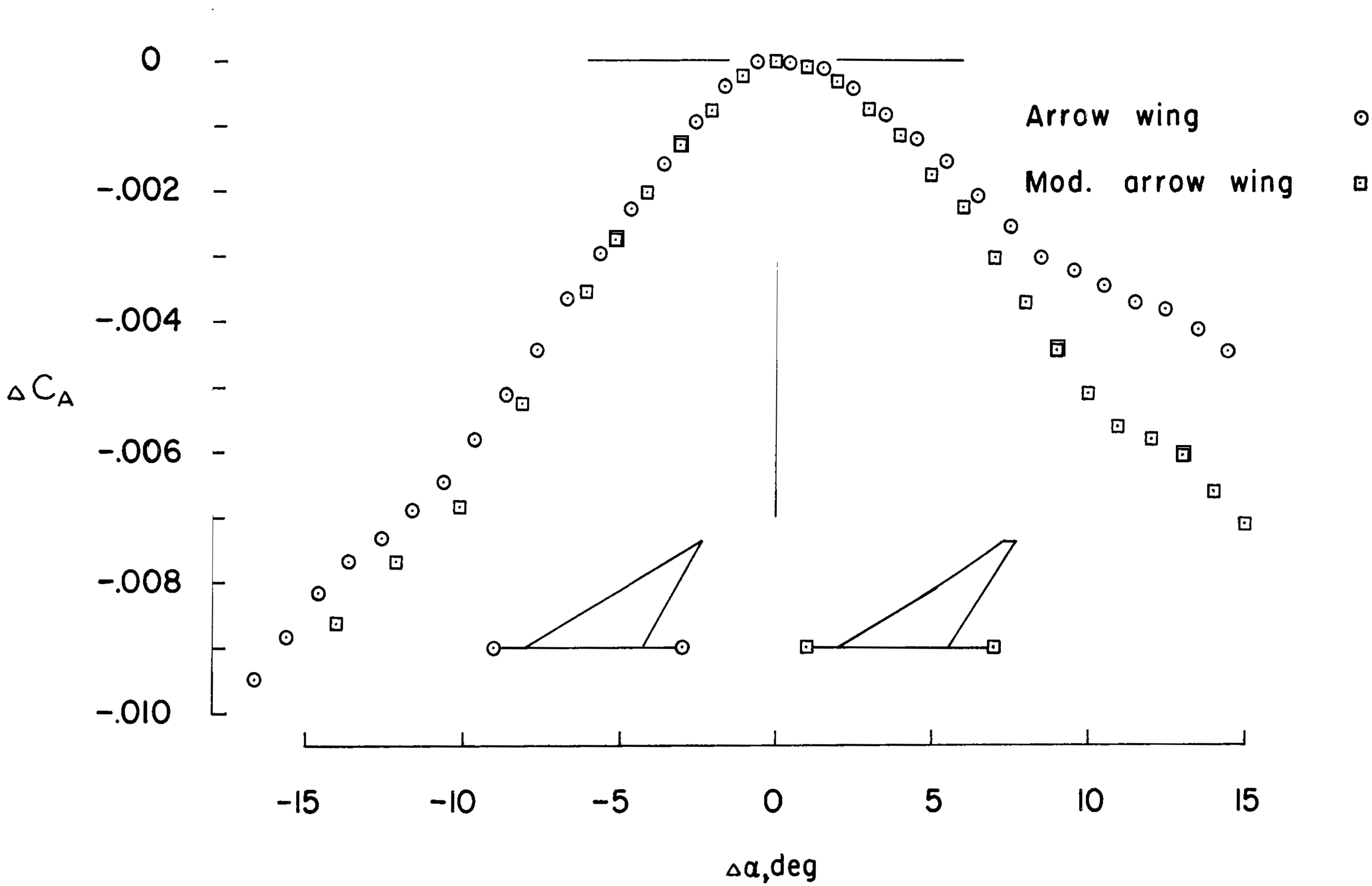

(c) $(r/c)_{le} = 0.00470.$

Figure 22.- Concluded.

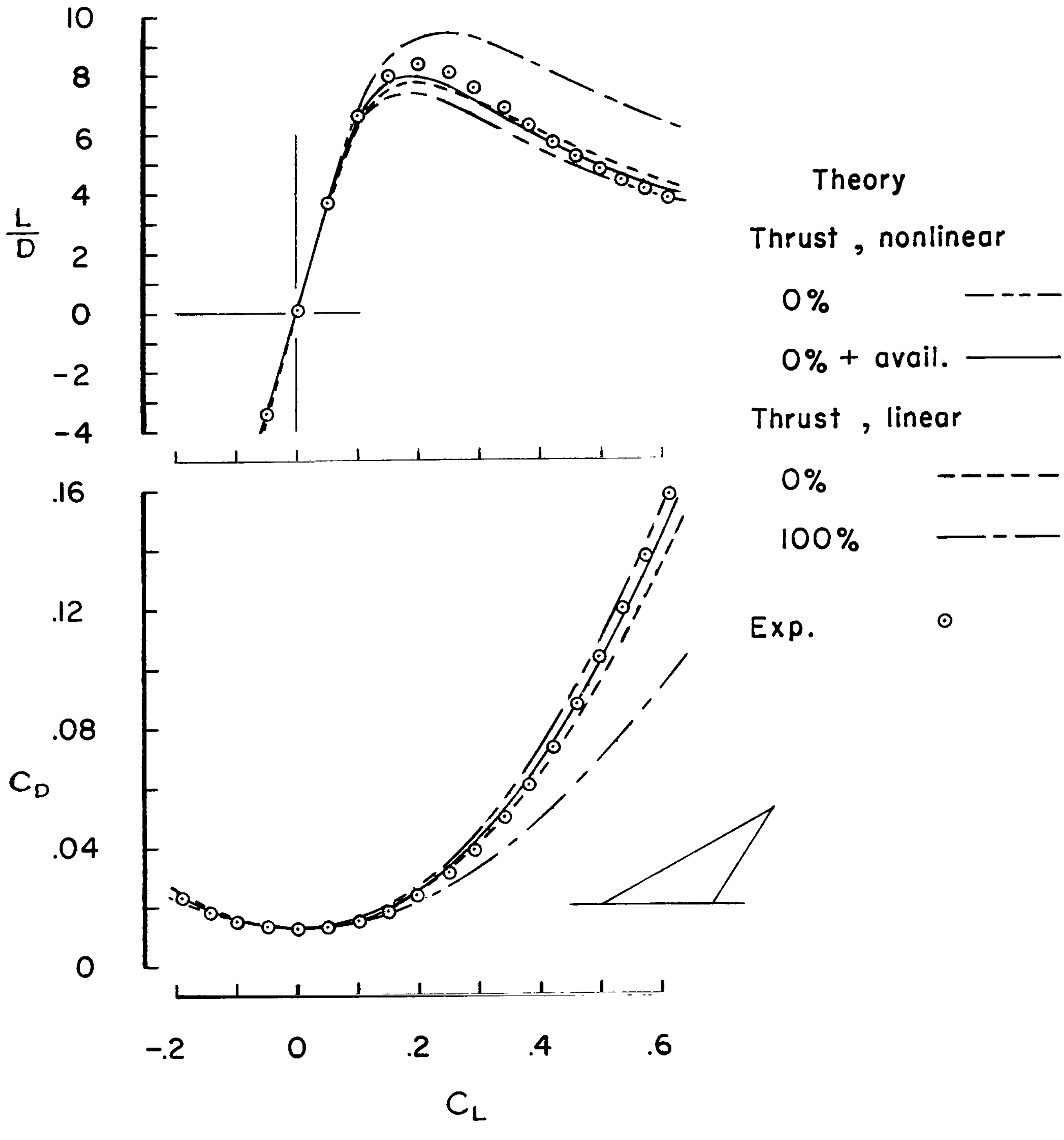

(a) Arrow wing with sharp leading edge.

Figure 23.- Comparison of theoretical and experimental wing performance at $M = 1.6$ and $R = 2.0 \times 10^6$.

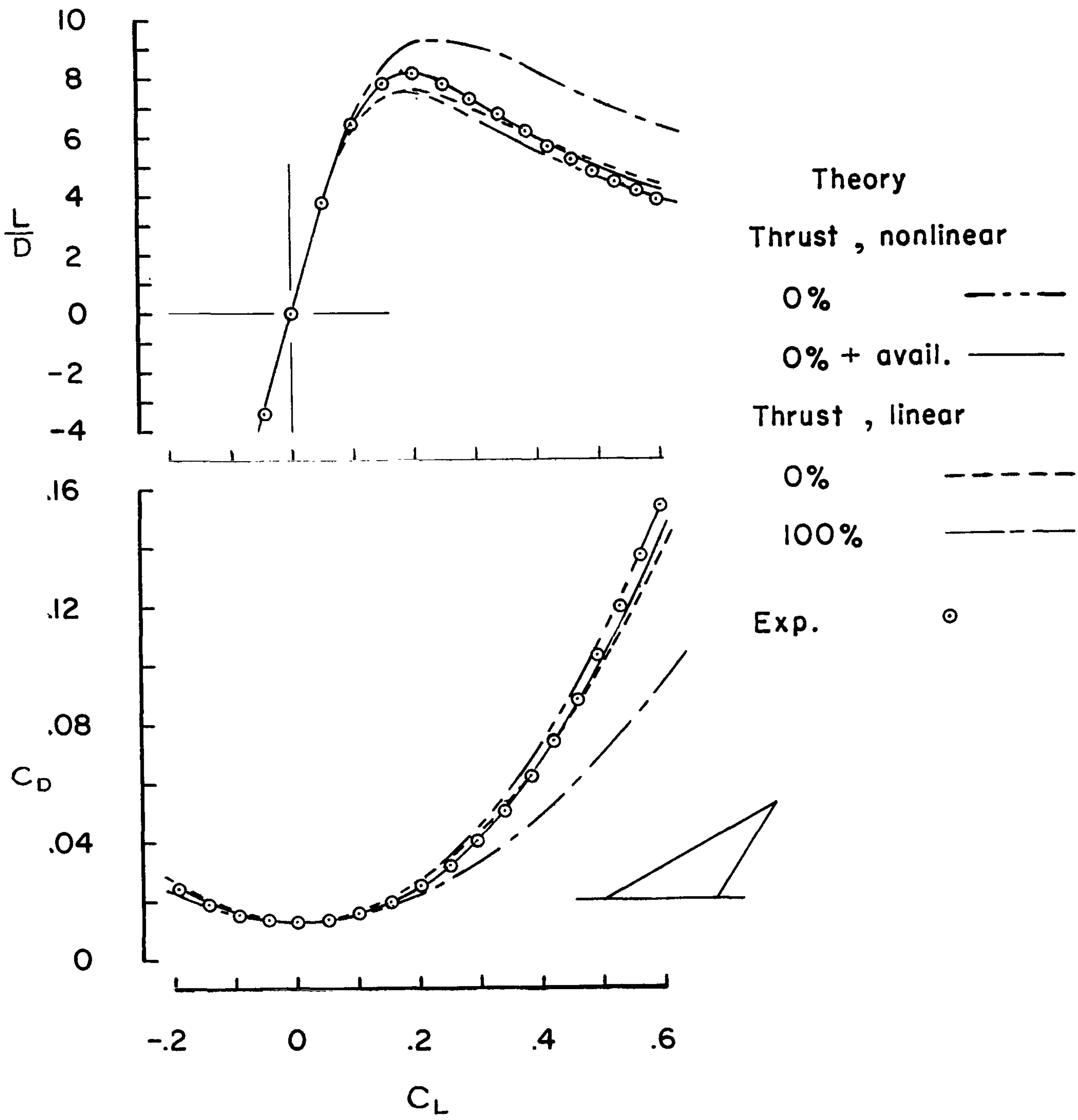

(b) Arrow wing with $(r/c)_{le} = 0.00235$.

Figure 23.- Continued.

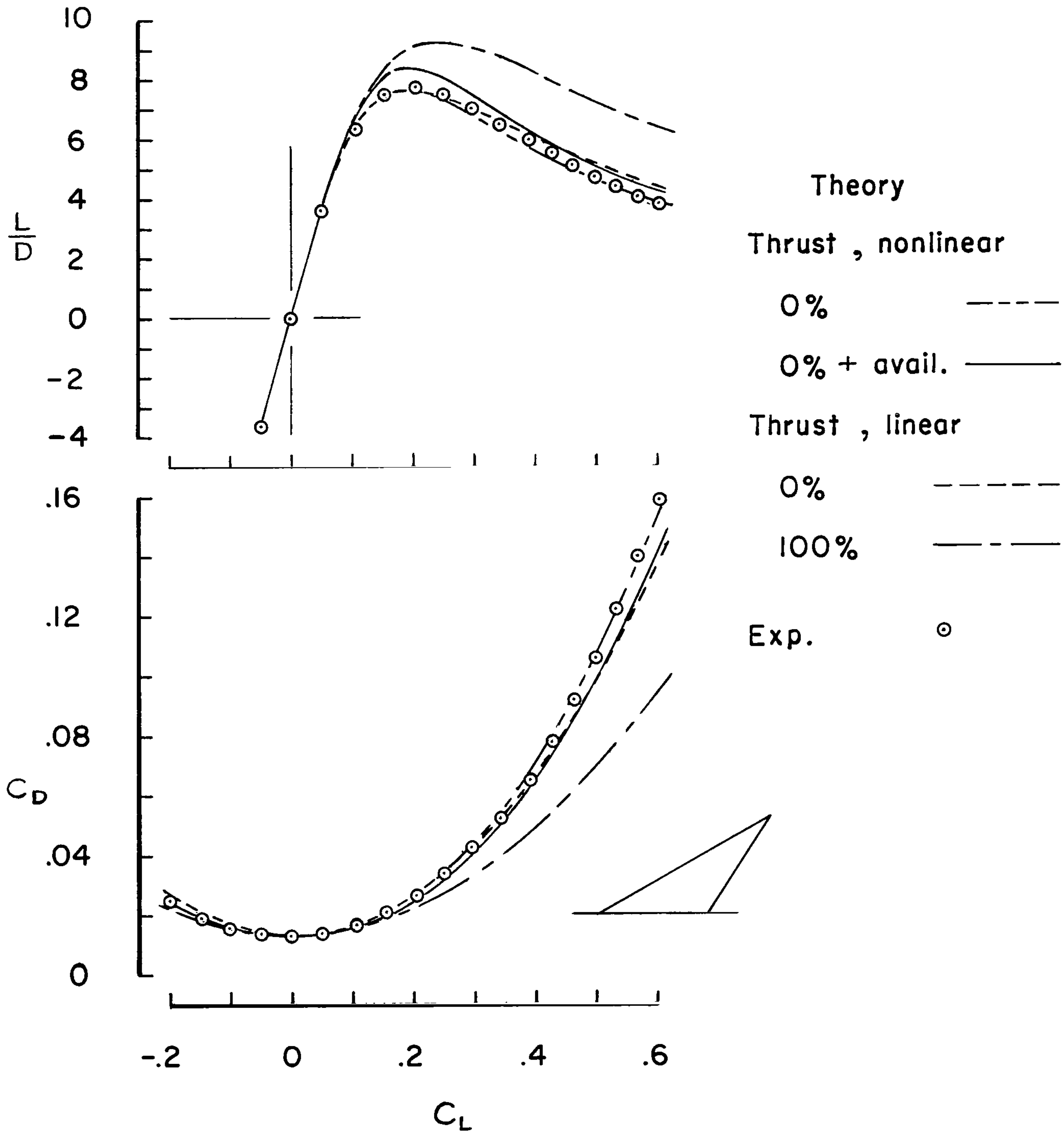

(c) Arrow wing with $(r/c)_{le} = 0.00470$.

Figure 23.- Continued.

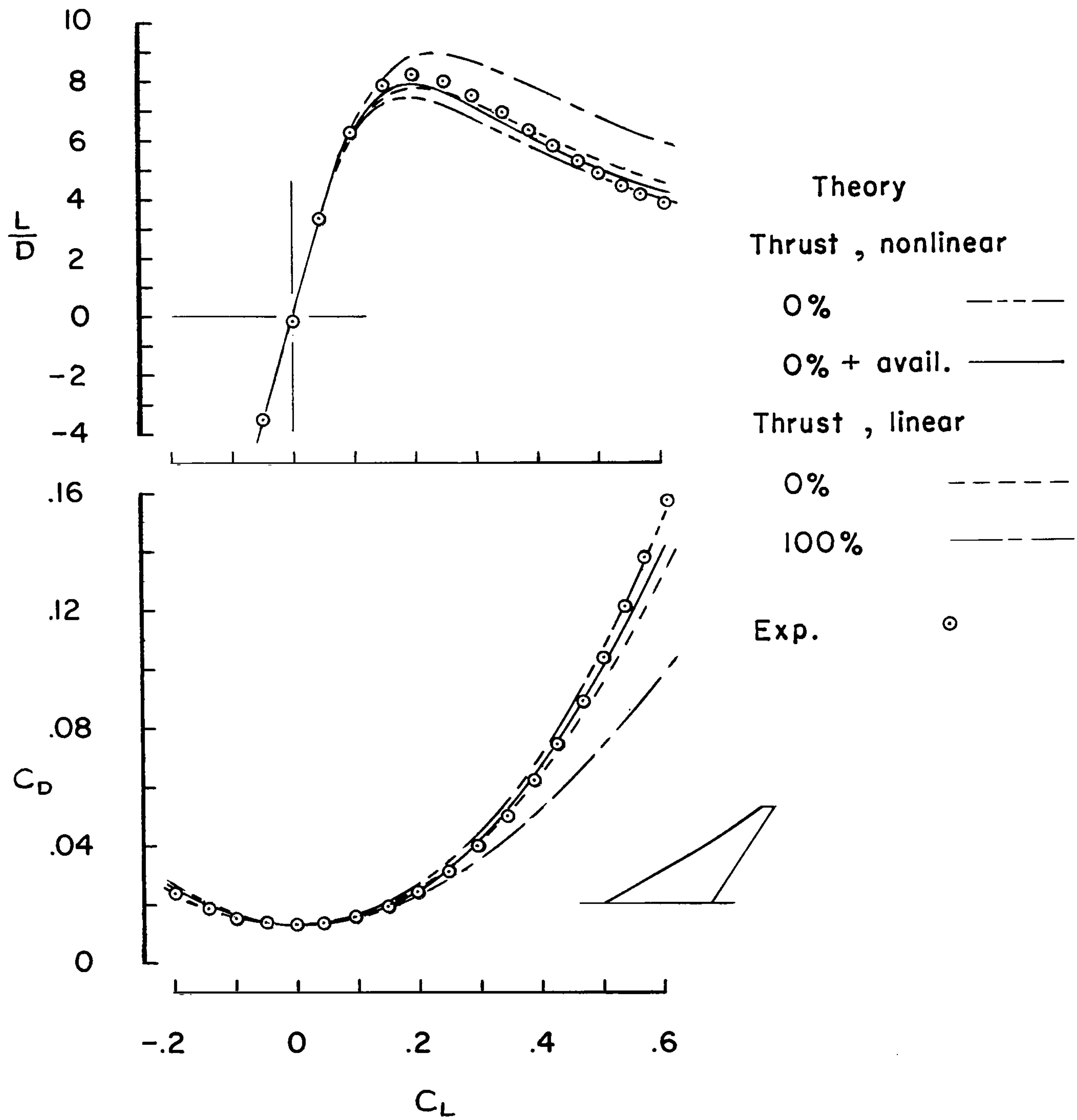

(d) Modified arrow wing with sharp leading edge.

Figure 23.- Continued.

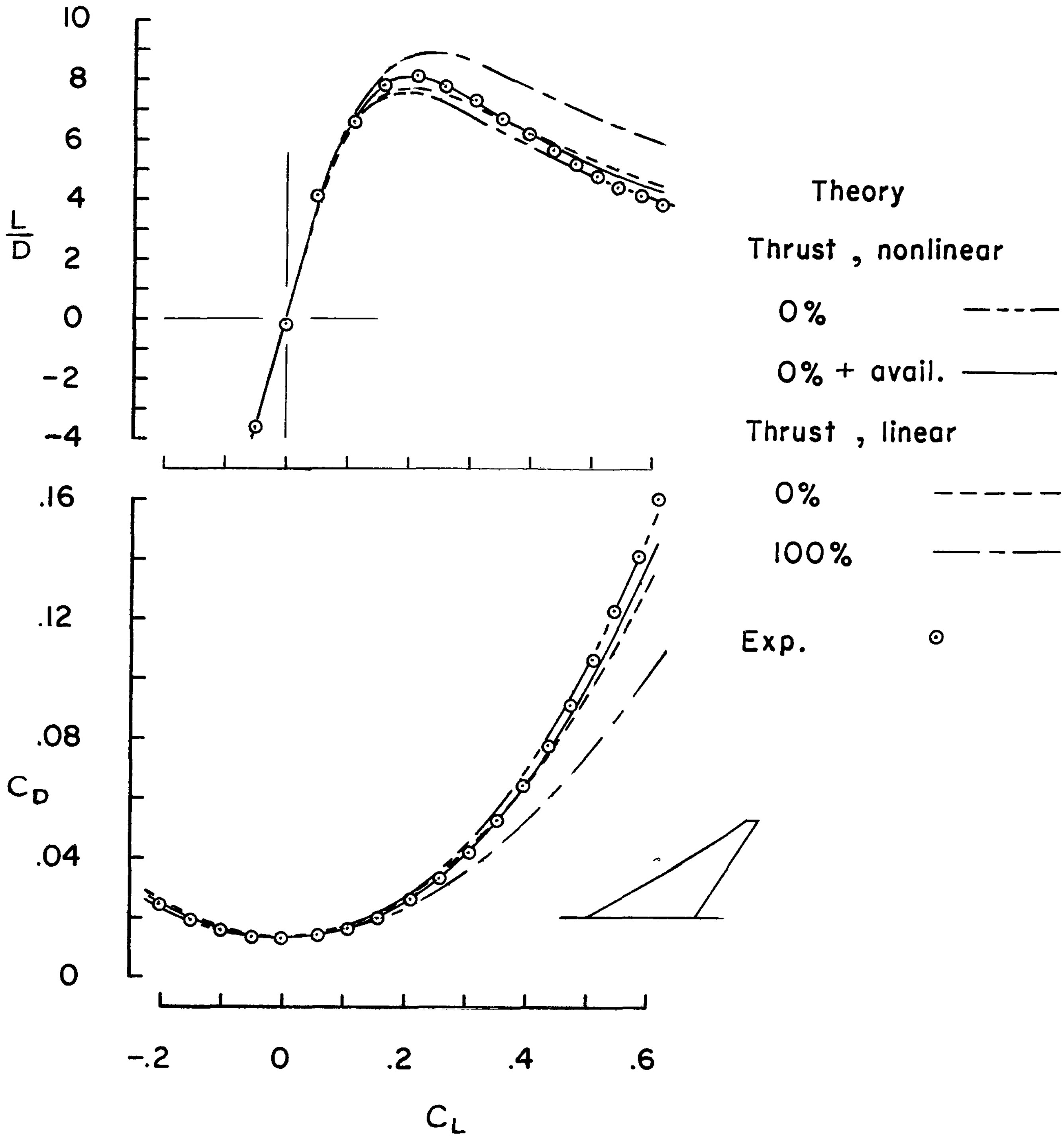

(e) Modified arrow wing with $(r/c)_{le} = 0.00235$.

Figure 23.- Continued.

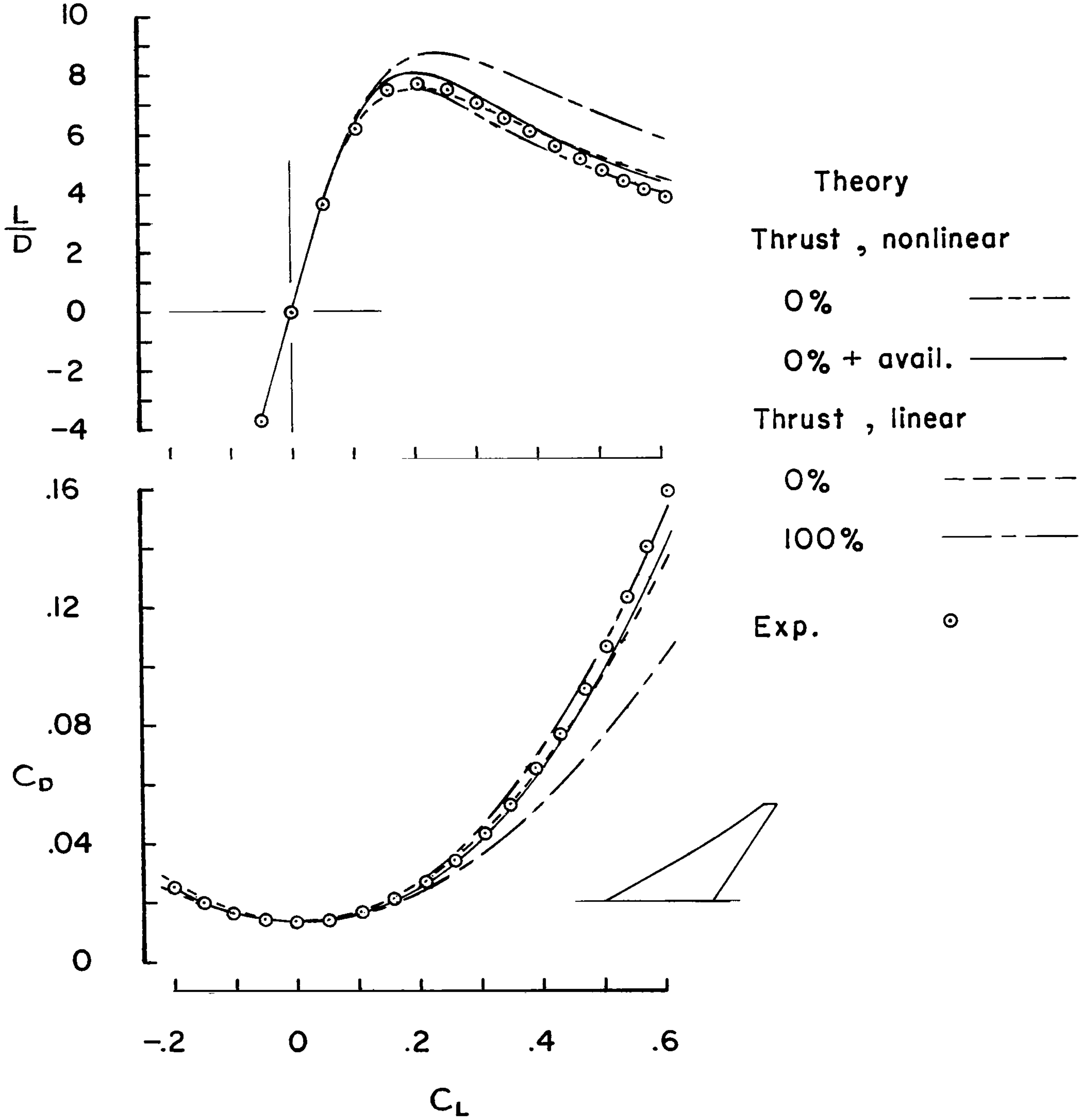

(f) Modified arrow wing with $(r/c)_{le} = 0.00470$.

Figure 23.- Concluded.

1. Report No.	2. Government Accession No.	3. Recipient's Catalog No.
NASA TP-2167		

4. Title and Subtitle	5. Report Date
WIND-TUNNEL INVESTIGATION OF LEADING-EDGE THRUST ON ARROW WINGS IN SUPERSONIC FLOW	August 1983
	6. Performing Organization Code 505-31-73-01
7. Author(s) Robert J. Mack	8. Performing Organization Report No. L-15535
9. Performing Organization Name and Address NASA Langley Research Center Hampton, VA 23665	10. Work Unit No.
	11. Contract or Grant No.
12. Sponsoring Agency Name and Address National Aeronautics and Space Administration Washington, DC 20546	13. Type of Report and Period Covered Technical Paper
	14. Sponsoring Agency Code

15. Supplementary Notes

16. Abstract

Six wing models were tested in the Langley Unitary Plan Wind Tunnel to identify and study leading-edge thrust at supersonic speeds. The tests were conducted at Mach numbers of 1.6, 1.8, 2.0, and 2.16, at a stagnation temperature of 125.0°F, and at Reynolds numbers per foot of 2.0×10^6 and 5.0×10^6. Test results showed that significant benefits from leading-edge thrust and nonlinear thickness effects can be obtained with very little airfoil bluntness, that these benefits were lost when the airfoil was severely blunted, and that such benefits seem to be found on wings with supersonic as well as subsonic leading edges.

17. Key Words (Suggested by Author(s))	18. Distribution Statement
Leading-edge thrust Supersonic flow Wind-tunnel study Theoretical comparison	Unclassified - Unlimited Subject Category 02

19. Security Classif. (of this report)	20. Security Classif. (of this page)	21. No. of Pages	22. Price
Unclassified	Unclassified	78	A05

National Aeronautics and
Space Administration

Washington, D.C.
20546

Official Business
Penalty for Private Use, $300

THIRD-CLASS BULK RATE

Postage and Fees Paid
National Aeronautics and
Space Administration
NASA-451

U.S.MAIL

7 1 1U,A, 830810 S00903DS
DEPT OF THE AIR FORCE
AF WEAPONS LABORATORY
ATTN: TECHNICAL LIBRARY (SUL)
KIRTLAND AFB NM 87117

NASA

S

POSTMASTER: If Undeliverable (Section 158 Postal Manual) Do Not Return